

---

# Event shapes in hadronic Higgs decays

---

Institute for Theoretical Physics  
Theoretical Particle Physics

## Master Thesis

GUGLIELMO COLORETTI

Eidgenössische Technische Hochschule Zürich  
M. Sc. in Physics, Spring Semester 2021  
*gcoloretti@student.ethz.ch*

Supervised by  
Prof. Dr. AUDE GEHRMANN-DE RIDDER

# Abstract

We study next-to-leading order corrections in Quantum Chromodynamics to the most common event shapes for hadronic Higgs decays to three-jets events. The production is achieved via electron-positron annihilation. In particular, we isolate the contributions resulting from gluon-gluon final states. The study of jets of this nature is usually harder to conduct, since the dominant contributions come from other final states. The analysis is achieved via the antenna subtraction method and we present the first subtraction term for the case under study. Our results serve as a theoretical prediction for a future  $e + e -$  collider. The numerical evaluation of the event shapes is conducted with the efficiently designed program **EERAD3**, whereas checks on our results are computed with programs targeted to our purposes, such as **FORM** and **MadGraph5**.

## Acknowledgements

First of all, I would like to thank Prof. Dr. Aude Gehrmann-De Ridder for giving me the opportunity to work in her research group and learn such marvelous things under her guidance. The challenging pandemic period everyone witnessed recently, made tougher feeling part of the scientific community: Prof. Dr. Aude Gehrmann-De Ridder inspired me during my thesis, restoring an environment which allowed me to actively participate in research.

I would like to thank Marco Zanasi, to whom I am deeply grateful, for having believed in me. Without its support, none of this would have been possible.

I also would like to thank my friends, for sharing their lives with mine, and my colleagues, for fruitful discussions and insights.

Finally, I thank my brother and sisters, because we will never be alone. My father, for having wanted me before I came. And my mother: because the underground root of our hearts stands always by me.

# Contents

<b>Introduction</b>	<b>6</b>
<b>1 Preliminaries</b>	<b>9</b>
1.1 Amplitudes structure . . . . .	9
1.2 Phenomenology . . . . .	14
1.3 Infrared limits . . . . .	19
1.3.1 Soft limit . . . . .	21
1.3.2 Collinear limit . . . . .	22
1.3.3 Beyond tree level . . . . .	23
<b>2 Antenna subtraction method</b>	<b>25</b>
2.1 Generalities . . . . .	25
2.2 Definitions . . . . .	26
2.2.1 Jet cross section . . . . .	26
2.2.2 Jet variables . . . . .	27
2.2.3 Jet cross section: LO and NLO . . . . .	30
2.2.4 Jet cross section: NNLO . . . . .	34
2.2.5 Antennas . . . . .	34
2.2.6 Momentum mapping . . . . .	40
2.3 Types of antenna . . . . .	42
<b>3 Hadronic Higgs decays to three-jets</b>	<b>45</b>
3.1 Matrix elements up to NLO . . . . .	45
3.1.1 LO . . . . .	46
3.1.2 NLO . . . . .	49
3.2 Subtraction terms at NLO . . . . .	55
3.3 Numerical implementation . . . . .	65
3.4 Results . . . . .	69
<b>Conclusions and outlook</b>	<b>83</b>

Appendix A: angular terms	84
References	87

# Introduction

The Higgs boson is the last building block of the Standard Model and a precise study of all its properties is mandatory for accurate tests of this theory and for any predictions beyond it. The Higgs field has rather special features and is of major interest for theoretical particle physics, since it is related to the electroweak symmetry breaking scale and many other crucial aspects<sup>1</sup>.

The relatively high mass of the Higgs boson requires high energies for its production. In this regime, the strong force plays a fundamental role and can be treated perturbatively. Quantum Chromodynamics (QCD) perturbative corrections are thus needed for reliable predictions. In the past years, their progress has witnessed an incredible *exploit* due to new efficient techniques to compute scattering amplitudes.

QCD is the extremely successful theory able to explain the strong interaction, namely the force which binds nuclei together. It is included in the Standard Model and has been largely tested up to next-to-next-to-leading-order (NNLO) precision [2]. It is a Yang-Mills gauge symmetry theory on the Lie group  $SU(3)$  and describes the interaction between Dirac spinorial fields, known as quarks and antiquarks, which come in three different generations (flavours) and 8 vector boson gauge fields, known as gluons. All fields need to be charged under the  $SU(3)$  group: the former ones transform under the fundamental representation, whereas the latter under the adjoint<sup>2</sup>.

Quark and antiquark fields acquire masses in the Yukawa couplings to the Higgs field via spontaneous symmetry breaking of the electroweak sector  $U(1)_Y \times SU(2)_L$ , but in high energy physics these fields can be safely treated as massless. Gluonic fields are massless and since there is no mechanism at play which breaks  $SU(3)$  gauge symmetry<sup>3</sup>, we need a structure to explain the extreme short range of this

---

<sup>1</sup>Such as the hierarchy problem, viz. the distribution of the spectrum of the masses of the various fields in the Standard Model, and the so called lack of naturalness, viz. the fine tuning needed to account for cancellation of large quantum corrections to the Higgs boson mass [1].

<sup>2</sup>Here it is why there are exactly 8 gluonic fields.

<sup>3</sup>Spontaneous symmetry breaking of the  $U(1)_Y \times SU(2)_L$  gauge group provides heavy masses for weak gauge bosons too, which in turns yields a short range for the weak interaction mediated by them.

interaction. The solution is provided via the so called asymptotic freedom, namely the fact that the beta function of QCD yields a running coupling which becomes perturbative at high energies and manifests a Landau pole at low energies.

Therefore asymptotic freedom denies a direct detection of the constituents of QCD (viz. partons: quarks and gluons) in experiments and is translated in phenomena with colour confinement: since strong interaction is increasingly strong (sic) at low energies and acts only on colour charged fields, in turns, only colour singlets can be allowed at these energy scales. Therefore, at our daily energy scales, we can only collect bound (colour singlets) states of the latter, namely hadrons (mesons and baryons). In fact, partons interact among each other as long as they form colour singlets. This mechanism is known as hadronization. In order to compare theoretical predictions with experiments, we need to find a bridge among computations and data: this is provided by the notion of jets, namely the definition of a final state according to specific properties. The idea behind the definition of jet functions lies in the fact that resolving particles with an energy below the sensitivity threshold of the detectors (soft particles), is experimentally impossible, as well as distinguishing two particles which are more collinear than the available angle resolution of the instruments. Jet definitions do not only have an experimental physical motivation, but are also necessary for theoretical computations. In fact, both soft and collinear configurations manifest as singularities in the amplitudes while the integration of the squared matrix elements is carried out in phase space. Nevertheless, as expected, all singularities cancel in the total integrated cross sections [3], taking into account also loop processes of the same order. Hence, the required cancellation occurs between processes with different number of particles in the final state. This is why jet functions are a precise procedure for classifying a final state of hadrons (experimentally) or quarks and gluons (theoretically) according to the number of jets it contains. For instance, we could define a three-jets final state as composed by three particles which remains well separated with respect to a certain measure (the jet function) or by more than three particles which are recombined since too close to each others to be distinguished.

To be useful, a jet measure should give cross sections which, like the total cross section, are free of soft and collinear singularities when calculated in perturbation theory, and should also be relatively insensitive to the non-perturbative fragmentation of quarks and gluons into hadrons. Notably, experimental measurements of jet production observables (such as event shapes variables) are among the most sensitive tests of QCD and yield very accurate determinations of its parameters [2].

The collinear and soft limit thus are an experimental and theoretical obstacle which sits in specific regions of the phase space: we need to face them in a system-

atic way (and, possibly, independent from the definition of the jet measure, namely how final states are recombined) in order to perform numerical evaluations and produce theoretical results. Among others [4], [5], the antenna subtraction method [6] stands out, since it is flexible, derived from physical gauge invariant processes and, above all, it is the only one which has been fully extended to NNLO.

In this thesis we exploit this method to compute the next-to-leading (NLO) order QCD corrections to Higgs decays into three jets of hadrons produced via electron-positron annihilation and derive all most common event shapes variables related to this process. This process is attentively chosen, since initial colourless particles provide a clean environment that avoid initial QCD radiations and parton distribution functions. The energy fed into the system is close to resonance with the Higgs boson mass. Hence we can treat all quarks to be massless but the bottom and the top. However, the top mass is so heavy that we can push it (along with possible additional new heavy coloured particles not detected yet) to infinity and integrate out this field à la Wilson in the so called Higgs effective field theory (HEFT [7], [8]). In this way, the Higgs field couples directly to bottom and anti-bottom quarks with a Yukawa coupling and via an effective vertex to gluons. All computations (algebraic and numerical) avail of programs designed for these purposes: **FORM** [9], **MadGraph5** [10], **EERAD3** [11].

The thesis is organized as follows. After some preliminaries on the general behaviour of QCD amplitudes in infrared limits and a discussion on the antenna subtraction method, we provide a detailed formulation of the cross section involved in the computations up to NLO precision, presenting the matrix elements as well as the subtraction terms essential for its rigorous treatment. We also include several plots of the event shapes variables and provide a careful analysis of them. Our results are to be compared with the study of three-jets observables for hadronic decays of Z boson [12].



# Chapter 1

## Preliminaries

### 1.1 Amplitudes structure

To obtain the perturbative cross section to a scattering process, quantum field theories require to sum over all particles multiplicity channels contributing to that precision order. In general, each channel might contain both ultraviolet (UV) and infrared (IR) singularities, which arises from allowing both for infinitely short and long wavelengths of the fields. Of course, both of them need to be cured, since experimental results are finite. UV divergences are systematically handled via renormalisation procedures and running of the couplings. In fact, as well known, UV divergences are local, which means they do not depend on any of the energy scales introduced in the process; this implies a fundamental trait of quantum field theories, which is the insensitivity of physics at certain energies from everything depending on higher energy scales, modulo a redefinition of the couplings. Of course, for standard computations, absorbing physics at higher energies into couplings, is of any help only if the theory redefined in this way is still mild under perturbative approaches.

Soft and collinear IR poles, on the other hand, cancel among each other once all particles channels are summed over [3].

IR singularities arise in two different fashions: from virtual processes, namely loop diagrams; or from collinear and soft singularities in real amplitudes. These latter limits are easily understood, since experimental instruments cannot detect particles which have a distance smaller than a specific threshold, or particles with an energy below the available sensitivity. The idea of defining a specific distance to quantify such limiting behaviours, gives birth to the definition of jets observables. However, virtual and real singularities have another crucial difference, too: while purely virtual singularities are explicitly isolated in the matrix elements just by integrating over the loop momenta, real soft and collinear singularities become

explicit only after integration over the phase space appropriate to the jet observable under consideration. Hence, this integration involves the definition of the jet observable itself, such that an analytic integration is not feasible and also not well suited. Instead, we seek for a flexible method able to be adapted to different jet definitions. The solution is to closely understand the infrared structure of QCD amplitudes and introduce subtraction terms that **(I)** cancel their poles so that to allow for a numerical integration over the phase space and **(II)** are easy enough to be integrated analitically over the limiting regions of the phase space and reproduce the pole structure to be canceled with the virtual one. We notice they need to be local and, further, they should not introduce any new spurious singularity.

In the very end, the antenna subtraction method heavily hinges on the factorisation of the amplitudes under infrared limits and here it is why a complete knowledge of them is mandatory. Infrared limits of QCD amplitudes are successfully captured by colour ordered amplitudes in spinor-helicity formalism.

Non abelian Yang-Mills gauge theories have an additional structure, namely the one related to the gauge group. This additional degree of freedom hides inside the amplitudes and it would be ideal to disentangle it from the spinorial part. This is achieved by stripping the gauge dependence of the amplitude by the rest of it and work it out independently [13]. In general<sup>1</sup>, the leading idea is to organize the amplitudes in terms of string and traces of the generators of the Lie algebra of the gauge group in the fundamental representation [15]. This is possible by noticing that the structure constants of the algebra can be rewritten in terms of products and commutators of those. To give an example, pure gauge vertices depend on the structure constants of the group in such a way as to be symmetric under permutations of the incoming fields<sup>2</sup>. This behaviour depends only on the gauge group and we can separate it from the spinorial part of the amplitude by rewriting the structure constants as traces of commutators, i.e (Fig. 1.1):

$$f^{ABC} \equiv -\frac{i}{T_F} \text{Tr}([T^A, T^B]T^C) \quad (1.1)$$

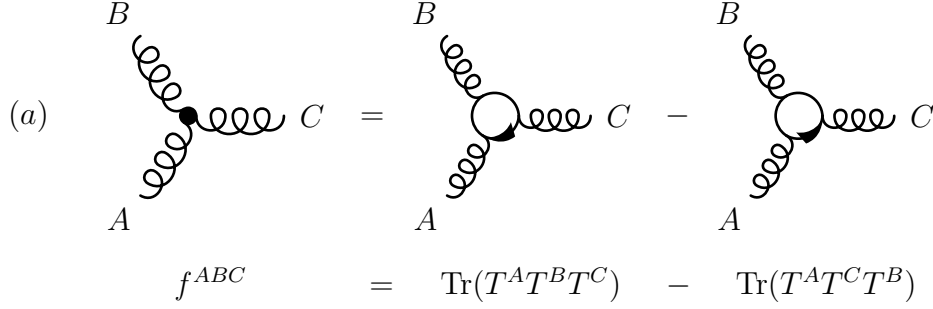
where  $T_F$  is the Casimir operator for the fundamental representation.

---

<sup>1</sup>There are other decompositions, which use a different basis for the gauge group part of the amplitudes. A remarkable one is the multiperipheral decomposition [14].

<sup>2</sup>Recall that for SU(N) gauge theories, having a compact semisimple real Lie algebra, the structure constants are antisymmetric under exchange of any indices [16].

(a)



$$f^{ABC} = \text{Tr}(T^A T^B T^C) - \text{Tr}(T^A T^C T^B)$$

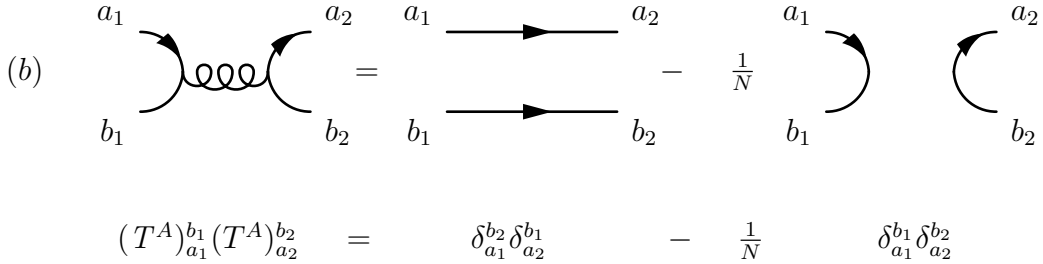
Figure 1.1: Pictorial representation of the decomposition of the structure constant in the pure gauge vertex into string of colour operators in the fundamental representation.

The amplitude is now decomposed in sum of strings of colour operators in the fundamental representation. We can then solve each of the strings and organize the amplitude in terms of the colour factors obtained by handling them. The colour algebra is carried out with the Fierz identity<sup>3</sup> for  $SU(N)$  (Fig. 1.2):

$$(T^A)_{a_1}^{b_1} (T^A)_{a_2}^{b_2} = \delta_{a_1}^{b_2} \delta_{a_2}^{b_1} - \frac{1}{N} \delta_{a_1}^{b_1} \delta_{a_2}^{b_2} \quad (1.2)$$

where uppercase indices span in the adjoint representation (**8**), whereas lowercase indices in the fundamental ( $a$  in the **3**) and  $b$  in the complex conjugate (**3**<sup>\*</sup>).

(b)



$$(T^A)_{a_1}^{b_1} (T^A)_{a_2}^{b_2} = \delta_{a_1}^{b_2} \delta_{a_2}^{b_1} - \frac{1}{N} \delta_{a_1}^{b_1} \delta_{a_2}^{b_2}$$

Figure 1.2: Pictorial representation of the Fierz identity. The non-abelian  $-\frac{1}{N}$  piece is responsible for the exchange of colours in quark-antiquark interaction, since the gluon carry  $SU(3)$  colour charge. This is crucially different from (Yang-Mills) abelian theories as QED, where photons are not charged under the  $U(1)$  gauge group.

For instance, a  $n$  pure gauge amplitude (viz. involving only  $n$  gauge bosons) contains only  $f^{ABC}$  colour factors in each vertex. Rewriting these structure constants with the help of eq. 1.1 and eq. 1.2, this class of amplitudes has the following typical structure:

<sup>3</sup>This identity just states that the  $T^A$  matrices form a complete set of traceless hermitian  $N \times N$  matrices. The  $-1/N$  term enforces the tracelessness condition.

$$\mathcal{M}_n^{tree}(\{k_i, \lambda_i, C_i\}) = g^{n-2} \sum_{\sigma \in S_n/Z_n} \text{Tr}(T^{C_{\sigma(1)}} \dots T^{C_{\sigma(n)}}) A_n^{tree}(\sigma(1^{\lambda_1}), \dots, \sigma(n^{\lambda_n})) \quad (1.3)$$

where  $g$  is the gauge coupling,  $k_i$ ,  $\lambda_i$  are the gluons momenta and helicities,  $C_i$  the adjoint colour indices,  $S_n$  is the set of all permutations of  $n$  object and  $Z_n$  the subset of cyclic permutations (therefore  $S_n/Z_n$  is the subset of all cyclically inequivalent permutations). Applying extensively and repeatedly the Fierz identity we can rewrite the gauge group part in terms of polynomials in the gauge group index  $N$ .

The amplitudes  $A_n^{tree}$  contains the spinorial structure and are the ones where the real work lies. In order to solve them, the so called colour ordered Feynman rules are used, namely a set of Feynman rules which respect the symmetry of the colour ordered amplitudes<sup>4</sup>. Another advantage of this technique is the appearance of additional symmetries in the amplitudes<sup>5</sup> which simplify the computations, allowing one to collect amplitudes with the same colour coefficient and rewrite the whole computations in a compact form. Finally, and perhaps more importantly, we recall that the partial colour ordered amplitudes are easier than the original ones, since the allowed singularities in a colour ordered amplitude are limited and localised in the ordering of the partons. For instance, an amplitude of the form  $A_4^{tree}(1^{\lambda_1}, 2^{\lambda_2}, 3^{\lambda_3}, 4^{\lambda_4})$ , can have infrared poles in the channel  $s_{12}$  but not in the channel  $s_{13}$  since parton 1 and parton 3 are not adjacent in the considered ordering, and thus cannot participate together in an infrared singularity.

We are then left only with the spinorial part of the amplitude which is handled with efficient methods, such as the spinor helicity formalism [17], [18]. Spinor-helicities formalism is a brilliant method whose main idea lies in a suited choice of the basis used to compute the amplitudes. At high energies, most particles can be treated as massless, where fermions transform as Weyl spinors and their chiralities coincide with their helicities. Therefore, for fermions, helicity needs to be conserved. Using helicity as a basis is thus much more natural, also because it provides one for massless gauge bosons, too<sup>6</sup>. In addition, although vector parti-

---

<sup>4</sup>For instance, the Feynman rule for the pure three-point gauge vertex is not anymore invariant under permutations of legs (apart from cyclic ones, which cannot be avoided without spoiling gauge invariance), since we have, precisely, introduced an ordering.

<sup>5</sup>For instance, photon decoupling identity for pure gauge amplitudes.

<sup>6</sup>The Lorentz group is equivalent to  $SL(2, \mathbb{C})/\mathbb{Z}$  (3 complex parameters, 6 real ones). In fact  $SL(2, \mathbb{C}) = SU(2) + iSU(2)$  and we can express the finite dimensional representations of the Lorentz group in terms of the finite ones of  $SU(2) \otimes SU(2)$ . This means that any finite representation of the Lorentz group can be obtained as the tensor product of two spinorial representations which allows to interpret a vector spin-1 representation as an object which lives in the tensor product of pairs of Weyl spinor spin-1/2 representations. Formally, this means that

cles do not conserve helicity, it turns out that the most helicity-violating processes vanish at tree level, due to a hidden supersymmetry that relates boson and fermion amplitudes<sup>7</sup> [19]. Another crucial aspect is that the spinor-helicity formalism exploits directly Mandelstam invariants and encapsulates the limiting behaviour of theories (such as gauge theories) in which vector fields auto-interact. In fact, this interaction would violate conservation of total angular momentum if their vertices would not depend on incoming momenta. This dependence thus reduces the singularities of soft and collinear limits which indeed manifest their appearance in the basic building blocks of spinor helicities formalism, viz. spinor products. [17]. A little drawback of spinor-helicity formalism is that it heavily relies on 4-dimensional spacetime and thus it is not suited for computations including loops, where, preserving gauge invariance, the most used and plain method is dimensional regularization [20] which however exploits the dimension as regulator and thus spoils spinor-helicity formalism.

Nevertheless, other powerful techniques have been found to decompose any loop amplitude into a basis of master integrals and derive compact results. Since for our purpose only one-loop amplitudes<sup>8</sup> are required, we just mention the Passarino-Veltman one-loop decomposition [13]. In order to regularize divergences of amplitudes, several schemes exist and one may use the one more suited to his needs. In fact, they preserve some symmetries of the theory and it is desirable to have a scheme which preserves as many of them as possible. Among others, dimensional regularization is the most used, since it preserves gauge symmetry, unitarity and deals with both UV and IR singularities in the same fashion. The most important ingredient of dimensional regularization is the continuation of the momenta of the unobserved particles into  $d \neq 4$  dimensions, thus rendering the integrals over these momenta finite. Having done this, one is left with a lot of freedom in how to treat the momenta of observed particles and the polarization vectors of all particles. The different choices lead to different versions of dimensional regularization<sup>9</sup>. Conventional dimensional regularisation treats all particles, both external and internal, on the same foot and hence ruins spinor helicity formalism hopelessly. A little variant of it, proposed by 't Hooft and Veltman [21], requires “observable” states, viz. external, to be kept in 4-dimensions. It decomposes all one loop amplitudes in terms of four types<sup>10</sup> of master integrals, called tadpoles and bubbles

---

spin-1 representations are read as spin-(1/2,1/2) representations.

<sup>7</sup>We are referring to supersymmetric Ward identities with  $N=1$  (SUSY  $N=1$ ).

<sup>8</sup>We actually are going to need also some two-loops amplitudes to define infrared safe three-jet observables at NLO precision, but since they are quite easy, we do not require a general formalism to attack them.

<sup>9</sup>Here there is a bottleneck, since unitarity is not always manifest if helicities and dimensions of the momenta of the particles are not treated on the same foot. Luckily, the 't Hooft-Veltman scheme has been proven to preserve it.

<sup>10</sup>There is also a rational term, which is tricky to compute, but there exist many ways to do

for UV divergences and triangles and boxes for IR divergences. All of these are well known and explicitly computed. The Passarino-Veltman decomposition is truly useful since, we recall, it allows to keep all legs, apart from the ones in the loops, in 4-dimensions<sup>11</sup> and thus recover all the tree level results for the rest of the amplitude with spinor-helicity techniques.

Having found where IR singularities hide in amplitudes, we can designed ad-hoc terms that resembles these limits and thus free the real matrix elements from divergences, such that a numerical integration of the matrix elements is performed quickly via suited computer techniques (Montecarlo methods). The goal is to manage to build these terms in such a way as to be able to analitically integrate them in the singular regions of the phase space, thus cancelling the poles of the virtual part of the amplitude explicitly. Since we ask for a method to encapsulate all possible IR limits of generic processes, we need to find the subtraction terms from physical matrix elements. In some cases, this requirement turns out to be quite tricky, but clever escamotages have been found to overcome these difficulties<sup>12</sup> and have gauge invariant subtraction terms.

## 1.2 Phenomenology

The process under study is Higgs decays into hadrons and the corrections we will address are purely QCD ones. We will focus on three-jets observables at next-to-leading order (NLO), i.e. contributions to order  $\alpha_s^2$ . The production of the Higgs boson is achieved via electron-positron annihilation. At resonance with the Higgs boson, the cross section factorizes and we can extract the respective decay width. This process is chosen since it avoids initial state QCD radiations (both for the  $e + e-$  scattering and the Higgs decays) and thus simplifies our study, not using parton distribution functions.

Before discussing the physics at our energetic regime, we briefly recall some fundamentals of QCD.

QCD is a non-abelian Yang-Mills gauge theory with SU(3) as gauge group. Its Lagrangian density, considering all the renormalisable terms, reads:

$$\mathcal{L}_{QCD} = \mathcal{L}_{YM} + \mathcal{L}_{gauge} + \mathcal{L}_{ghost} + \mathcal{L}_{\theta} \quad (1.4)$$

where:

$\mathcal{L}_{YM}$ : This is the standard Yang-Mills lagrangian density for a gauge theory with massless spin-1  $\mathcal{A}^A$  fields (gluons) transforming in the adjoint rep-

---

it (e.g. [22]).

<sup>11</sup>This is done via the so called Van Neerven-Vermaseren basis.

<sup>12</sup>See Section 2.3 on antenna subtractions to have a clear and non trivial example.

representation and massive spin-1/2 fields  $\psi^a$  (quarks) transforming in the fundamental representation, namely:

$$-\frac{1}{4}G^{\mu\nu,A}G_{\mu\nu,A} + \sum_f \bar{\psi}_a(\not{D}_{ab} + M_{ab})\psi_b$$

where: lowercase indices are in the fundamental representation and uppercase in the adjoint; the sum over  $f$  runs over the 6 flavours  $f = u, d, c, s, b, t$ ; the covariant derivative is in the fundamental representation, i.e.  $\not{D}_{ab} = \gamma^\mu(\partial_\mu\delta_{ab} + g_s T_{ab}^A \mathcal{A}_\mu^A)$  - notice that in  $\gamma^\mu$  and  $\psi^a$  spinor indices are suppressed. We recall that, since  $SU(3)$  is a non-abelian group, the term  $G^{\mu\nu,A}$  contains also terms proportional to the structure constant of the  $su(3)$  algebra, i.e.

$$G^{\mu\nu,A} = \partial_\mu \mathcal{A}_\nu^A - \partial_\nu \mathcal{A}_\mu^A - g_s f^{ABC} \mathcal{A}_\mu^B \mathcal{A}_\nu^C$$

The additional terms proportional to the structure constants give rise to triple and quartic self-interactions among gluons and, ultimately, to asymptotic freedom.

The masses of quarks are encoded in the mass matrix  $M$  and are due to spontaneous symmetry breaking of the  $U(1)_Y \times SU(2)_L$  gauge group of the Standard Model lagrangian. They arise in the coupling between fermions and the Higgs field via spontaneous breaking of the terms

$$\mathcal{L}_{mass} = -Y_{ij}^d \bar{Q}^i H d_R^j - Y_{ij}^u \bar{Q}^i \tilde{H} u_R^j + h.c.$$

where:  $Y^u, Y^d$  are the Yukawa matrices containing the couplings;  $Q^i$  denotes the left-handed quark doublets charged under  $U(1)_Y \times SU(2)_L$  and its index runs over the three different flavour generations;  $u_R^j, d_R^j$  are up-like and down-like right-handed quark fields and their indices run over flavour generations as well;  $H$  is the Higgs field and  $\tilde{H} \equiv i\sigma_2 H^*$  with  $\sigma_2 = \begin{pmatrix} 0 & -i \\ i & 0 \end{pmatrix}$ . After spontaneous symmetry breaking, these terms generate the mass matrix as well as an interaction among the Higgs boson field and the quarks. In our high energy regime, we will neglect the mass matrix  $M_{ab}$  and retain only the couplings among the Higgs boson field and the quarks. As for them, still at our energy scales, they can be all considered irrelevant but the top and bottom ones. The top quark has a mass far larger than the Higgs boson and thus, at energy scales around 125.18 GeV, we can safely integrate out the top field, generating an effective coupling (see below 1.3) among gluons and

Higgs boson. Therefore, the only remnant of the the above equation is just in the Yukawa coupling for the bottom quark.

$\mathcal{L}_{gauge}$ : Quantization of gauge theories requires the introduction of a term to prevent over-counting physical equivalent field configurations. This term, in fact, select the gauge, namely define which representatives are taken in the equivalence classes of the gauge group. There are in principle infinite possibilities to choose how to fix the gauge; the standard way to do it in a covariant manner is via a parameter  $\zeta$  and yields:

$$\mathcal{L}_{gauge} = -\frac{1}{2\zeta}(\partial^\mu \mathcal{A}_\mu^A)^2$$

$\mathcal{L}_{ghost}$ : In non-abelian gauge theories, fixing the gauge leaves and additional term in the path integral. With the standard Faddeev-Popov procedure [23], we can take account of this term adding new spurious fields known as ghosts  $\eta^A$ , which are unphysical and only needed in computations where triple and quartic gluon-gluon interactions appear. They are scalar colour charged odd-grassmannian fields and are required to cancel the propagation of unphysical degrees of freedoms of gluons thus ensuring gauge invariance. Using the covariant class of gauges parametrised by  $\zeta$ , these fields are introduced in the lagrangian with the term:

$$\mathcal{L}_{ghost} = \partial_\mu \eta^{A,\dagger} (D_{AB}^\mu \eta^B)$$

where the covariant derivative is in the adjoint representation and couples ghosts to gluons. We notice here that this term depends on the gauge fixing part of the lagrangian. In general, covariant gauges are used in loop computations since the Feynman propagator has a clean spinorial structure, whereas for external legs the so called axial gauges simplify the computations much more. In fact, in axial gauges the ghost-gluons interaction decouples in  $\mathcal{L}_{ghost}$  and we can integrate out the ghost fields [24]. However, loop computations in axial gauges have some subtleties which render them quickly too complicated. Luckily, different gauges for external and internal lines can be used, which allows us to neglect ghosts as external legs and use Feynman propagators in internal lines.

$\mathcal{L}_\theta$ : This term is responsible for possible CP violating effects, which have been found extremely small in actual experiments [25]. This term reads:



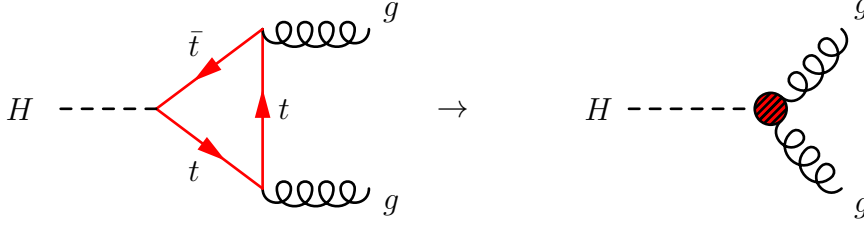


Figure 1.3: Higgs effective theory at one loop.

$$\mathcal{L}_\theta = \frac{\theta g_s^2}{32\pi^2} \frac{1}{2} \epsilon_{\mu\nu\rho\sigma} G_A^{\rho\sigma} G^{A\mu\nu}$$

It is a total derivative and can be safely ignored in perturbation theory. Further, even allowing its presence, and thus considering non perturbative effects [26], in the massless regime it can be swiped away via a chiral rotation<sup>13</sup> [30].

We now turn to Higgs decays and analyse the QCD correction to it. In the Standard Model, the Higgs boson couples directly to quarks and antiquarks through Yukawa couplings and interacts with gluons through virtual loops of quark and antiquarks. At Higgs mass energy scale, we can safely treat all quarks to be massless but the top and the bottom.

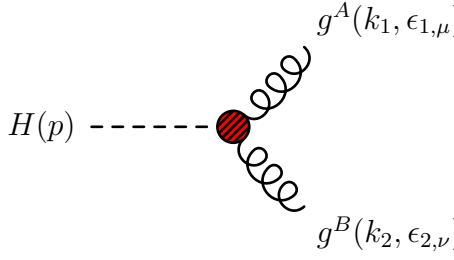
The top quark has a mass much larger than the energetic regime considered: it cannot be produced as final state since there is not enough available energy and it enters amplitudes only via loops of virtual particles. Hence we would like to integrate out this degree of freedom à la Wilson. This is done via the Higgs effective field theory (HEFT) [31], [7], [8], [32]. This theory shrinks loops of top generation<sup>14</sup> and results in an interaction among Higgs boson and gluons (Fig. 1.3). The interaction term in the lagrangian between the Higgs field  $H$  and the gluon stress field tensor  $G_{\mu\nu}^A$  reads:

$$\mathcal{L}_{int} = -\frac{\lambda}{4!} H G^{\mu\nu,A} G_{\mu\nu,A} \quad (1.5)$$

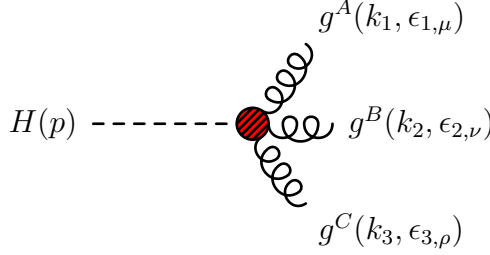
Feynman rules can be easily derived from this interaction term:

<sup>13</sup>This is due to the anomaly of the QCD lagrangian under chiral rotational symmetry. We point out that, even with masses, there are theoretical mechanisms which explain the fine tuning of the small  $\theta$  parameter, being actually a coupling. The general idea hinges on the introduction of an additional U(1) symmetry [27] which is spontaneously broken giving rise to axion-like fields [28], [29].

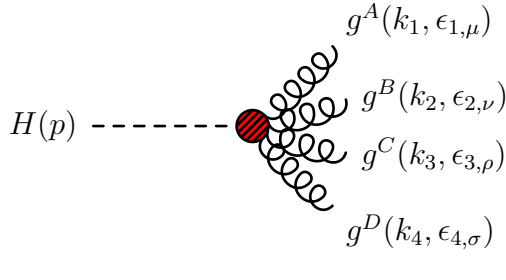
<sup>14</sup>In principle, any colour charged massive particles heavier than the top generation could hide in this effective vertex.



$$= i\lambda\delta^{ab}(g^{\mu\nu}k_1 \cdot k_2 - k_1^\nu k_2^\mu) \quad (1.6)$$



$$= -g_s\lambda f^{abc}(g^{\mu\nu}(k_1^\rho - k_2^\rho) + g^{\nu\rho}(k_2^\mu - k_3^\mu) + g^{\rho\mu}(k_2^\nu - k_3^\nu)) \quad (1.7)$$



$$= -g_s^2\lambda \left[ f^{abe}f^{cde}(g^{\mu\rho}g^{\nu\rho} - g^{\mu\sigma}g^{\nu\rho}) + f^{ade}f^{bce}(g^{\mu\nu}g^{\rho\sigma} - g^{\mu\rho}g^{\nu\sigma}) + f^{ace}f^{dbe}(g^{\mu\sigma}g^{\nu\rho} - g^{\mu\nu}g^{\rho\sigma}) \right] \quad (1.8)$$

At Higgs mass energies, neglecting energies above top mass, HEFT gives calculations accurate within 5% and thus it is sufficiently reliable. This theory is well established: the two loop beta function, needed to run the coupling  $\lambda$  to the desired energy, is known in purely QCD and the renormalization constant for this coupling is given by:

$$Z_\lambda = \frac{1}{1 - \beta(\alpha_s)/\epsilon} = 1 - \frac{\alpha_s}{2\pi} \frac{\beta_0}{\epsilon} + \left( \frac{\alpha_s}{2\pi} \right)^2 \left[ \frac{\beta_0^2}{\epsilon^2} - \frac{\beta_1}{\epsilon} \right] + \mathcal{O}(\alpha_s^3) \quad (1.9)$$

with  $\beta_0$  and  $\beta_1$  the first two coefficients of the QCD- $\beta$  function in dimensional regularisation ( $\overline{\text{MS}}$ ), namely:

$$\beta_0 = \frac{11N - 2N_F}{6}, \quad \beta_1 = \frac{34N^3 - 13N^2N_F + 3N_F}{12N} \quad (1.10)$$

where  $N = C_A$ , viz. the Casimir operator of  $\text{su}(3)$  Lie algebra, and  $N_F$  is the number of active flavours.

As for the remaining quarks, all are treated as massless. To be precise, we keep the mass of the bottom generation, which appears in the Yukawa coupling between the latter and the Higgs boson. Nevertheless, in actual computations at the Higgs mass energy scale, neglecting its mass in all other elements, we can safely ignore it, since it accounts for less than 2% of accuracy.

For the Yukawa coupling, all matrix elements are already known, as well as the renormalisation group equation (up to two loops in QCD) to run the coupling to the desired energy scale [33], [34].

We therefore work in perturbative massless QCD with  $N_F = 5$  active flavours, considering the QCD lagrangian at energies close to the Higgs boson mass, thus without the  $\mathcal{L}_\theta$  term, neglecting the mass matrix  $M$  and with the additional interaction in eq. 1.5. Therefore, the Higgs boson couples only to bottom-antibottom pairs via a Yukawa coupling and to gluons via HEFT vertices.

Hence, in our analysis the contributions to three-jets events come from two configurations: (i) a bottom-antibottom pair; (ii) a pair of gluons. The branching functions for these two processes give a ratio of 97% against 0.03%, respectively [2]. This is due to the fact that, as mentioned above, the coupling of the Higgs field to the gluons happens via an effective vertex, whereas the coupling to the bottom generation is the Yukawa vertex of the Standard Model.

In the following, we will treat the LO case for both contributions, and extend our analysis to NLO precision for gluon-gluon final states. In general, jets coming from this contribution are more difficult to extract, given their small contribution to the whole decay width of the Higgs boson.

## 1.3 Infrared limits

Unitarity is the requirement for probabilities of all possible physical processes (amplitudes) to add up to one (i.e. certainty): a simple physical aspect, which nevertheless leads to several insights on quantum field theories. The generality of the consequences derived from it follows from the nature of this inspection, which, in fact, does not require perturbation theory and thus holds even beyond it. Among others<sup>15</sup>, the one we will exploit is the factorization of arbitrary scattering amplitudes whenever the energy in a channel allows for an intermediate state to be produced. All that is required is that the operators<sup>16</sup> involved in the amplitudes overlap with some fields which transform under an irreducible representation of the Poincaré group. The amplitude then factorizes when the available energy is near resonances corresponding to the masses of these fields [35].

---

<sup>15</sup>Such as a non-perturbative demonstration of LSZ formula, or, assuming a gauge theory, the necessity for spin-1 fields to transform under the adjoint representation.

<sup>16</sup>Of course, including elementary fields too, viz. the ones appearing in a Lagrangian.

In purely massless QCD, the case under study, amplitudes factorize whenever an intermediate leg goes on-shell. If we consider only single unresolved partons, this could happen in two cases, namely whenever a particle approaches null energies or a pair of particles become collinear. For the sake of clarity, considering a two particle channel and defining  $s_{ij} = P^2 = (p_i + p_j)^2$ , the propagator is<sup>17</sup>

$$\frac{-i g_{\mu,\nu}}{s_{ij}} \quad \text{for gluons,} \qquad \frac{\not{p}}{s_{ij}} \quad \text{for fermions.} \quad (1.11)$$

The propagators diverge whenever  $s_{ij} = p_i^2 + p_j^2 + 2p_{i,\mu}p_j^\mu = 2p_{i,\mu}p_j^\mu = 0$  which can only happen if either

- $p_{i,\mu} = 0, p_{j,\mu} = 0 \quad \longrightarrow$  soft limits
- or
- $2p_{i,\mu}p_j^\mu = 0 \quad \longrightarrow$  collinear limit

Spinor-helicity formalism is extremely convenient to describe these limits at tree level since with it the factorization of the amplitude is particularly manifest. Using spinor-helicity formalism it is in fact possible to prove a much more powerful result, that goes under the Britto-Cachazo-Feng-Witten (BCFW) on-shell recursion relation [36], [37]. The idea behind the proof is that at tree-level amplitudes are plastic, viz. continuously deformable, analytic functions of the momenta involved in the scattering. Using complex analysis, it should then be possible to reconstruct the behaviour of the whole amplitude by inspecting the singular kinematic regions. In general, multivariable complex analysis is far from being easy. BCFW are extensively exploited since they use only a single complex parameter and, luckily, this family explores enough of the singular regions to recover a recursion relation for the original amplitude. All is in a well suited and cleverly chosen shift of pairs of spinors by a complex parameter. The choice must be done with care, since the amplitude should also vanish whenever the complex parameter reaches the boundaries of the phase space. Calling this parameter  $z$  and a generic tree level  $n$  point amplitude  $A_n$ , we can then invoke Cauchy theorem and write:

$$0 = \frac{1}{2\pi} \oint_C dz \frac{A_n(z)}{z} = A_n(0) + \sum_k \text{Res} \left[ \frac{A_n(z)}{z} \right] \Big|_{z=z_k} \quad (1.12)$$

with the contour  $C$  pushed to infinity where the amplitude vanishes, and  $z_k$  being the poles of the amplitude.  $A_n(0)$  is just the original amplitude, thus, solving the above equation for it, we have a formula to compute it in terms of a sum of on-shell amplitudes with fewer legs. Since the parton going on-shell can propagate

---

<sup>17</sup>Recalling our massless regime, t and u channel will only have a minus sign before them.

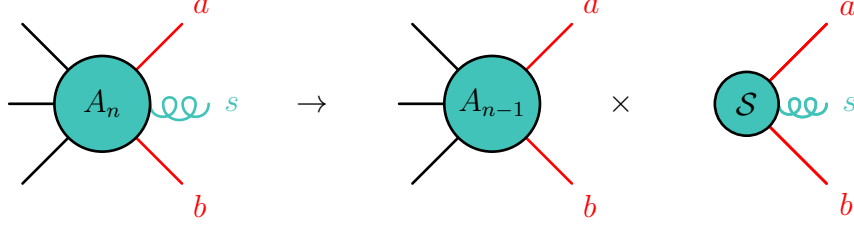


Figure 1.4: Factorization of tree-level amplitudes under soft limit of gluon  $s$ .

an arbitrary distance, the amplitudes in which the original one is factorized into, are causally disconnected. A sketch of the proof can be found in [17].

The way the amplitudes factorize depends heavily on the vertices attached to the ends of the propagators going on-shell. Since in QCD they could be of limited types, there are compact formulas for soft and collinear limits.

### 1.3.1 Soft limit

Soft limit occurs when the momentum of a gluon  $k_s$  scales uniformly to zero. In the following, we will refer *only* to colour ordered amplitudes and will use the notation from spinor-helicity formalism as in<sup>18</sup> [18]. Let us consider an amplitude  $A_n^{tree}(1, 2, \dots, a, s^\pm, b, \dots, n)$ , where the soft gluon is labelled with  $s$  and its helicity is in superscript. Recalling that the amplitude is colour ordered, the soft gluon  $s$  is emitted between the two hard radiators  $a$  and  $b$  adjacent to it. Soft factorization reads:

$$A_n^{tree}(1, \dots, a, s^\pm, b, \dots, n) \xrightarrow{k_s \rightarrow 0} \mathcal{S}(a, s^\pm, b) \times A_{n-1}^{tree}(1, \dots, a, b, \dots, n) \quad (1.13)$$

As expected, the amplitude strictly factorizes and the singularity is fully encapsulated in the soft (eikonal) factor

$$\mathcal{S}(a, s^+, b) = \frac{\langle ab \rangle}{\langle as \rangle \langle sb \rangle} \quad ; \quad \mathcal{S}(a, s^-, b) = -\frac{[ab]}{[as][sb]} \quad (1.14)$$

This factorization might look obvious for fewer point amplitudes, such as a 5 point amplitude, but it is highly non trivial already for a 6 point amplitude. In fact, for a 5 point amplitude, it could be obtained rearranging the expression of the scattering process, whereas in a 6 point amplitude more terms appear summed together and only in the soft limit we recover the factorization shown (see [13], section 2.4.4). Pictorially, it is represented in Fig. 1.4.

<sup>18</sup>Apart from the standard Van der Waerden notation of spinors, we recall that in our conventions all partons have outgoing momenta.

An interesting feature of the soft factorization is that the eikonal factor is universal: it does not depend on the types of partons from which the soft gluon is radiated; it does not rely on their helicities; not even on the magnitude of their momenta (just the directions of them). The independence from spin can be understood considering the nature of this limit. Being a low energy behaviour, it is long-wavelength and thus intrinsically classic<sup>19</sup>. After squaring the amplitudes and summing over helicities, we obtain the factorization of the matrix element squared that enters the integral which yields the cross section. We will need it in the future; considering parton  $b$  to be soft, it reads:

$$\mathcal{S}_{abc} = \frac{2s_{ac}}{s_{ab}s_{bc}} \quad (1.15)$$

where  $s_{ij}$  is the Mandelstam invariant for partons  $i$  and  $j$ .

### 1.3.2 Collinear limit

Collinear limit occurs when the momenta of two partons  $k_a$  and  $k_b$  become parallel  $K_P^2 = k_a^2 + k_b^2 + 2 k_a \cdot k_b \xrightarrow{a||b} 0$ , where  $K_P$  is the “parent” parton whose propagator goes on shell in this limit. In order to describe the limit properly, we need to specify the momentum fraction of the original parton carried by the collinear partons:

$$k_a \approx z K_P, \quad k_b \approx (1 - z) K_P$$

where  $z$  is the fraction of the original momentum  $K_P$  and  $0 < z < 1$ . Mind that if  $z = 0$  or  $z = 1$ , one of the partons becomes soft. Relating this to spinor-helicity notation, the respective spinors  $\lambda$  and  $\tilde{\lambda}$  scale with the square root of it, namely:

$$\begin{aligned} \lambda_a &\approx \sqrt{z} \lambda_P, & \lambda_b &\approx \sqrt{1 - z} \lambda_P \\ \tilde{\lambda}_a &\approx \sqrt{z} \tilde{\lambda}_P, & \tilde{\lambda}_b &\approx \sqrt{1 - z} \tilde{\lambda}_P \end{aligned}$$

Labelling with  $P$  the splitting parent parton and  $a, b$  the collinear ones, the factorization in this limit reads:

$$A_n^{tree}(1, \dots, a^{\lambda_a}, b^{\lambda_b}, \dots, n) \xrightarrow{a||b} \sum_{\lambda_P=\pm} \text{Split}_{-\lambda_P}(a^{\lambda_a}, b^{\lambda_b}; z) A_{n-1}^{tree}(1, \dots, P^{\lambda_P}, \dots, n) \quad (1.16)$$

---

<sup>19</sup>Due to its spin independence, the soft factor can be computed pretending the hard radiator partons are scalars, and just using QED Feynman rules and Schouten identity [17].

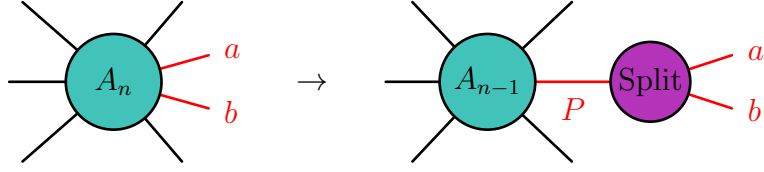


Figure 1.5: Factorization of tree-level amplitudes under collinear limit of particles  $a$  and  $b$ .

where  $\lambda$  indicates the helicity of the parton considered. Again, all singularities are captured by the splitting functions  $\text{Split}(z)$ . We depict this limit in the diagrams of Fig. 1.5. Notice that there appears a sum over the intermediate helicities of the parent parton<sup>20</sup> and that its helicity is reversed with respect to the one it had in the original amplitude (again, our conventions yield all momenta to be outgoing). The right-hand-side of eq. 1.16 is found by merging the intermediate parton according to the possible vertices in QCD:  $g \rightarrow gg, g \rightarrow q\bar{q}, q \rightarrow qg, \bar{q} \rightarrow \bar{q}g$ . A crucial difference with respect to the eikonal factor, is that the splitting functions depend on the configurations of final partons  $a$  and  $b$  and on their helicities as well. All splitting functions can be readily computed from general processes and are well known. Collinear singularities of initial state radiations resemble the DGLAP evolution equations for parton distributions. In fact, after squaring the amplitudes and summing over helicities, we obtain the correct splitting probabilities  $P(z)$ . Since we will need them in the following sections, we briefly list them:

$$\begin{aligned} P_{qg \rightarrow Q}(z) &= \left( \frac{1 + (1-z)^2 - \epsilon z^2}{z} \right), \\ P_{q\bar{q} \rightarrow G}(z) &= \left( \frac{z^2 + (1-z)^2 - \epsilon}{1-\epsilon} \right), \\ P_{gg \rightarrow G}(z) &= 2 \left( \frac{z}{1-z} + \frac{1-z}{z} + z(1-z) \right) \end{aligned}$$

where the computation has been carried out in conventional (or 't Hooft-Veltman) regularization scheme and the notation is understood.

### 1.3.3 Beyond tree level

Since the antenna formalism exploits factorization of one-loop amplitudes and we will need the following results in later sections, we briefly recall them.

<sup>20</sup>This is not always the case, or better: if the parent parton is a quark or antiquark, helicity conservation requires only one term in the sum to survive, whereas for an intermediate gluon both helicities are allowed.

A similar factorization as the tree-level one occurs at one-loop level in general gauge theories, too [38], [39]. From it, it is possible to derive the factorization for collinear and soft limits at one-loop. For instance, the collinear one reads:

$$A_n^{loop}(1, \dots, a^{\lambda_a}, b^{\lambda_b}, \dots, n) \xrightarrow{a||b} \sum_{\lambda=\pm} \left( \text{Split}_{-\lambda_P}^{tree}(z, a^{\lambda_a}, b^{\lambda_b}) A_{n-1}^{loop}(1, \dots, P^{\lambda_P}, \dots, n) \right. \\ \left. + \text{Split}_{-\lambda_P}^{loop}(z, a^{\lambda_a}, b^{\lambda_b}) A_{n-1}^{tree}(1, \dots, P^{\lambda_P}, \dots, n) \right)$$

where the notation is meant to be in the same fashion as the above equations for tree limits. As expected, the singular behaviour is controlled by the splitting function  $\text{Split}^{tree}$  and its one-loop counter part  $\text{Split}^{loop}$ . The splitting functions are also well known and process independent. They depend only on the configurations of the splitting partons (gluons or quarks), their helicities and momenta, just as in the tree level case. Pictorially, one-loop collinear limits can be represented as:

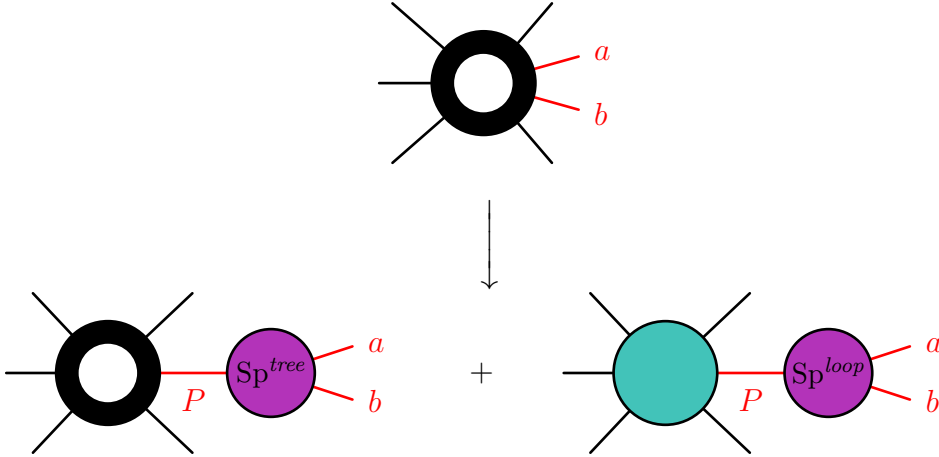


Figure 1.6: Factorisation of one-loop-level amplitudes under collinear limit of particles  $a$  and  $b$ .

where with circles we indicate tree amplitudes, with donuts one-loop and with Sp splitting kernels. For soft limits, a similar factorization exists [40]. The relevant conclusion is that amplitudes factorise in a precise manner under infrared limits also at one-loop level, and we can thus design subtraction terms for higher orders in perturbation theory, especially at NNLO.



# Chapter 2

## Antenna subtraction method

### 2.1 Generalities

As previously discussed, QCD cross sections are affected by singular limits coming from multiple radiations of real partons. The nature of the singularities is twofold: infrared singularities coming from loops are easily overcome, being manifest in the matrix elements and explicit already after the loop integration; the ones coming from real matrix elements arise only after integration in phase space of the matrix elements and are thus somewhat hidden in the cross section. This suggests the definition of jets and infrared safe quantities. Roughly speaking, knowing real singularities needs to be canceled with the ones coming from loop integrals with a different number of final states, we can organize the contributions to the same order in such a way as to free the cross section from singularities.

Having done this, we still have a major issue: jet definitions require recombination of collinear or soft partons into a single object and this procedure has plenty of freedom. Definitions mainly propose integral measures of phase space which treat singular regions<sup>1</sup> in certain ways. Hence, the integration of cross sections in phase space avoid singularities depending on the jet functions. As a result, analytical integration is not feasible and, more relevantly, not quite appropriate so that each jet observable should in principle be treated differently. Instead, one would aspire to a flexible method, independent from the jet definition and thus suited to all kind of jet observables. Thus, the poles of real matrix elements need to be extracted from the integration via infrared subtraction terms, namely add to the real contributions additional matrix elements which match their behaviour in the singular regions of the phase space. Of course, these terms need to be inserted back in the cross section, but if they are simple enough to be analytically

---

<sup>1</sup>With singular regions, we mean a section of phase space which encompasses all regions corresponding to singular configurations of real matrix elements.

integrated in the singular regions, the poles obtained will be explicitly canceled by the ones coming from the virtual contributions. This is accomplished only due to the definition of the jet cross section and a last key ingredient, namely the factorization of phase space over singular regions which allows to treat the factors entering the subtraction terms independently.

Therefore infrared subtraction terms need to fulfill some crucial requirements: **(I)** approximating the full real matrix elements in *all* singular limits; **(II)** being still sufficiently simple to be integrated *analytically* over the singular regions of the phase space; **(III)** being *local*, thus not introducing additional spurious infrared singularities apart from the ones they are aimed at.

The antenna subtraction method is a systemic approach designed precisely for this purpose and<sup>2</sup> it has some desirable advantages. First of all, it has been fully extended at NNLO accuracy; further, it uses a single phase space mapping for the two possible collinear limits of a parton, as we will discuss in the following. This method considers the parton who becomes singular surrounded by a pair of other partons which are redefined into the two hard final ones: we have an antenna composed by two hard radiators which emits a soft or collinear parton between them. Before analysing the construction of the different antennas, we prefer to highlight the general setting we will adopt.

## 2.2 Definitions

### 2.2.1 Jet cross section

The order of accuracy to a jet observable depends on the number of jets in the final state and is computed in terms of powers of the couplings, starting from the leading configurations to the selected number of jets. In order to be clean with the notation, we specify our definitions. We follow closely [6].

We define the tree-level  $n$ -parton contribution to the  $m$ -jet cross section<sup>3</sup> in  $d$  dimensions by:

$$d\sigma^B = \mathcal{N} \sum_n d\Phi_n(p_1, \dots, p_n; q) \frac{1}{S_n} |\mathbf{M}_n(p_1, \dots, p_n)|^2 J_m^{(n)}(p_1, \dots, p_n) \quad (2.1)$$

where the normalisation factor  $\mathcal{N}$  includes all factors which does not depend on the QCD Lagrangian as well as the dependence on the *renormalised* QCD coupling

---

<sup>2</sup>There exist other methods to build subtraction terms, such as the closely related Catani-Seymour dipole formalism [41].

<sup>3</sup>Actually, for tree level process of course we need to set  $n = m$ . However, since we will use the same expression for NLO cross section, we leave  $n \neq m$ .

constant  $\alpha_s$ ;  $\sum_n$  denotes the sum over all configurations of the matrix element  $\mathbf{M}$  with  $n$  partons in the final state;  $d\Phi_n$  is the standard phase space for a  $n$ -parton final state with total four-momentum  $q^\mu$  in  $d = 4 - 2\epsilon$  space-time dimensions, namely

$$d\Phi_n(p_1, \dots, p_n; q) = \frac{d^{d-1}p_1}{2E_1(2\pi)^{d-1}} \cdots \frac{d^{d-1}p_n}{2E_n(2\pi)^{d-1}} (2\pi)^d \delta^d(q - p_1 - \cdots - p_n); \quad (2.2)$$

$S_n$  is a symmetry factor for identical partons in the final state. Finally, we recall  $|\mathbf{M}_n|^2$  denotes a squared, colour-ordered tree-level  $n$ -parton matrix element, where each particle is color connected with the adjacent ones (see Fig. 2.1).

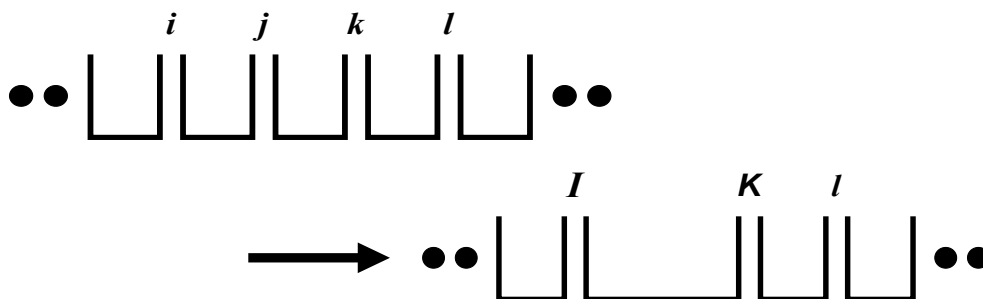


Figure 2.1: Color connection of real radiation under singular IR limits. The parent partons are  $(i, j, k)$  with  $j$  becoming unresolved. The new recombined partons are  $(I, K)$ .

In every jet function definition, all colour orderings are summed over  $\sum_m$  with the appropriate colour weighting. The jet function  $J_m^{(n)}$  defines the procedure to reconstruct  $m$  jets from  $n$  partons. In general, it contains  $\theta$  and  $\delta$  functions and its main property is that it is infrared safe [2]. Roughly, this means the variables defined must be insensitive to the emission of soft or collinear partons; in particular, if  $p_i$  is any three-momentum occurring in its definition, it must be invariant under the branching

$$p_i \rightarrow p_j + p_k \quad (2.3)$$

whenever  $p_j$  and  $p_k$  are parallel or one of them is soft. Quantities made out of linear sums of momenta meet this requirement.

## 2.2.2 Jet variables

In the past years, several variables have been defined in order to characterize the final states of an event. They depend on the number of particles in the final states.

Here we briefly summarise the most common ones requiring three particles in the final states.

Among others, event shapes variables are extensively used and called so since they inquire the geometric behaviour of the distribution of jets. We recall that, in order to define a jet observable quantitatively, we need to introduce the concept of a jet measure, i.e. a procedure for classifying a final state of hadrons (experimentally) or quarks and gluons (theoretically) according to the number of jets it contains. To be useful, a jet measure should give cross sections which, like the total cross section, are free of soft and collinear singularities when calculated in perturbation theory, and should also be relatively insensitive to the non-perturbative fragmentation of quarks and gluons into hadrons.

**Thrust  $T$ :** The idea is indeed to define a quantity which characterize the shape of the event, being “pencil like”, planar, spherical and so on. The thrust variable is defined as<sup>4</sup>:

$$T = \max_{\mathbf{n}} \left( \frac{\sum_i |\mathbf{p}_i \cdot \mathbf{n}|}{\sum_i |\mathbf{p}_i|} \right) \quad (2.4)$$

where  $\mathbf{p}_i$  are final state hadron (or parton) momenta and  $\mathbf{n}$  is an arbitrary unit vector. The unit vector  $\mathbf{n}$  is varied to find the thrust direction  $\mathbf{n}_T$  which maximises the expression in parentheses. The maximum value of thrust,  $T \rightarrow 1$ , is obtained in the limit where there are only two particles in the event (“pencil-like event”) and in this case the thrust direction  $\mathbf{n}_T$  lies along the jets. For a three-particle event the minimum value of thrust is  $T = 2/3$ .

**Heavy jet mass  $\rho$ :** The customary definition considers the event as divided by the two hemispheres  $H_i$  separated by the plane orthogonal to the thrust axis. In each of them, the hemisphere invariant mass is computed as:

$$M_i^2/s = \frac{1}{E_{\text{vis}}^2} \left( \sum_{k \in H_i} p_k^\mu \right)^2 \quad (2.5)$$

The heavy jet mass observable  $\rho$  is determined by the larger of the two hemisphere invariant masses:

---

<sup>4</sup>In this section, for the sake of clarity, we use bold font to denote vectors in three space.

$$\rho \equiv M_H^2/s = \max(M_1^2/s, M_2^2/s). \quad (2.6)$$

The behaviour of this variable is such that in the two particles limit  $\rho \rightarrow 0$ , while for a three particles event  $\rho \leq 1/3$ .

**Jet broadening**  $B_W, B_T$ :

The event is divided again in the two hemispheres  $H_i$  separated by the plane orthogonal to the thrust axis. In each of them, the hemisphere broadening is defined as:

$$B_i = \frac{\sum_{k \in H_i} |\mathbf{p}_k \times \mathbf{n}_T|}{2 \sum_k |\mathbf{p}_k|} \quad (2.7)$$

The wide and total jet broadening are then determined, respectively, as:

$$B_W = \max(B_1, B_2) \quad (2.8)$$

$$B_T = B_1 + B_2 \quad (2.9)$$

These variables are designed such that in the two particles limit they both tend to zero  $B_W, B_T \rightarrow 0$ . For a three particles event, the maximum jet broadening is  $B_T = B_W = 1/(2\sqrt{3})$ .

**C parameter:**

A further quantity of interest is related to the following linearised tensor in momentum space:

$$\Theta^{\alpha\beta} = \frac{1}{\sum_k |\mathbf{p}_k|} \sum_k \frac{p_k^\alpha p_k^\beta}{|\mathbf{p}_k|}, \quad (\alpha, \beta = 1, 2, 3) \quad (2.10)$$

Its three eigenvalues  $\lambda_i$  are used to identify the  $C$  parameter<sup>5</sup>:

$$C = 3(\lambda_1 \lambda_2 + \lambda_2 \lambda_3 + \lambda_3 \lambda_1) \quad (2.12)$$

---

<sup>5</sup>This definition is actually equivalent to:

$$C = 3(\Theta^{11}\Theta^{22} + \Theta^{22}\Theta^{33} + \Theta^{33}\Theta^{11} - \Theta^{12}\Theta^{12} - \Theta^{23}\Theta^{23} - \Theta^{31}\Theta^{31}) \quad (2.11)$$

**Jet transition variable  $Y_3$ :** Another observable commonly studied is the jet transition variable  $Y_3$ . It is defined as the value of the jet resolution parameter  $y_{cut}$  for which an event changes from a three-jets to a two-jets configuration with some jet defining scheme. The  $Y_3$  parameter defines a distance in energy for the radiated partons and the condition under which two partons needs to be recombined into a single jet. There are several measures that fulfills this task and it is desirable to have a definition which resembles the experimental results, namely identifies two partons being “close” as two partons which in the experimental detection are truly soft or collinear. The most used is the DURHAM algorithm<sup>6</sup>:

$$y_{ij,D} = \frac{2\min(E_i^2, E_j^2)(1 - \cos \theta_{ij})}{s_{ij}} \quad (2.13)$$

where  $E$  is the energy of the particle  $i$  or  $j$  and  $s_{ij}$  their Mandelstam invariant. The pair with the lowest  $y_{ij,D}$  is replaced by a pseudoparticle whose four-momentum is given by the sum of the four-momenta of particles  $i$  and  $j$  (recombination scheme). This procedure is repeated as long as pairs with invariant mass below the predefined resolution parameter  $y_{ij,D} < y_{cut}$  are found. Once the clustering is terminated, the remaining (pseudo-)particles are the jets. In our analysis, focusing on three jets observables, we will compute  $Y_3$ , namely the transition parameter from 2 to 3 jets. Of course transition parameters from  $n - 1$  to  $n$  jets are defined analogously.

### 2.2.3 Jet cross section: LO and NLO

We finally give the operative definitions for the cross section we will use to compute NLO corrections to three-jets QCD cross sections.

Recalling the definition for a jet cross section as in Section 2.2.1, we obtain the leading order approximation to the  $m$ -jet cross section by integration over the appropriate phase space:

$$d\sigma_{LO} = \int_{d\Phi_m} d\sigma^B \quad (2.14)$$

---

<sup>6</sup>There are also other algorithms, such as the JADE algorithm. When  $Y_3$  is small, the sensitivity is pushed to its extreme value and thus soft and collinear singularities become more and more relevant; this is resembled in theoretical computation by typical terms  $O(\alpha_s^n \ln^{2n} y)$  which needs to be resummed. However, the JADE algorithm is not practically suited for this type of operation, whereas the DURHAM meets this need.

We note that, depending on the jet function used, this cross section can still be differential in certain kinematical quantities.

As for the NLO contributions to  $m$ -jets, we need to consider  $(m + 1)$ -partons real radiation and one-loop processes. The latter are to be integrated in the  $m$ -particles phase space against a  $m$ -jets function and thus their integration is easily achieved numerically, since poles of these matrix elements are explicitly manifest after integration over loop momenta and the  $m$ -jets functions prevent the final state partons to become unresolved and thus introduce additional IR singularities. Instead, for the real radiation matrix elements, the integration is carried out in  $(m + 1)$ -particles phase space; the  $m$ -jet function recombines the final states to obtain  $m$ -particles and we need to account for single unresolved parton processes and IR singularities arising from them. In order to perform an efficient and jet function independent numerical integration, we introduce subtraction terms which are designed to free real matrix elements from IR divergences. These subtraction terms need to resemble the real radiation matrix elements in every IR limits without introducing additional spurious singularities. Of course, we need to add the subtraction terms back in our definition of the cross section and we require them to be mild enough to be analytically integrated in the single regions of the phase space i.e. the reduced factorised antenna phase space, hence reproducing the explicit one-loop matrix elements virtual poles to be correctly cancelled with.

Therefore, we consider the following  $m$ -jet cross section:

$$d\sigma_{NLO} = \int_{d\Phi_{m+1}} (d\sigma_{NLO}^R - d\sigma_{NLO}^S) + \left[ \int_{d\Phi_{m+1}} d\sigma_{NLO}^S + \int_{d\Phi_m} d\sigma_{NLO}^V \right] \quad (2.15)$$

where:

$d\sigma_{NLO}^R$  : Born cross section, namely tree-level contributions with one additional real radiation parton. It is equivalent to  $d\sigma_{NLO}^B$  as in eq. 2.1 but with  $m \rightarrow m + 1$ .

$d\sigma_{NLO}^V$  : one-loop virtual correction to the  $m$ -parton Born cross section  $d\sigma^B$  in eq. 2.1.

$d\sigma_{NLO}^S$  : subtraction term. It has the same *unintegrated* singular behaviour as  $d\sigma_{NLO}^R$  in all singular unresolved parton limits. Their difference is free of divergence and can be integrated *numerically*. This term needs also to be *analytically* integrated over all singular regions of the  $(m + 1)$ -parton phase space. The resulting cross section, added to the virtual contribution, yields an infrared safe observable.

Using the antenna subtraction method, the subtraction term at NLO can then be written as:

$$\begin{aligned} d\sigma_{NLO}^S = & \mathcal{N} \sum_{m+1} d\Phi_{m+1}(p_1, \dots, p_{m+1}; q) \times \\ & \frac{1}{S_{m+1}} \sum_j X_{ijk}^0 |\mathbf{M}_m(p_1, \dots, \tilde{p}_I, \tilde{p}_K, \dots, p_{m+1})|^2 J_m^{(m)}(p_1, \dots, \tilde{p}_I, \tilde{p}_K, \dots, p_{m+1}) \end{aligned} \quad (2.16)$$

where the notation has already been clarified in Section 2.2.1. We recall, nevertheless, what our notation points out: the subtraction term involves the  $m$ -parton amplitude depending *only* on the redefined on shell momenta  $p_1, \dots, \tilde{p}_I, \tilde{p}_K, \dots, p_{m+1}$  where  $\tilde{p}_I, \tilde{p}_K$  are linear combinations of  $p_i, p_j, p_k$ ; on the other hand, the tree antenna function  $X_{ijk}^0$  (as well as the factorised antenna phase space  $d\Phi_{X_{ijk}}$ ) depends *only* on  $p_i, p_j, p_k$ .  $X_{ijk}^0$  describes all of the configurations for this colour-ordered amplitude where parton  $j$  is unresolved. Again, this method finds its roots in the particular factorization properties of colour-ordered amplitudes, as previously described in the above sections.

We recall another fundamental aspect, as discussed before, namely the phase space mapping from the three partons of the antenna involved in the limiting process to the two recombined ones. The crucial feature is that, in the singular regions, the new redefined momenta are independent from the single unresolved ones and are functions of a mixture of them. Thus the jet function  $J_m^{(m)}$  in eq. 2.16 does not depend on the individual momenta  $p_i, p_j, p_k$ , but only on a combination of them, namely  $\tilde{p}_I, \tilde{p}_K$ . The  $(m+1)$ -phase space disentangles into the  $m$ -particles phase space depending on  $p_1, \dots, \tilde{p}_I, \tilde{p}_K, \dots, p_{m+1}$  and the antenna phase space depending only on  $p_i, p_j, p_k$ . This allows us to *analytically* perform the integration of the antenna in the reduced antenna phase space and explicitly recover the poles of the virtual contribution. The factorization of the phase space reads:

$$\begin{aligned} d\Phi_{m+1}(p_1, \dots, p_{m+1}; q) \\ \longrightarrow d\Phi_m(p_1, \dots, \tilde{p}_I, \tilde{p}_K, \dots, p_{m+1}; q) \cdot d\Phi_{X_{ijk}}(p_i, p_j, p_k; \tilde{p}_I + \tilde{p}_K) \end{aligned} \quad (2.17)$$

where the notation has already been clarified. We notice that the NLO antenna phase space  $d\Phi_{X_{ijk}}$  is proportional to the three-particle phase space. In fact, selecting  $m = 2$  in the last formula we obtain<sup>7</sup>:

---

<sup>7</sup>We recall that the two-particle phase space is a constant, which in conventional dimensional



$$d\Phi_3 = P_2 d\Phi_{X_{ijk}} \quad (2.18)$$

Therefore, regarding the analytical integration, we can exploit eq. 2.17 to write each subtraction term in the following form:

$$|\mathbf{M}_m|^2 J_m^{(m)} d\Phi_m \int d\Phi_{X_{ijk}} X_{ijk}^0 \quad (2.19)$$

where

- $|\mathbf{M}_m|^2, J_m^{(m)}, d\Phi_m$  depend *only* on  $p_1, \dots, \tilde{p}_I, \tilde{p}_K, \dots, p_{m+1}$
- $X_{ijk}^0, d\Phi_{X_{ijk}}$  depend *only* on  $p_i, p_j, p_k$

Hence, the analytical integral of the subtraction term is defined as the antenna function integrated over the *fully inclusive* antenna phase space, normalised appropriately<sup>8</sup>:

$$\mathcal{X}_{ijk}^0(s_{ijk}) = (8\pi^2(4\pi)^{-\epsilon} e^{\epsilon\gamma}) \int d\Phi_{X_{ijk}} X_{ijk}^0 \quad (2.20)$$

Again, probably being pedantic, we remind the reader that the integration 2.19 is performed analytically in  $d$  dimensions and the poles obtained cancel exactly the one coming from loop virtual integration. The normalisation factor  $(8\pi^2(4\pi)^{-\epsilon} e^{\epsilon\gamma})$  is related to the normalisation of the normalised coupling constant, and its relation to the bare coupling parameter  $g = \sqrt{4\pi\alpha_0}$  appearing in the QCD Lagrangian density:

$$\alpha_0 \mu_0^{2\epsilon} S_\epsilon = \alpha_s \mu^{2\epsilon} \left[ 1 - \frac{\beta_0}{\epsilon} \left( \frac{\alpha_s}{2\pi} \right) + \left( \frac{\beta_0^2}{\epsilon^2} - \frac{\beta_1}{2\epsilon} \right) \left( \frac{\alpha_s}{2\pi} \right)^2 + \mathcal{O}(\alpha_s^3) \right] \quad (2.21)$$

with  $S_\epsilon = (4\pi)^\epsilon \exp^{-\epsilon\gamma}$  and Euler constant  $\gamma = 0.5772\dots$ . The mass parameter  $\mu_0$  is the one introduced in dimensional regularisation to maintain the coupling adimensional in the Lagrangian density, the coefficient  $\beta_1$  and  $\beta_2$  are the same as in eq. 1.10. The normalisation factor  $(8\pi^2(4\pi)^{-\epsilon} \exp^{\epsilon\gamma}) = 8\pi^2/S_\epsilon$  included is particular convenient. In fact, loop amplitudes are proportional to powers of  $(\alpha_s/2\pi)$ . Checking the cancellation of the integrated subtraction terms with the

---

regularisation reads:

$$P_2 = \int d\Phi_2 = 2^{-3+2\epsilon} \pi^{-1+\epsilon} \frac{\Gamma(1-\epsilon)}{\Gamma(2-2\epsilon)} (q^2)^{-\epsilon}$$

For a detailed discussion on phase space up to four-particles, used in the antenna subtraction method up to NNLO, we remind the reader to [42].

<sup>8</sup>Recall that calligraphic notation stands for integrated form of matrix elements.

virtual parts is thus more handy, since both contributions are multiplied by the same overall prefactor:

$$\begin{aligned} \text{Tree } (m+1)\text{-partons:} & \propto g_s^{2(m+1)} / \underbrace{8\pi^2}_{\text{Normalisation of } d\Phi_{X_{ijk}^0}} \\ \text{Virtual } m\text{-partons:} & \propto \left(\frac{\alpha_s}{2\pi}\right) g_s^{2m} \end{aligned}$$

## 2.2.4 Jet cross section: NNLO

In this section, we limit ourselves to briefly discuss the subsequent NNLO corrections to  $m$ -jet cross sections. The new contributions come from two-loops corrections to  $m$ -partons final state, one-loop corrections to  $(m+1)$ -partons final state and real radiation  $(m+2)$ -partons final state. The tricky part is that now we allow for up to two partons to become unresolved and thus, apart from the singular limit already discussed at NLO, we also find double unresolved configurations. These have a non-trivial colour structure, since the connection of the unresolved partons with the rest of the matrix element depends on the configuration considered. The phase space mapping definition from  $(m+2)$  to  $(m+1)$ -partons is also much more involved, since it needs a precise and unique way to identify the colour orderings. Nevertheless, the antenna subtraction method brilliantly extends at NNLO, too. A relevant example of its application can be found in [11], where jet rates and event shapes are computed for Z boson decays at NNLO in QCD. These results will be used as a matter of comparison to our analysis.

## 2.2.5 Antennas

The antennas are matrix elements which encapsulate the IR limits of specific processes. In fact, we recall that amplitudes under these limits factorise into two disconnected parts, one involving the partons at play in the IR singularity and the other containing the remaining states. Antenna are then built selecting three partons, considering a pair of them which remain hard (radiators) and the remaining one becoming unresolved (emitter) in between them. The order strictly matters, since the factorization of the amplitudes is colour ordered. Ordering of emissions means that the two hard radiator partons defining the antenna are identified, and that each unresolved parton can become singular only with the two particles which are adjacent to it, i.e. the two radiators. The main advantage compared to other known methods [41], apart from the full and detailed extension to NNLO, is the possibility to use the same phase space mappings independently from the radiators onto which the unresolved parton collapses to. All antennas are derived from

physical processes, which in turns renders them gauge invariant. Further, since we care only about the singular structure in phase space and wish to apply the same method to all possible scatterings, we get rid of couplings and initial states by normalising each antenna by the Born cross section of the same process. The factorization is represented pictorially by Fig. 2.2. It is the same one undergone by the phase space, as it is discussed later.

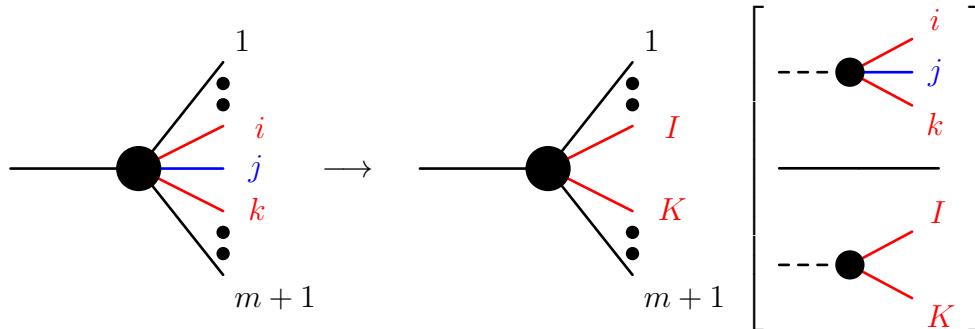


Figure 2.2: Illustration of antenna factorization (at NLO): the picture represents the factorization of both the matrix elements and the  $(m+1)$ -particle phase space. The term in brackets, where the fraction line stands for the normalisation by the Born element, denotes both the antenna  $X_{ijk}^0$  and the antenna phase space  $d\Phi_{X_{ijk}}$ .

Each antenna is a function of the invariants formed by the momenta of the final state particles. To be precise, they are given by a colour connected pair of partons which emit radiation between them and determined by both the external state and the pair of hard partons they collapse to. They are derived from colour ordered matrix elements, normalised by Born processes and stripped off of couplings and colour factors. The physical process examined is always the decays of a field. Considering the possible combinations of fields allowed by QCD vertices, we have three different types of antennas depending on the hard radiators: quark-antiquark, gluon-gluon and quark-gluon (antiquark-gluon). They are derived from the following processes:

1. quark-antiquark :  $\gamma^* \longrightarrow q\bar{q} + \text{partons}$
2. gluon-gluon :  $H \longrightarrow \text{partons}$
3. quark-gluon :  $\tilde{\chi} \longrightarrow \tilde{g} + \text{partons}$

Generic antennas are denoted by  $X$ . The detailed classification is not given

here, but we remind the reader to Section 3 of [6] for the notation. We will only give a couple of examples in Section 2.3.

At tree level and for singular unresolved configurations, the antenna is defined as<sup>9</sup>:

$$X_{ijk}^0 = S_{ijk,IK} \frac{|\mathbf{M}_{ijk}^0|^2}{|\mathbf{M}_{IK}^0|^2} \quad (2.22)$$

where  $S_{ijk}$  is a symmetry factor accounting for more than one singular behaviour in the process (to be considered later),  $\mathbf{M}_{ijk}^0$  is the tree level<sup>10</sup> coloured ordered matrix element of the process considered with final states labelled as  $i, j, k$  and  $j$  becoming unresolved, and  $\mathbf{M}_{IK}^0$  is the Born coloured ordered matrix element with final states partons  $I, K$ , namely the two recombined hard partons from the  $i, j, k$  ones. Under the IR limit in which parton  $j$  becomes unresolved (see section 1.3), the antenna reads:

$$X_{ijk}^0 \xrightarrow{j \text{ unresolved}} S_{ijk,IK} \mathcal{R}^0(ijk) \frac{|\mathbf{M}_{IK}^0|^2}{|\mathbf{M}_{IK}^0|^2} \quad (2.23)$$

where with  $\mathcal{R}^0(ijk)$  we denote either a splitting function or the eikonal factor, at tree level. Hence, the antenna clearly captures the singular behaviour of the limits.

There exist also antennas for double unresolved configurations at tree-level. These necessarily have four-partons in the final state. We will need them to write the four-real partons contribution at tree-level to three-jets events. To define them, we should understand the structure of double unresolved IR limits of tree amplitudes, which, in principle, is an application of the BCFW relation. Nevertheless, since we will not deal with NNLO corrections and double unresolved configurations, we will just use their definitions to write the matrix elements in terms of them. The double unresolved antenna at tree level is derived from the colour ordered squared matrix elements of decays of fields into four partons. It is given by:

$$X_{ijkl}^0 = S_{ijkl,IL} \frac{|\mathbf{M}_{ijkl}^0|^2}{|\mathbf{M}_{IL}^0|^2} \quad (2.24)$$

where the notation is understood.

As for one loop antennas, we closely look at the factorization of amplitudes under IR limits and, following a similar idea to the tree level three-partons case, we define:

---

<sup>9</sup>We indicate, here and in the following, colour-ordered matrix elements with bold font, whereas with calligraphic font we denote general non-colour-ordered matrix elements.

<sup>10</sup>0 superscript denotes tree level process.

$$X_{ijk}^1 = S_{ijk,IK} \frac{|\mathbf{M}_{ijk}^1|^2}{|\mathbf{M}_{IK}^0|^2} - X_{ijk}^0 \frac{|\mathbf{M}_{IK}^1|^2}{|\mathbf{M}_{IK}^0|^2} \quad (2.25)$$

where the notation is the same as before and the 1 at superscript denotes one loop process<sup>11</sup>. Under IR limits (see section 1.3), using eq. 2.23 we have that  $X(ijk) \rightarrow \mathcal{R}^0(ijk)$ , and thus the one loop antenna reads:

$$X_{ijk}^1 \xrightarrow{j \text{ unresolved}} S_{ijk,IK} \frac{\mathcal{R}^1(ijk)|\mathbf{M}_{IK}^0|^2 + \mathcal{R}^0(ijk)|\mathbf{M}_{IK}^1|^2}{|\mathbf{M}_{IK}^0|^2} - \mathcal{R}^0(ijk) \frac{|\mathbf{M}_{IK}^1|^2}{|\mathbf{M}_{IK}^0|^2} \quad (2.26)$$

where  $\mathcal{R}^1(ijk)$  is the one loop counterpart of  $\mathcal{R}^0(ijk)$ . Again, the one loop antenna has the desired behaviour under the limits considered.

Although we are not presenting the complete classification of antennas, we would like to give some more details on the general structure of them. Since they are given in terms of kinematical invariants of the momenta of the amplitudes, in general, antennas include more than one singular configuration. This is due to their definition in terms of matrix elements which makes them invariant under certain symmetries, among which there is cyclic permutations of partons. This is somehow a problem for the identification of the partons and in turns allows more kinematic limits to be present with respect to the ones we are aiming to. Invariance under cyclic permutation is, however, unavoidable: gauge symmetry enforces it. Nevertheless, for the numerical implementation in terms of momentum mappings (to be discussed in the next section), a unique identification of hard radiators and unresolved partons is mandatory and the emission is also required to be ordered. Therefore we need to face two problems: (I) unique identification of partons in antennas from ordered emission; (II) decomposition of non-ordered emissions into different terms in the same fashion.

In the first case, it is possible to disentangle different contributions in the antennas such as to separate them into distinct terms, each of which holds a unique identification of hard radiators and unresolved partons<sup>12</sup>. This is typical of antennas made out of gluons in final states; for instance, for a three gluons final state, we have several ways to choose the antenna configuration of radiators and unresolved particles, obtained by cyclic permutations of the triplets: separating these configurations gives three sub-antennas in which partons are uniquely identified and colour ordered.

As for the second issue, non-ordered emission is present only in subleading colour terms (namely contributions proportional to  $-\frac{1}{N}$ ). In this elements, gluons

---

<sup>11</sup>The notation could be misleading, but it is standard: with  $|\mathbf{M}_{ijk}^1|^2$  we denote  $2\text{Re}[\mathbf{M}_{ijk}^0 \mathbf{M}_{ijk}^{1,\dagger}]$ .

<sup>12</sup>The different parts in which antennas are decomposed in this way, are denoted with lowercase font [6]

behave effectively as photons and thus cannot couple, which amounts to miss the collinear limit of them and have ambiguous colour ordering of partons. In order to overcome these problems, partial fractioning is heavily exploited as to uniquely identify the partons involved in the emission. However, this procedure introduces spurious non-physical propagators, namely invariants at denominators which do not correspond to any combination of momenta in the amplitude. This is not a problem for numerical integration, but crucial for analytical one. Although in principle feasible, analytical integration of non-physical propagators is more involved and requires a larger set of master integrals. To avoid this problem we use the ordered sub-antenna functions in the numerical implementation, and ensure that all ordered contributions to a given antenna function are taken together with the same phase space factorization, *but different momentum mappings*. In this way, the ordered contributions to the sub-antennas can be recombined to form the full antenna functions (related to physical matrix elements), which are then integrated analytically in phase space.

The singular behaviour of the antenna can be extracted conveniently with the operators  $\mathbf{I}^{(1)}$  [43], which extracts the IR poles of one-loop amplitudes. In fact, the infrared structure of QCD amplitudes follows a specific pattern and their poles can be extracted in a way such that the cancellations between real radiation and virtual loop is made explicit. For this purpose, following again [6], it is convenient to introduce two operators which separate the pole structure from the finite parts. For instance, the poles of the integrated antenna<sup>13</sup>  $\mathcal{X}$  in the relative antenna phase space will be denoted with

$$\mathcal{Poles}(\mathcal{X})$$

It is important to note that the infrared structure operators  $\mathbf{I}^{(1)}$  used to extract the poles of the matrix elements as in [43], contains also finite contributions. These come from the expansion of  $\mathbf{I}^{(1)}$ , which can contain terms of the type  $(\epsilon \ln(s))^n$  (where  $s$  is the invariant mass of a pair of momenta or the total one of the particles in the antenna) and transcendental constants resulting from the normalisation factors that appear in their definitions<sup>14</sup>. The *remaining* finite parts can be identified with

$$\mathcal{Finite}(\mathcal{X}) = \mathcal{X} - \mathcal{Poles}(\mathcal{X})$$

We notice that, since virtual loops manifest their infrared structure explicitly at the level of unintegrated matrix elements, we can apply the above operators

---

<sup>13</sup>We recall again that calligraphic letters always denote integrated antennas in the respective antenna phase space.

<sup>14</sup>They are defined with running coupling in the  $\overline{\text{MS}}$  scheme, using conventional dimensional regularisation [43]

directly to the one-loop matrix elements.

An important remark is that the  $\mathbf{I}^{(1)}$  operators, in the formulation of [43], are tensors in colour space and contain imaginary parts coming from analytic continuation of loop amplitudes from the Euclidean to the Minkowskian region. Nevertheless, since we are considering only colour ordered matrix elements, the  $\mathbf{I}^{(1)}$  operators turn into scalars in colour space. Further, since in the computations described in Chapter 3 we will define infrared safe observables, when we use these operators to extract real radiation singularities, we can neglect the imaginary contributions. In fact, for three jets observables at NLO, in order to cancel all poles and fulfill the KNL theorem [3], we need to consider the two-loop-times-tree-level and one-loop-times-one-loop two partons amplitudes, too [44]. These matrix elements are only considered to recover the required and necessary cancellations among poles of cross sections, but no finite parts of them compete to the three-jets observables. Once both contributions are taken into account, the imaginary parts of the  $\mathbf{I}^{(1)}$  operators cancel.

The operators depend on the different partons entering the process as well as their kinematic invariants. Following again [6], we denote them as

$$\mathbf{I}_{ij}^1(\epsilon, s_{ij}) \quad \text{and} \quad \mathbf{I}_{ij,F}^1(\epsilon, s_{ij})$$

where  $ij = \{q\bar{q}, qg, g\bar{q}, gg\}$ , and the second operator, with an additional  $F$  subscript, describes the contributions arising from the splitting of a gluon into a quark-antiquark pair, which are proportional to the number of light active flavours  $N_F$ .

The operators are given by:

$$\begin{aligned}
\mathbf{I}_{q\bar{q}}^1(\epsilon, s_{q\bar{q}}) &= -\frac{e^{\epsilon\gamma}}{2\Gamma(1-\epsilon)} \left[ \frac{1}{\epsilon^2} + \frac{3}{2\epsilon} \right] \text{Re}(-s_{q\bar{q}})^{-\epsilon} \\
\mathbf{I}_{qg}^1(\epsilon, s_{qg}) &= -\frac{e^{\epsilon\gamma}}{2\Gamma(1-\epsilon)} \left[ \frac{1}{\epsilon^2} + \frac{5}{3\epsilon} \right] \text{Re}(-s_{qg})^{-\epsilon} \\
\mathbf{I}_{gg}^1(\epsilon, s_{gg}) &= -\frac{e^{\epsilon\gamma}}{2\Gamma(1-\epsilon)} \left[ \frac{1}{\epsilon^2} + \frac{11}{6\epsilon} \right] \text{Re}(-s_{gg})^{-\epsilon} \\
\mathbf{I}_{q\bar{q},F}^1(\epsilon, s_{q\bar{q}}) &= 0 \\
\mathbf{I}_{qg,F}^1(\epsilon, s_{qg}) &= \frac{e^{\epsilon\gamma}}{2\Gamma(1-\epsilon)} \frac{1}{6\epsilon} \text{Re}(-s_{qg})^{-\epsilon} \\
\mathbf{I}_{gg,F}^1(\epsilon, s_{gg}) &= \frac{e^{\epsilon\gamma}}{2\Gamma(1-\epsilon)} \frac{1}{3\epsilon} \text{Re}(-s_{gg})^{-\epsilon}
\end{aligned} \tag{2.27}$$

The antiquark-gluon operator are obtained by charge conjugation:

$$\mathbf{I}_{g\bar{q}}^{(1)}(\epsilon, s_{g\bar{q}}) = \mathbf{I}_{q\bar{q}}^{(1)}(\epsilon, s_{q\bar{q}}) \quad \text{and} \quad \mathbf{I}_{g\bar{q},F}^{(1)}(\epsilon, s_{g\bar{q}}) = \mathbf{I}_{q\bar{q},F}^{(1)}(\epsilon, s_{q\bar{q}})$$

At two loops, several other operators appear, as listed in [6]. In general, the one-loop matrix elements, integrated in the fully inclusive phase space, contain them, since we are formally considering a double unresolved limit. In fact, the contributions are to be cancelled by higher perturbative orders. Nevertheless, in the following Chapter 3, we will integrate the one-loop matrix elements against the  $(m)$ -jets-to- $(m)$ -jets jet function, ensuring all final states are kept hard, and thus IR singularities coming from phase space integration of one-loop matrix elements will not bother us. All other operators, indeed, enters the formalisation of NNLO corrections to  $(m)$ -jets events and, for the purpose of this thesis, aimed at NLO corrections only, we will only need the operators listed above to display the required cancellation of poles in the cross section.

### 2.2.6 Momentum mapping

A crucial property of the antenna subtraction method is the factorization, under IR limits, not only of the matrix elements, but of the phase space as well (see Fig. 2.2, and Fig. 2.1). In fact, we can define a momentum mapping which uniquely identifies two partons, obtained with combinations of the two hard radiators and



the unresolved parton involved in the antenna. This is of fundamental importance for this method, since it allows to carry the analytical integration of the antenna in the factorised phase space and thus recover the pole structure to be canceled with the virtual contribution of the cross section. The momentum mapping is a function that maps [45]:

$$\{p_i, p_j, p_k\} \rightarrow \{\tilde{p}_I, \tilde{p}_K\}$$

where  $i, k$  are the hard radiators in the antenna,  $j$  the unresolved parton and  $I, K$  the new redefined hard momenta.

The momentum mapping needs to fulfill some requirements:

1. momentum conservation:  $\tilde{p}_I + \tilde{p}_L = p_i + p_j + p_k$  ;
2. the new momenta should be on-shell:  $\tilde{p}_I^2 = \tilde{p}_L^2 = 0$  ;
3. the new momenta should reduce to the appropriate original momenta in the exact singular limits;
4. the mapping needs not to introduce spurious singularities;
5. the momenta are to be considered colour ordered.

In the IR limits where parton  $j$  becomes unresolved, the momenta of the partons  $i, j, k$  are mapped to  $\tilde{p}_I = (\tilde{i}j)$  and  $\tilde{p}_K = (j\tilde{k})$  in the following way:

$$\begin{aligned}\tilde{p}_I &= x p_i + r p_j + z p_k \\ \tilde{p}_K &= (1-x)p_i + (1-r)p_j + (1-z)p_k\end{aligned}\tag{2.28}$$

where

$$\left\{ \begin{array}{l} x = \frac{1}{2(s_{ij}+s_{ik})} \left[ (1+\rho)s_{ijk} - 2rs_{jk} \right] \\ z = \frac{1}{2(s_{jk}+s_{ik})} \left[ (1-\rho)s_{ijk} - 2rs_{ij} \right] \\ \rho^2 = 1 + \frac{4r(1-r)s_{ij}s_{jk}}{s_{ijk}s_{ik}} \end{array} \right.$$

This mapping depends on the choice of the parameter  $r$ . It could be taken such that the cases in which momentum  $j$  becomes collinear with momentum  $i$  and the one in which become collinear with momentum  $k$  are treated in a symmetric way. Conveniently, we set it to [46]:

$$r = \frac{s_{jk}}{s_{ij} + s_{jk}}$$

## 2.3 Types of antenna

The available vertices for partons in QCD determines the possible types of antennas, uniquely identified by the hard radiators (see section 2.2.5). Since we want them to be gauge invariant, the processes from which are derived must be attentively chosen. We remind again to [6] for a complete reference and we discuss here the main ideas behind the different processes used to obtain the wanted antennas.

**Quark-antiquark:** Photons couple to quark and antiquark via the QED vertex. The gauge group for QED is  $U(1)$  and gauge bosons are not charged under it. Therefore, Ward-identities hold with off-shell photons too and we can consider one of these to decay into a pair of quark-antiquarks. Through this matrix elements, we can obtain the colour ordered antennas for quark-antiquark hard radiators [12].

**Gluon-gluon:** The only field that couples to a pair of gluons is the gluon itself. However, gluons are charged under  $SU(3)$  and Slavnov-Taylor identities prevent them to be off-shell. Higgs boson, on the other hand, is a colour singlet and couples to a pair of gluons via loops of quarks. In the limit of infinitely massive quarks, these loops give rise to an effective lagrangian in the so called Higgs Effective Theory HEFT. We can then use this lagrangian to derive gluon-gluon antennas [44]. The details of the interaction lagrangian and the Feynman rules were given in the previous sections, since this, in the end, is exactly the decay under study.

**Quark-gluon/antiquark-gluon:** Here we have the same problem as for gluon-gluon antennas. In fact, matching the correct quantum numbers, we need to consider the decay of an off-shell spin-1/2 particle into an on-shell spin-1/2 particle (massless quark) and an on-shell spin-1 particle (gluon). The final state quark is in the triplet (fundamental) representation of  $SU(3)$  and the gluon is in the octet (adjoint) representation. This requires the initial spin-1/2 particle to be in the triplet representation as well. Nevertheless, gauge invariance prevents off-shell colour charged external states.

Luckily, factorisation of amplitudes in QCD happens in colour ordered matrix elements, where the spinorial structure is disentangled from the gauge group dependence. In this formulation, a parton in the adjoint representation is actually seen as a superposition of two partons (with identical momenta) in the fundamental representation. Considering then a final state made out of a spin-1/2 octet

and a spin-1 octet, we can regard these fields as being a quark-antiquark pair and a gluon and therefore obtain the quark-gluon and antiquark-gluon antennas from the same process. In our massless regime<sup>15</sup>, we only need a spin-1/2 colour singlet in the initial state, since, being neutral under SU(3), it can be taken as external off-shell state and let it decay.

In QCD, spin-1/2 fields can only be triplets since SU(3) gauge invariance forces them to transform in the fundamental representation. We can impose a new symmetry on the lagrangian<sup>16</sup>, relating spins of the Standard Model fields to new additional ones, among which there exist what we are looking for: neutralinos<sup>17</sup> (spin-1/2 singlet) and gluinos (spin-1/2 octet). The lagrangian we will use is thus the one of the Minimal Supersymmetric Standard Model [1]. Neutralinos decay into gluinos and gluon is mediated via loops of supersymmetric particles. As for the gluon-gluon antennas, we can integrate out these degrees of freedom, resulting in an effective vertex described by the following interaction term<sup>18</sup>:

$$\mathcal{L}_{int} = i\eta\bar{\psi}_{\tilde{g}}^A\sigma^{\mu\nu}\psi_{\tilde{\chi}}G_{\mu\nu}^A + \text{h.c.} \quad (2.29)$$

which allows to couple the gluino field  $\bar{\psi}_{\tilde{g}}^A$  and the neutralino field  $\psi_{\tilde{\chi}}$  to the gluon stress field tensor  $G_{\mu\nu}^A$  via the vertex  $\eta$  which has inverse mass dimension. Feynman rules are easily derived for this lagrangian [47] and<sup>19</sup>, given our aim to find the infrared structure of QCD amplitudes, we only need to consider QCD corrections to neutralinos decays.

We now briefly check the correct colour structure in the final states. The basic decay of a neutralino into gluon (1) and gluino (2) has a simple colour structure:

$$i\eta\delta^{A_1A_2}\mathbf{M}_{g\tilde{g}}^0(p_1, p_2) \quad (2.30)$$

The colour structure of the final states is, however, hidden in this factor. To make it manifest, we can multiply eq. 2.30 by  $\sqrt{2} T_{a_1a_2}^A$ ; in fact, this term in squared matrix elements will yield:

$$\sqrt{2} T_{a_1a_2}^A \sqrt{2} T_{a_2a_1}^{A'} = \delta^{AA'} \quad (2.31)$$

---

<sup>15</sup>Of course, we recall that, if the quarks had been taken massive, we could have used an on-shell state to decay into the other partons and simply overcome this problem.

<sup>16</sup>This is formally done extending ordinary space-time to the so called superspace, namely considering fields which also depends on fermionic (spinorial) degrees of freedom.

<sup>17</sup>There exist several extension of the Standard Model via supersymmetry. We will consider the minimal possible extension, in which there exist 4-neutralinos (one for each electro-weak gauge boson). The one we will use does not matter.

<sup>18</sup>We recall that standard notation yields  $\sigma^{\mu\nu} = \frac{i}{2}[\gamma^\mu, \gamma^\nu]$ .

<sup>19</sup>A technical remark: besides QCD Feynman rules and the ones for the interaction term above, we will also need the rule for the coupling among gluon-gluino-gluino.

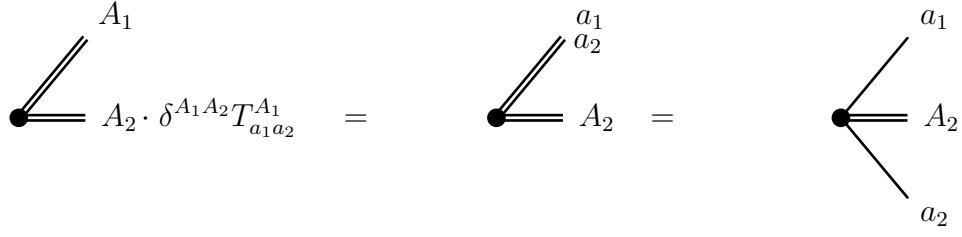


Figure 2.3: Colour structure of the matrix element 2.32 for the decay of a neutralino into gluon and gluino ( $\tilde{\chi} \rightarrow \tilde{g}g$ ). This contains a quark-gluon as well as an antiquark-gluon antenna. The diagram is displayed with 't Hooft notation. Upper case is for adjoint representation indices, lower case for fundamental.

and thus the insertion of it will cause no harm. Therefore, the colour structure of the amplitude turns out be:

$$i\eta\sqrt{2} T_{a_1 a_2}^{A_2} \mathbf{M}_{\tilde{g}g}^0(p_1, p_2) \quad (2.32)$$

From it, we can see that the amplitude actually contains two antennas:

- A quark-gluon antenna: quark with momentum  $p_1$  and colour index  $a_1$ , gluon with momentum  $p_2$  and colour index  $A_2$ .
- An antiquark-gluon antenna: antiquark with momentum  $p_1$  and colour index  $a_2$ , gluon with momentum  $p_2$  and colour index  $A_2$ .

As a technical remark, we point out that we freely identified the gluino with a quark or an antiquark: this is feasible due to its Majorana nature. The colour connection of the antenna is displayed pictorially in Fig. 2.3.

# Chapter 3

## Hadronic Higgs decays to three-jets

### 3.1 Matrix elements up to NLO

We here provide three-jets LO matrix elements for Higgs decays into a bottom-antibottom pair or two gluons as well as NLO three-jets matrix elements for gluon-gluon final state.

The three-jets contribution involves, of course, three partons in the final state at leading order. At next-to-leading order, we will consider one-loop three partons matrix elements as well as tree-level four-partons matrix elements. As a normalisation factor, we will use the leading order Born process, to cancel the couplings coming from the Higgs vertex, so to clear the background and enlight QCD corrections proportional to  $\alpha_s$ .

The Born squared matrix elements, at Higgs mass energy, read:

$$\mathbf{H} \rightarrow \mathbf{gg} : |\mathbf{M}_B(gg)|^2 = \frac{1}{4}\lambda^2(N^2 - 1)M_H^4$$

$$\mathbf{H} \rightarrow \mathbf{b\bar{b}} : |\mathbf{M}_B(b\bar{b})|^2 = 2y_b^2 M_H^2 N$$

where  $M_H$  is the Higgs boson mass,  $\lambda$  the effective coupling of HEFT,  $y_b$  the Yukawa coupling for the bottom mass, and  $N$  the gauge group dimension. Although in QCD  $N = 3$ , in all computations we will leave it as a free parameter.

We will further weight each contribution by the respective branching functions, to separate the contributions of QCD radiation from a pair of gluons final state with respect to a bottom-antibottom pair final state. Regarding the branching functions, taking for instance as final state a pair of gluons, they are computed as:

LO	$H \rightarrow ggg$	tree level
	$H \rightarrow gq\bar{q}$	tree level
NLO	$H \rightarrow ggg$	one loop
	$H \rightarrow gq\bar{q}$	one loop
	$H \rightarrow gggg$	tree level
	$H \rightarrow gq\bar{q}q$	tree level
	$H \rightarrow q\bar{q}q'\bar{q}'$	tree level

Table 3.1: Partonic contributions to three-jets events in perturbative QCD from gluon-gluon final state.

$$\text{Br}(gg) = \frac{\Gamma(gg)}{\Gamma(gg) + \Gamma(b\bar{b})} \quad (3.1)$$

where  $\Gamma$  is the decay rate of the Higgs boson in the final states in parenthesis. These quantities are computed in perturbation theory order by order.

The NLO cross section receives contributions from matrix elements with different final states; we summarize them in Table 3.1. In the following, we will provide the matrix elements in terms of antenna functions. This will simplify the analysis of the limits and the investigation of the subtraction terms, since the limits of all antennas have been closely studied [6]. Further, antennas immediately provide matrix elements weighted by the respective Born process, by definition of them. In order to understand the colour structure and thus obtain the correct symmetry factors in the equations of section 2.2.5, we computed the matrix elements again, working out the algebra with the help of the program FORM [9]. We further ensure our results checking them numerically with the program MadGraph5 [10], which, producing also diagrams of the decays as a check to ours, helped as well in understanding the infrared structure of the final states of the amplitudes.

### 3.1.1 LO

As for the leading order, we compute the decay rate for both QCD radiations of a parton from a pair of gluons and from a bottom-antibottom pair. At leading order, we do not need any subtraction term, since the three-jets functions keep all final states hard.

For the radiation coming from a bottom-antibottom pair we refer to [33].

For the radiation coming from a pair of gluons, we have two different final state configurations:  $H \rightarrow ggg$  and  $H \rightarrow gq\bar{q}$ . Analyzing the colour structure we immediately realize that for the  $(ggg)$  final state, it needs to be  $(N^2 - 1)N^2$ . This is easily derived, as any pure gauge interactions at tree level cannot have subleading  $-\frac{1}{N}$  terms<sup>1</sup>. As for the  $(gq\bar{q})$ , we only have a single colour structure which, summing over the active flavours, brings a factor of  $(N^2 - 1)N_F$ .

To express the LO matrix elements in terms of tree-level antennas, we need to understand the symmetry factors  $S_{ijk}$  present in equation 2.22. The symmetry factors are introduced in the definitions of the antennas, in order to account for multiple singular configurations leading to different antennas in the same matrix element. In fact, we recall antennas are derived from physical matrix elements. For instance, in an antenna obtained by three final state gluons, cyclic symmetry is unavoidable and thus there are more than one way to identify the hard radiators and the unresolved parton undergoing the singular limit. Actually, the degree of symmetry is larger than the one yielded by colour ordered Feynman rules, since the antennas are given by squared matrix elements and the symmetry is attained at the level of momenta invariants in the integration. Hence, the symmetry factors are actually given by just all the possible permutations allowed by the bosonic or fermionic nature of their final states.

*The symmetry factor is found to be equal to all possible identical configurations present in the non-colour-ordered squared matrix elements used to derive the antenna, normalised by the ones in the Born process.*

In the  $(gg)$  final state corrections, the Born matrix element  $H \rightarrow gg$  has a symmetry factor of  $2!$ , since we can swap the two gluons in the final state and we would not recognize any difference while performing the integral. For the same reason, the symmetry factor for the  $H \rightarrow ggg$  amounts to  $3!$ . For convenience, when we will perform the numerical implementation of the problem, we specify we include the symmetrization of the phase space<sup>2</sup> directly in the squared matrix elements. In this way, the numerical program always uses the same phase space to carry out the integration, independently of the process studied, and modifying the code for one's needs is straightforward. Therefore, the antenna will be:

$$X_{ijk}^0(1_g, 2_g, 3_g) = \frac{3!}{2!} \frac{\frac{1}{3!} |\mathbf{M}_3^0(1_g, 2_g, 3_g)|^2}{\frac{1}{2!} |\mathbf{M}_2^0(1_g, 2_g)|^2} \quad (3.2)$$

---

<sup>1</sup>This result is straightforward via exploitation of photon decoupling identity and reflection symmetry of colour ordered amplitudes in spinor-helicity formalism.

<sup>2</sup>To avoid any misunderstanding, we remind the reader that the  $n$  phase space used in cross sections is given by  $\frac{1}{\sum_i (b_i)!} d\Phi_n$ , where  $b_i$  is the number of  $i$  identical bosons present in the amplitude.

In the following, we will use the standard notation introduced in [6] and call the above antenna  $F_3^0(1_g, 2_g, 3_g)$ , where the labelling of gluons matters, since the antennas are colour ordered.

Exploiting the Feynman rules presented in Section 1.2, we notice that this contribution has a single colour structure<sup>3</sup>  $f^{A_1 A_2 A_3}$

$$\mathcal{M}_3^0(g, g, g) = i\lambda g_s f^{A_1 A_2 A_3} \mathbf{M}_3^0(1_g, 2_g, 3_g) \quad (3.3)$$

We recall here again the notation used.  $\mathcal{M}(g, g, g)$  denotes the whole amplitude;  $\mathbf{M}(i_g, j_g, k_g)$  refers to colour-ordered matrix elements, with the ordering specified in the parenthesis and stripped by colour factors and couplings.

Using colour ordered matrix elements, the contribution proportional to  $N^2$  can be written in terms of the antennas as:

$$\begin{aligned} \frac{\frac{1}{3!} |\mathcal{M}_3^0(g, g, g)|^2}{\frac{1}{2!} |\mathcal{M}_2^0(g, g)|^2} &= g_s^2 N \left( \frac{\frac{1}{3!} |\mathbf{M}_3^0(1_g, 2_g, 3_g)|^2}{\frac{1}{2!} |\mathbf{M}_2^0(1_g, 2_g)|^2} + \frac{\frac{1}{3!} |\mathbf{M}_3^0(1_g, 3_g, 2_g)|^2}{\frac{1}{2!} |\mathbf{M}_2^0(1_g, 2_g)|^2} \right) = \\ &= g_s^2 N \frac{1}{3} \left( F_3^0(1_g, 2_g, 3_g) + F_3^0(1_g, 3_g, 2_g) \right) = \\ &= g_s^2 N \frac{1}{3} \sum_{(i,j) \in P(2,3)} F_3^0(1_g, i_g, j_g) \end{aligned} \quad (3.4)$$

The second final state configuration is  $H \rightarrow gq\bar{q}$ . It has a single colour structure  $T_{a_2 a_3}^{A_1}$  and thus one colour ordering:

$$\mathcal{M}_3^0(g, q, \bar{q}) = i\lambda g_s T_{a_2 a_3}^{A_1} \mathbf{M}_3^0(1_g, 2_q, 3_{\bar{q}}) \quad (3.5)$$

The symmetry factor for its related antenna comes only from the Born normalisation matrix element, since the final state given by  $gq\bar{q}$  has no symmetry in swapping the particles. In terms of the antennas, summing over all active light flavours, still relating to the notation of [6], it can be written as:

$$\begin{aligned} \frac{|\mathcal{M}_3^0(g, q, \bar{q})|^2}{\frac{1}{2!} |\mathcal{M}_2^0(g, g)|^2} &= g_s^2 N_F \frac{|\mathbf{M}_3^0(1_g, 2_q, 3_{\bar{q}})|^2}{\frac{1}{2!} |\mathbf{M}_2^0(1_g, 2_g)|^2} = \\ &= g_s^2 N_F \frac{1}{2} G_3^0(1_g, 2_q, 3_{\bar{q}}) \end{aligned}$$

---

<sup>3</sup>Here, instead of using increasing letters to label adjoint indices as  $f^{ABC}$ , we prefer to use numbers as  $f^{A_1 A_2 A_3}$ . We make sure there are no misunderstandings with the notation in the following.



Therefore, the squared matrix element for three-jets coming from gluon-gluon final state at LO reads:

$$\begin{aligned}
d\sigma_{LO}^R &= \frac{|\mathcal{M}_{LO}|^2}{|\mathcal{M}_B|^2} d\Phi_3(p_1, p_2, p_3; q) J_3^{(3)}(p_1, p_2, p_3) = \\
&= g_s^2 \left[ \frac{1}{3} \sum_{(i,j) \in P(2,3)} N F_3^0(1_g, i_g, j_g) + 2 N_F G_3^0(1_g, 2_q, 3_{\bar{q}}) \right] \\
&\quad \times d\Phi_3(p_1, p_2, p_3; q) J_3^{(3)}(p_1, p_2, p_3) \tag{3.6}
\end{aligned}$$

### 3.1.2 NLO

We consider now the next correction to the gluon-gluon final state. At NLO, we need to include both the tree-level four parton real radiation final states, as well the one loop three-parton contributions.

#### Real 4-partons

There are four possible final state configurations, namely  $(g, g, g, g)$ ,  $(g, q, \bar{q}, g)$ ,  $(q, \bar{q}, q', \bar{q}')$ ,  $(q, \bar{q}, q, \bar{q})$ , where with primes we denote different flavour contributions. The latter matrix element for the same flavour quarks final state, is actually found to be of minor importance and neglected in the computations. Further, it does not contain any single unresolved singular configuration in phase space.

Since we will introduce a subtraction term for each color contribution, for the sake of clarity we divide their treatment into separate subsections.

#### $N^2$

This colour contribution comes from the final state in which only gluons appear. As for the three gluons final state, for exactly the same reasons, we expect that these colour matrix elements has only  $N^2(N^2 - 1)$  as colour factor. The non-cyclic permutations are six, and, as for any pure gauge amplitudes in QCD, given by fixing one of the gluons and considering all possible permutations of the others:

$$\mathcal{M}_4^0(g, g, g, g) = i\lambda g_s^2 \sum_{(i,j,k) \in P(2,3,4)} \text{Tr}(T^{A_1} T^{A_i} T^{A_j} T^{A_k}) \mathbf{M}_3^0(1_g, i_g, j_g, k_g) \tag{3.7}$$

The symmetry factor for this matrix element is  $4!$  since, at the level of the integration in phase space, we can permute the gluons without producing any

change. Minding the factor  $2!$  at denominator coming from the Born amplitude, the overall symmetry factor turns into 12. Therefore, in terms of the antennas, we can write the normalised matrix element as:

$$\begin{aligned} \frac{\frac{1}{4!} |\mathcal{M}_4^0(g, g, g, g)|^2}{\frac{1}{2!} |\mathcal{M}_2^0(g, g)|^2} &= g_s^4 N^2 \frac{1}{\frac{1}{2!} |\mathbf{M}_2^0(1_g, 2_g)|^2} \frac{1}{4!} \sum_{(i,j,k) \in P(2,3,4)} |\mathbf{M}_4^0(1_g, i_g, j_g, k_g)|^2 = \\ &= g_s^4 N^2 \frac{1}{12} \sum_{(i,j,k) \in P(2,3,4)} F_4^0(1_g, i_g, j_g, k_g) \end{aligned} \quad (3.8)$$

### $\mathbf{NN_F}$

The final state considered here is composed by two gluons and a pair of quark-antiquark. There are two colour structures, arising from interchanging the gluons (or the quark with the antiquark):

$$\mathcal{M}_4^0(g, g, q, \bar{q}) = i\lambda g_s^2 \sum_{(i,j) \in P(1,2)} (T^{A_i} T^{A_j})_{a_1 a_2} \mathbf{M}_4^0(i_g, 3_q, 4_{\bar{q}}, j_g) \quad (3.9)$$

The colour factor here splits into a leading term proportional to  $N(N^2 - 1)$  and a subleading term proportional to  $-\frac{1}{N}(N^2 - 1)$ . In both cases, the symmetry factor comes from swapping the two gluons and thus, being  $2!$ , cancels with the one of the Born matrix element. Therefore there is no symmetry factor for this antenna. Summing over quark flavours, we also gain a  $N_F$  factor. The leading colour term for this final states then reads:

$$\begin{aligned} \frac{\frac{1}{2!} |\mathcal{M}_{4,\text{lead}}^0(g, g, q, \bar{q})|^2}{\frac{1}{2!} |\mathcal{M}_2^0(g, g)|^2} &= g_s^4 N_F N \frac{1}{\frac{1}{2!} |\mathbf{M}_2^0(1_g, 2_g)|^2} \frac{1}{2!} \sum_{(i,j) \in P(1,2)} |\mathbf{M}_4^0(i_g, 3_q, 4_{\bar{q}}, j_g)|^2 = \\ &= g_s^4 N_F N \sum_{(i,j) \in P(1,2)} G_4^0(i_g, 3_q, 4_{\bar{q}}, j_g) \end{aligned} \quad (3.10)$$

### $-\mathbf{N_F/N}$

The final state is the same as above. In the subleading colour term, the gluons behave as photons, namely they do not interact between each other and thus there is no collinear limit for two of them. The symmetry factor is again the same as the previous contribution and this element in terms of the antennas can be written as:

$$\begin{aligned}
\frac{\frac{1}{2!} |\mathcal{M}_{3,\text{sub-lead}}^0(q, \bar{q}, g, g)|^2}{\frac{1}{2!} |\mathcal{M}_2^0(g, g)|^2} &= g_s^4 \left( -\frac{N_F}{N} \right) \frac{1}{\frac{1}{2!} |\mathbf{M}_2^0(1_g, 2_g)|^2} \frac{1}{2!} \left| \sum_{(i,j) \in P(1,2)} \mathbf{M}_4^0(i_g, 3_q, 4_{\bar{q}}, j_g) \right|^2 = \\
&= g_s^4 \left( -\frac{N_F}{N} \right) \tilde{G}_4^0(1_g, 3_q, 4_{\bar{q}}, 2_g) \tag{3.11}
\end{aligned}$$

where in the standard antennas notation, the subleading terms are denoted by a tilde.

## $\mathbf{N_F^2}$

The final states here are two pairs of quark-antiquark. There is only one colour structure but two different flavour structures in the case of identical quark flavours, namely:

$$\mathcal{M}_4^0(q, \bar{q}, q', \bar{q}') = i\lambda g_s^2 \left[ T_{a_1 a_2}^{A_1} T_{a_3 a_4}^{A_1} \mathbf{M}_4^0(1_q, 2_{\bar{q}}, 3_{q'}, 4_{\bar{q}'} ) - \delta_{qq'} T_{a_1 a_4}^{A_1} T_{a_3 a_2}^{A_1} \mathbf{M}_4^0(1_q, 4_{\bar{q}}, 3_{q'}, 2_{\bar{q}'} ) \right] \tag{3.12}$$

When they are of different flavours, the colour factor amounts to  $(N^2 - 1)$ . The symmetry factor here is  $2!$ , since we can swap the pair of quarks among each other, being of the same flavour. This, as above, cancels with the one coming from the Born matrix element normalisation. In terms of the antennas, summing over quark flavours, this contribution reads:

$$\begin{aligned}
\frac{\frac{1}{2!} |\mathcal{M}_4^0(q, \bar{q}, q', \bar{q}')|^2}{\frac{1}{2!} |\mathcal{M}_2^0(g, g)|^2} &= g_s^4 N_F^2 \frac{\frac{1}{2!} |\mathbf{M}_4^0(1_q, 2_{\bar{q}}, 3_{q'}, 4_{\bar{q}'} )|^2}{\frac{1}{2!} |\mathbf{M}_2^0(1_g, 2_g)|^2} = \\
&= g_s^4 N_F^2 H_4^0(1_q, 2_{\bar{q}}, 3_{q'}, 4_{\bar{q}'} ) \tag{3.13}
\end{aligned}$$

All together, the contributions to the tree-level four-real partons final states can be written as:

$$\begin{aligned}
d\sigma_{NLO}^R &= \frac{|\mathcal{M}_{NLO}^R|^2}{|\mathcal{M}_B|^2} d\Phi_4(p_1, \dots, p_4; q) J_3^{(4)}(p_1, \dots, p_4) = \\
&= g_s^4 \left\{ \frac{1}{12} N^2 \sum_{(i,j,k) \in P(2,3,4)} F_4^0(1_g, i_g, j_g, k_g) + \right. \\
&\quad N_F \left[ N \sum_{(i,j) \in P(1,2)} G_4^0(i_g, 3_q, 4_{\bar{q}}, j_g) - \frac{1}{N} \tilde{G}_4^0(1_g, 3_q, 4_{\bar{q}}, 2_g) \right] + \\
&\quad \left. N_F^2 H_4^0(1_q, 2_{\bar{q}}, 3_{q'}, 4_{\bar{q}'} \right\} \\
&\times d\Phi_4(p_1, \dots, p_4; q) J_3^{(4)}(p_1, \dots, p_4)
\end{aligned} \tag{3.14}$$

where, as discussed above, we have explicitly neglected the  $-N_F/N$  contribution accounting for different flavours of quark-antiquark pairs in the final state. We again notice that the four-partons real matrix elements are integrated in the four-particles phase space against the jet function  $J_3^{(4)}$  which recombine four partons into three.

### Virtual 3-partons

The virtual contributions are given by the interference between one-loop and tree-level amplitudes with three partons as final states. These are the same as the ones of the tree-level three partons final state case. Hence, the symmetry factors are the same. Regarding the colour structures, there are several. They have been computed with the algebraic program FORM and they amount to the ones present in the four partons real final states, as expected, due to the foreseen cancellation of real radiation poles with virtual loop integrals.

To reproduce virtual matrix elements in terms of antennas, we need to compute also the one-loop matrix elements for two partons final states, since the antennas capture only the one-loop splitting functions and one-loop soft current, and to retrieve the one-loop matrix elements we need to recover the (one-loop-two-partons)  $\times$  (tree-level-two-partons) as can be seen in eq. 2.25. We further notice that, since antennas are defined to resemble the limiting behaviour of amplitudes and one-loop virtual matrix elements are integrated against a three-jets-to-three-jets functions (thus keeping all final states hard), while writing one-loop matrix elements in terms of one-loop antennas, the contribution given by the one-loop two partons process in 2.25 is integrated in the two-particles phase space. In fact,

as discussed before, the phase space strictly factorises and can be treated independently. Referring to the standard notation of [6], we find two structures: one proportional to  $N(N^2 - 1)$ , namely  $\mathcal{F}_2^1$ ; one flavour dependent<sup>4</sup> proportional to  $N_F(N^2 - 1)$ , namely  $\hat{\mathcal{F}}_2^1$ . Notice that the calligraphic notation denotes the fact that these are integrated two-partons antennas.

To summarize: the contributions coming from (one-loop-two-partons)  $\times$  (tree-level-two-partons) matrix elements are removed in the one-loop antennas and thus added back to write the one-loop virtual matrix elements in terms of antennas.

## $N^2$

These contributions come from one-loop amplitudes with three gluons as final states. These compete to two colour factors and here we examine the term proportional to  $N^2$ . The symmetry factor is the same as the tree-level matrix elements, having the same final states. The colour structure proportional to  $N^2$  is given by fixing the first gluon and considering all possible permutations of the other two. Thus, as the tree-level counterpart, there are two different colour ordered matrix elements. Using the structure of equation 2.25, we can write the one-loop contribution proportional to  $N^2$  as:

$$\frac{\frac{1}{3!}|\mathcal{M}_3^1(g, g, g)|^2}{\frac{1}{2!}|\mathcal{M}_2^0(g, g)|^2} = g_s^2 \frac{\alpha_s}{2\pi} N^2 \frac{1}{3} \sum_{(i,j) \in P(2,3)} \left[ F_3^1(1_g, i_g, j_g) + F_3^0(1_g, i_g, j_g) \mathcal{F}_2^1(s_{123}) \right] \quad (3.15)$$

We notice that, as mentioned at the end of Section 2.2.3, we wrote the couplings in the above way to match our results with the overall constant of the antenna phase space.

## $NN_F$

These contributions come from two different final state configurations, viz. three gluons or a gluon and a quark-antiquark pair. Again, the final state being equal, the symmetry factor are the same as the tree-level counterparts. Regarding the colour ordering, as for the tree-level counterparts, the only gluons final state has two distinct configurations contributing to the same colour factor. These matrix elements can then be written in terms of antennas as:

---

<sup>4</sup>As one could guess, in the standard notation the flavour dependent antennas are denoted with a hat.

$$\frac{\frac{1}{3!}|\mathcal{M}_3^1(g, g, g)|^2}{\frac{1}{2!}|\mathcal{M}_2^0(g, g)|^2} = g_s^2 \frac{\alpha_s}{2\pi} N N_F \textcolor{red}{3} \sum_{(i,j) \in P(2,3)} \left[ \hat{F}_3^1(1_g, i_g, j_g) + F_3^0(1_g, i_g, j_g) \hat{\mathcal{F}}_2^1(s_{123}) \right] \quad (3.16)$$

As for the gluon-quark-antiquark final state, we have two different colour factors, referred as leading and subleading. The leading one has the same colour structure as the three gluons final state above and it reads:

$$\frac{|\mathcal{M}_{3,\text{lead}}^1(g, q, \bar{q})|^2}{\frac{1}{2!}|\mathcal{M}_2^0(g, g)|^2} = g_s^2 \frac{\alpha_s}{2\pi} N N_F \textcolor{red}{2} \left[ G_3^1(1_g, 2_q, 3_{\bar{q}}) + G_3^0(1_g, 2_q, 3_{\bar{q}}) \mathcal{F}_2^1(s_{123}) \right] \quad (3.17)$$

$-\mathbf{1}/\mathbf{N}$

This contribution could come only from the gluon-quark-antiquark pair final states. Again, the symmetry factor is the same as in the tree-level case. Here, as every subleading colour contribution, the gluons (including the internal ones) are treated as photon-like. Since there is no one-loop two-partons contribution proportional to this colour factor, the antenna does not need to add it back. This is due to the factorisation undergone by this one-loop matrix element. Therefore, in terms of the antennas, it reads:

$$\frac{|\mathcal{M}_{3,\text{sub-lead}}^1(g, q, \bar{q})|^2}{\frac{1}{2!}|\mathcal{M}_2^0(g, g)|^2} = g_s^2 \frac{\alpha_s}{2\pi} \left(-\frac{1}{N}\right) \textcolor{red}{2} \tilde{G}_3^1(1_g, 2_q, 3_{\bar{q}}) \quad (3.18)$$

$\mathbf{N_F^2}$

This contribution arises from the quark dependent part of the gluon-quark-antiquark final state. Again, the symmetry factor is the same as the tree-level counterpart. In terms of the antennas, it can be written as:

$$\frac{|\mathcal{M}_{3,\text{flav}}^1(g, q, \bar{q})|^2}{\frac{1}{2!}|\mathcal{M}_2^0(g, g)|^2} = g_s^2 \frac{\alpha_s}{2\pi} N_F^2 \textcolor{red}{2} \left[ \hat{G}_3^1(1_g, 2_q, 3_{\bar{q}}) + G_3^0(1_g, 2_q, 3_{\bar{q}}) \hat{\mathcal{F}}_2^1(s_{123}) \right] \quad (3.19)$$

All together, the contributions to the one-loop three-partons final states read:

$$\begin{aligned}
d\sigma_{NLO}^V &= \frac{|\mathcal{M}_{NLO}^V|^2}{|\mathcal{M}_B|^2} d\Phi_3(p_1, \dots, p_3; q) J_3^{(3)}(p_1, \dots, p_3) = \\
&= g_s^2 \frac{\alpha_s}{2\pi} \left\{ N \left[ \frac{1}{3} N \sum_{(i,j) \in P(2,3)} (F_3^1(1_g, i_g, j_g) + F_3^0(1_g, i_g, j_g) \mathcal{F}_2^1(s_{123})) + \right. \right. \\
&\quad \left. \frac{1}{3} N_F \sum_{(i,j) \in P(2,3)} (\hat{F}_3^1(1_g, i_g, j_g) + F_3^0(1_g, i_g, j_g) \hat{\mathcal{F}}_2^1(s_{123})) \right] + \\
&\quad N_F \left[ 2N(G_3^1(1_g, 2_q, 3_{\bar{q}}) + G_3^0(1_g, 2_q, 3_{\bar{q}}) \mathcal{F}_2^1(s_{123})) + \right. \\
&\quad \left. 2\left(-\frac{1}{N}\right) \tilde{G}_3^1(1_g, 2_q, 3_{\bar{q}}) + \right. \\
&\quad \left. \left. 2N_F(\hat{G}_3^1(1_g, 2_q, 3_{\bar{q}}) + G_3^0(1_g, 2_q, 3_{\bar{q}}) \hat{\mathcal{F}}_2^1(s_{123})) \right] \right\} \\
&\quad \times d\Phi_3(p_1, \dots, p_3; q) J_3^{(3)}(p_1, \dots, p_3) \tag{3.20}
\end{aligned}$$

Again, we notice that the three-partons one-loop matrix elements are integrated in the three-particles phase space against the  $J_3^{(3)}$  jet function which enforces all final state partons to be hard.

All matrix elements obtained in the above has been checked with the ones computed in [44]. In particular, for each colour factor, every symmetry factor reproduces the correct poles structure once we integrate the matrix elements in the respective antenna phase space.

## 3.2 Subtraction terms at NLO

In order to find the subtraction terms, we first need to have a look at the IR limits of the real four-partons matrix elements. To compute them, we refer to [6]. What we need to do is take the four-partons real matrix elements and consider all possible singular configurations of their final states. In this section, we will only carefully derive the subtraction terms for the  $NN_F$  contribution, since it is the

most involved, being formed by both gluons and quark-antiquark pairs in the final states.

The antenna which describes this leading colour contribution is  $G_4^0(1_g, 3_q, 4_{\bar{q}}, 2_g)$ . The possible singular unresolved IR limits are soft limit of both gluons, quark-gluon collinear limits, quark-antiquark collinear limit, and, since the gluons are truly coupling<sup>5</sup>, gluon-gluon collinear limit. In this configurations, the antenna approaches the following expressions:

1. Soft limits:

$$\begin{aligned} G_4^0(1_g, 3_q, 4_{\bar{q}}, 2_g) &\xrightarrow{1_g \rightarrow 0} \mathcal{S}_{213} G_3^0(2_g, 3_q, 4_{\bar{q}}) \\ G_4^0(1_g, 3_q, 4_{\bar{q}}, 2_g) &\xrightarrow{2_g \rightarrow 0} \mathcal{S}_{124} G_3^0(1_g, 3_q, 4_{\bar{q}}) \end{aligned} \quad (3.21)$$

2. Collinear limits:

$$\begin{aligned} G_4^0(1_g, 3_q, 4_{\bar{q}}, 2_g) &\xrightarrow{1_g || 2_g} \frac{1}{s_{12}} P_{gg \rightarrow G}(z) G_3^0((\tilde{1}2)_g, 3_q, 4_{\bar{q}}) + \text{ang.} \\ G_4^0(1_g, 3_q, 4_{\bar{q}}, 2_g) &\xrightarrow{3_q || 4_{\bar{q}}} \frac{1}{s_{34}} P_{q\bar{q} \rightarrow G}(z) F_3^0(1_g, (\tilde{3}4)_g, 2_g) + \text{ang.} \\ G_4^0(1_g, 3_q, 4_{\bar{q}}, 2_g) &\xrightarrow{1_g || 3_q} \frac{1}{s_{13}} P_{qg \rightarrow Q}(z) G_3^0(2_g, (\tilde{1}3)_q, 4_{\bar{q}}) + \text{ang.} \\ G_4^0(1_g, 3_q, 4_{\bar{q}}, 2_g) &\xrightarrow{4_{\bar{q}} || 2_g} \frac{1}{s_{24}} P_{qg \rightarrow Q}(z) G_3^0(1_g, 3_q, (\tilde{2}4)_{\bar{q}}) + \text{ang.} \end{aligned} \quad (3.22)$$

where the notation follows section 1.3. We notice here that the collinear limits of antenna functions contain additional terms denoted with *ang.*, whereas soft limits do not. This is due to the spin dependence (helicity) of the collinear splitting functions appearing in the factorization of amplitudes (see eq. 1.16). This dependence forbids a plain factorization of the squared matrix elements and the interference generated is reflected in the so called angular terms [48]. However, this terms cause no harm, since they analytically integrate to zero in the antenna phase space. In principle we could ignore them, being that they can be neglected in the analytic cancellation of poles; nevertheless, aiming to subtraction terms which are local to speed up the numerical evaluation, we require an algorithm to cancel them. This is needed only at NNLO when four-partons antenna functions are used to resemble five-partons matrix elements IR limits. For our purposes, we can thus ignore them and remind the interested reader to Appendix A 3.4.

---

<sup>5</sup>Recall that in the subleading contribution  $\tilde{G}_4^0(1_g, 3_q, 4_{\bar{q}}, 2_g)$ , gluons behave like photons.



To find the subtraction terms we can proceed in two ways: either consider final states in Feynman diagrams and build antenna function from the possible configurations, or examine the limits of three-partons antenna functions and pick the ones who match the limits of the matrix elements above. We followed the first line of thoughts, since it appears more intuitive to us, and then check that our subtraction terms have the expected singular limits.

We first draw the colour ordered Feynman diagrams for the amplitudes contributing to the squared matrix element<sup>6</sup>  $G_4^0(1_g, 3_q, 4_{\bar{q}}, 2_g)$ :

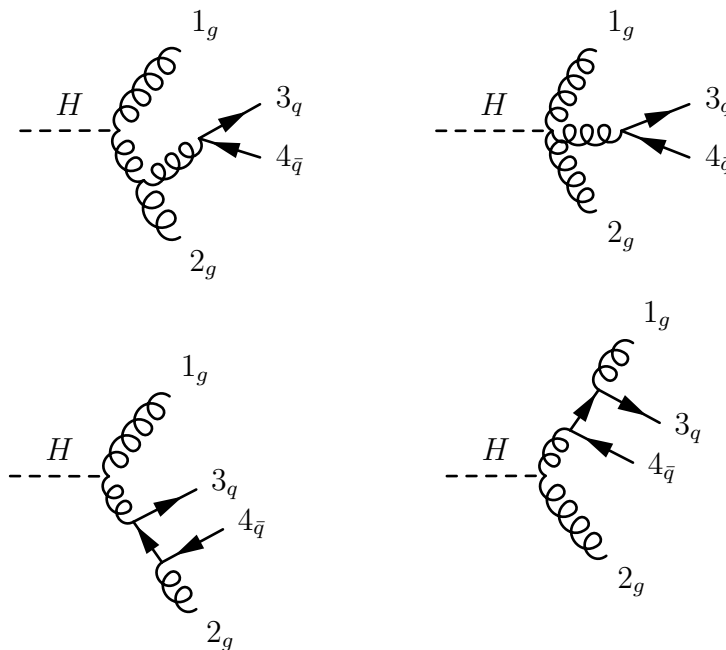


Figure 3.1: Diagrams for amplitudes in antenna  $G_4^0(1_g, 3_q, 4_{\bar{q}}, 2_g)$ .

The diagrams clearly depict the possible infrared limits. In the first one, we have the collinear limit for quark-antiquark; in the second one, we see the additional gluon-gluon collinear limit; in the last two diagrams, there are the collinear limit for quark and antiquark with gluons as well as the soft limit for both gluons. The possible antennas are given by selecting three colour ordered partons, identifying the two hard radiators and the emitter.

<sup>6</sup>The contribution proportional to the colour factor  $NN_F$ , actually includes also a different colour ordering, namely  $G_4^0(2_g, 3_q, 4_{\bar{q}}, 1_g)$ . The analysis for this term is exactly the same up to relabelling of gluons  $1 \leftrightarrow 2$ .

Starting from gluon 1 and proceeding clockwise<sup>7</sup>, the first configuration gives gluon 1 and antiquark 4 as hard radiators and quark 3 as emitter (Fig. 3.2). The possible singular limits are the collinear quark-gluon and the collinear quark-antiquark. There is no antenna which undergoes both limits, since it would require one of the radiators to change type of parton. We thus retain the collinear quark-antiquark limit and leave the remaining limit to another antenna. This because there exist antennas which have only quark-antiquark collinear limit but none which has only quark-gluon collinear limit, due to the fact that gluon can be soft but a quark soft limit would violate conservation of helicity. Thinking about the matrix elements or just looking at the limits of the antennas in [6], the ones to use are  $G_3^0(g, q, \bar{q})$  or  $E_3^0(q, q', \bar{q}')$ . We further notice that the collinear limit is also present in the configuration with quark 3 and gluon 2 as hard radiators and antiquark 4 as emitter (Fig. 3.3). This configuration has exactly the same limits up to relabelling of gluons  $1 \leftrightarrow 2$  and reordering of the partons. Therefore, for the sake of the stability of the numerical implementation, we split in half the quark-antiquark collinear limit between this two antennas. Hence, we have the following subtraction terms for these configurations:

$$\frac{1}{2}E_3^0(1_{q'}, 3_q, 4_{\bar{q}})F_3^0((\tilde{1}\tilde{3})_g, (\tilde{3}\tilde{4})_g, 2_g) + \frac{1}{2}E_3^0(2_{q'}, 3_q, 4_{\bar{q}})F_3^0(1_g, (\tilde{3}\tilde{4})_g, (\tilde{4}\tilde{2})_g) \quad (3.23)$$

The quark-antiquark merges into a gluon and the remaining three hard partons in the matrix elements are only gluons. The factorised matrix elements are in fact given by  $F_3^0(g, g, g)$  antennas. The notation for the mapping of the momentum from four-partons to three-partons follows section 2.2.6. The subtraction terms have been tested with both  $G_3^0(g, q, \bar{q})$  and  $E_3^0(q, q', \bar{q}')$ , reproducing the same results within the statistical errors<sup>8</sup>.

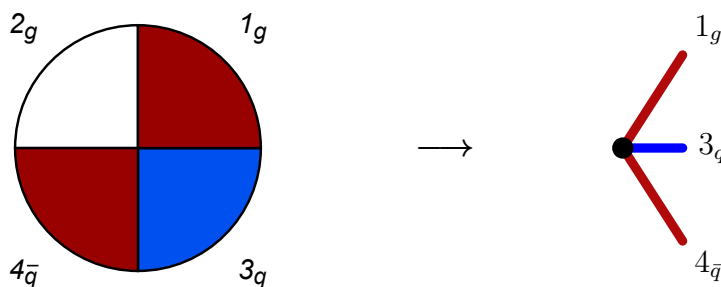


Figure 3.2: Colour connection in  $G_3^0(1_g, 3_q, 4_{\bar{q}})$  or  $E_3^0(1_q, 3_q, 4_{\bar{q}})$  antenna.

<sup>7</sup>Our analysis yields the same conclusions under cyclic permutations.

<sup>8</sup>Both for the NLO perturbative coefficient and the NLO correction to the cross section. See section 3.4 for details.

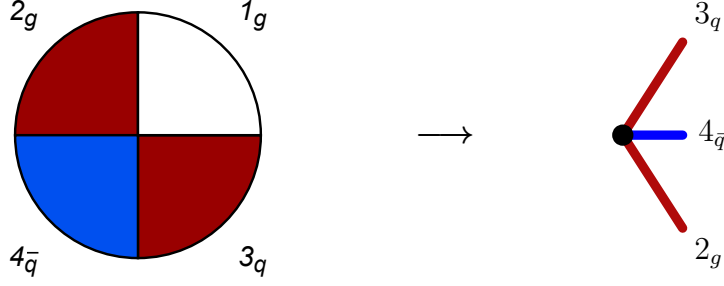


Figure 3.3: Colour connection in  $G_3^0(2_g, 3_q, 4_{\bar{q}})$  or  $E_3^0(2_q, 3_q, 4_{\bar{q}})$  antenna.

We proceed the analysis considering the next configuration, namely the one given by antiquark 4 and gluon 1 as hard radiators and gluon 2 as emitter (Fig. 3.4). The singular configurations are soft limit for gluon 2, collinear limit for gluon 2 with antiquark 4 and collinear limit for the gluons. The antenna which has all the limits listed is the quark-gluon one  $D_3^0(q, g, g)$ . However, this antenna has additional singular configurations with respect to the desired ones. In fact, due to its construction (see section 2.3), it contains two antennas and we need to disentangle them. In principle, this is not a problem for the cancellations of the real poles with the ones in the subtraction term, since the additional limits of the antenna  $D_3^0(q, g, g)$  are recovered in the last singular configuration to be considered, namely the one in which gluon 2 and quark 3 are hard radiators and gluon 1 acts as emitter (Fig. 3.5). Nevertheless, as discussed in section 2.2.5, in order to obtain the factorization of the phase space in the singular regions, we need to uniquely identify the radiators and the emitter and thus to disentangle the two antennas present in  $D_3^0(q, g, g)$ . This is possible, as reported in [6]. In the disentangled antenna  $d_3^0(q, g, g)$ , one of the gluon is meant to be hard so that the unwanted singular configurations present in  $D_3^0(q, g, g)$  are shielded. The  $d_3^0(q, g, g)$  has exactly the limits we are looking for. The subtraction term then reads:

$$d_3^0(4_{\bar{q}}, 2_g, 1_g) G_3^0((\tilde{1}2)_g, 3_q, (\tilde{2}4)_{\bar{q}}) \quad (3.24)$$

The gluon 2 collapses onto the hard radiators which persist as a quark and a gluon. The reduced matrix element is in fact a  $G_3^0(g, q, \bar{q})$  antenna.

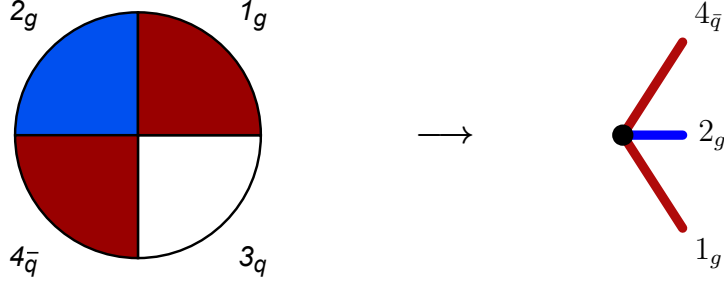


Figure 3.4: Colour connection in  $d_3^0(4_{\bar{q}}, 2_g, 1_g)$  antenna.

The next configuration is very similar to the one presented above (Fig. 3.5). We have quark 3 and gluon 2 as radiators and gluon 1 as emitter. With it, we would like to precise a subtlety. The collinear limit of the gluons in the  $d_3^0(q, g, g)$  antennas, actually do not match the splitting function for a gluon-gluon collinear singularity and thus, in this limit, the subtraction term in eq. 3.24 does not exactly cancel the poles of the respective real contributions. This is the drawback of separating the two sub-antennas in  $D_3^0(q, g, g)$ . Nevertheless, in the configuration we are considering now, the subtraction term is given again by a  $d_3^0(q, g, g)$  antenna, and the gluons undergoing the collinear limit are the same as before. Therefore, summing the two subtraction terms, we recover the correct gluon-gluon splitting function in the collinear limit. Again referring to [6], we correctly have:

$$d_3^0(4_{\bar{q}}, 2_g, 1_g) + d_3^0(3_q, 1_g, 2_g) \xrightarrow{1_g \parallel 2_g} P_{gg \rightarrow G}(z) \quad (3.25)$$

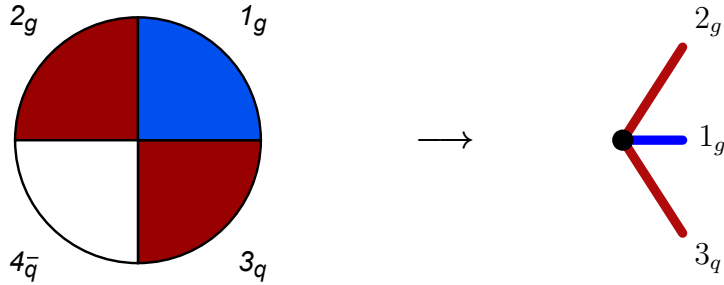


Figure 3.5: Colour connection in  $d_3^0(3_q, 1_g, 2_g)$  antenna.

In the end, the subtraction term for the full<sup>9</sup>  $NN_F$  colour factor reads:

---

<sup>9</sup>In this section we built step by step the subtraction term for the  $G_4^0(1_g, 3_q, 4_{\bar{q}}, 2_g)$  matrix ele-

**Matrix element:**

$$\sum_{(i,j) \in P(1,2)} G_4^0(i_g, 3_q, 4_{\bar{q}}, j_g) \quad (3.26)$$

**Subtraction term:**

$$\begin{aligned} & \sum_{(i,j) \in P(1,2)} \left[ d_3^0(4_{\bar{q}}, j_g, i_g) G_3^0((\tilde{i}j)_g, 3_q, (\tilde{j}4)_{\bar{q}}) + d_3^0(3_q, i_g, j_g) G_3^0((\tilde{j}i)_g, (\tilde{i}3)_q, 4_{\bar{q}}) \right] + \\ & \sum_{(i,j) \in P(1,2)} \left[ \frac{1}{2} E_3^0(i_{q'}, 3_q, 4_{\bar{q}}) F_3^0((\tilde{i}3)_g, (\tilde{3}4)_g, j_g) + \right. \\ & \left. \frac{1}{2} E_3^0(j_{q'}, 3_q, 4_{\bar{q}}) F_3^0(i_g, (\tilde{3}4)_g, (\tilde{4}j)_g) \right] \quad (3.27) \end{aligned}$$

A similar analysis allows to build the subtraction terms for the remaining matrix elements. The subtraction terms for the contributions to the real four-partons matrix elements 3.14, is found to be:

---

ment. The contribution proportional to  $NN_F$  includes also the ordering in which we interchange gluons  $1 \leftrightarrow 2$ , i.e.  $G_4^0(2_g, 3_q, 4_{\bar{q}}, 1_g)$ .

$$\begin{aligned}
d\sigma_{NLO}^S &= \frac{|\mathcal{M}_{NLO}^S|^2}{|\mathcal{M}_B|^2} d\Phi_4(p_1, \dots, p_4; q) J_3^{(4)}(p_1, \dots, p_4) = \\
&= g_s^4 \left\{ \frac{1}{12} N^2 \sum_{(i,j,k) \in P(2,3,4)} \left[ f_3^0(k_g, 1_g, i_g) F_3^0((\tilde{k}1)_g, (\tilde{1}i)_g, j_g) \times J_3^{(3)}((\tilde{k}1)_g, (\tilde{1}i)_g, j_g) \right. \right. \\
&\quad f_3^0(1_g, i_g, j_g) F_3^0((\tilde{1}i)_g, (\tilde{i}j)_g, k_g) \times J_3^{(3)}((\tilde{1}i)_g, (\tilde{i}j)_g, k_g) \quad + \\
&\quad f_3^0(i_g, j_g, k_g) F_3^0((\tilde{i}j)_g, (\tilde{j}k)_g, 1_g) \times J_3^{(3)}((\tilde{i}j)_g, (\tilde{j}k)_g, 1_g) \quad + \\
&\quad \left. \left. f_3^0(j_g, k_g, 1_g) F_3^0((\tilde{j}k)_g, (\tilde{k}1)_g, i_g) \times J_3^{(3)}((\tilde{j}k)_g, (\tilde{k}1)_g, i_g) \right] \right. + \\
&\quad N_F \left[ N \sum_{(i,j) \in P(1,2)} \left( d_3^0(4_{\bar{q}}, j_g, i_g) G_3^0((\tilde{i}j)_g, 3_q, (\tilde{j}4)_{\bar{q}}) \times J_3^{(3)}((\tilde{i}j)_g, 3_q, (\tilde{j}4)_{\bar{q}}) \right. \right. \\
&\quad \left. \left. d_3^0(3_q, i_g, j_g) G_3^0((\tilde{j}i)_g, (\tilde{i}3)_q, 4_{\bar{q}}) \times J_3^{(3)}((\tilde{j}i)_g, (\tilde{i}3)_q, 4_{\bar{q}}) \right. \right. \\
&\quad \sum_{(i,j) \in P(1,2)} \left( \frac{1}{2} E_3^0(i_{q'}, 3_q, 4_{\bar{q}}) F_3^0((\tilde{i}3)_g, (\tilde{3}4)_g, j_g) \times J_3^{(3)}((\tilde{i}3)_g, (\tilde{3}4)_g, j_g) \right. \\
&\quad \left. \left. \frac{1}{2} E_3^0(j_{q'}, 3_q, 4_{\bar{q}}) F_3^0(i_g, (\tilde{3}4)_g, (\tilde{4}j)_g) \times J_3^{(3)}(i_g, (\tilde{3}4)_g, (\tilde{4}j)_g) \right) \right. + \\
&\quad \left. - \frac{1}{N} \sum_{(i,j) \in P(1,2)} \left( A_3^0(4_q, i_g, 3_{\bar{q}}) G_3^0(j_g, (\tilde{3}i)_q, (\tilde{i}4)_{\bar{q}}) \times J_3^{(3)}(j_g, (\tilde{3}i)_q, (\tilde{i}4)_{\bar{q}}) \right) \right] + \\
&\quad N_F^2 \left[ \frac{1}{2} E_3^0(2_{\bar{q}}, 3_{q'}, 4_{\bar{q}'}) G_3^0((\tilde{3}4)_g, 1_q, (\tilde{2}3)_{\bar{q}}) \times J_3^{(3)}((\tilde{3}4)_g, 1_q, (\tilde{2}3)_{\bar{q}}) \right. + \\
&\quad \frac{1}{2} E_3^0(1_q, 3_{q'}, 4_{\bar{q}'}) G_3^0((\tilde{3}4)_g, (\tilde{4}1)_q, 2_{\bar{q}}) \times J_3^{(3)}((\tilde{3}4)_g, (\tilde{4}1)_q, 2_{\bar{q}}) \quad + \\
&\quad \frac{1}{2} E_3^0(4_{\bar{q}'}, 1_q, 2_{\bar{q}}) G_3^0((\tilde{1}2)_g, 3_{q'}, (\tilde{4}1)_{\bar{q}'}) \times J_3^{(3)}((\tilde{1}2)_g, 3_{q'}, (\tilde{4}1)_{\bar{q}'}) \quad + \\
&\quad \left. \left. \frac{1}{2} E_3^0(3_{q'}, 1_q, 2_{\bar{q}}) G_3^0((\tilde{1}2)_g, (\tilde{2}3)_{q'}, 4_{\bar{q}'}) J_3^{(3)}((\tilde{1}2)_g, (\tilde{2}3)_{q'}, 4_{\bar{q}'}) \right] \right\} \\
&\times d\Phi_4(p_1, \dots, p_4; q)
\end{aligned}$$

The  $N^2$  colour factor subtraction term, correctly has only gluon-gluon antennas with final state gluons, owing a cancellation for pure gauge contributions. In it, as we highlighted for the  $D_3^0(q, g, g)$  antenna above, we have to disentangle the singular configurations included in the  $F_3^0(g, g, g)$ . This contains three different sub-antennas  $f_3^0(g, g, g)$ , one for each possible identification of the partons in the matrix elements as hard radiators and emitter.

The  $-N_F/N$  colour factor subtraction term, needs to cancel the subleading colour contribution where the gluons behave as photons (and thus cannot undergo a collinear limit). This means that we can drag them around without affecting the colour ordering. We can thus pull one of the gluons between the quark and the antiquark out of the antenna. The quark and the antiquark participate in the colour ordering and are uniquely identified as the hard radiators. Therefore, the antenna to be used is the quark-antiquark one.

Finally the  $N_F^2$  colour factor subtraction term, has antennas which have only quark-antiquark collinear limit. In it, as for the  $N_F N$  colour factor, we separate the contribution symmetrically between the configurations at play<sup>10</sup>.

In writing the antennas, sometimes it could appear the ordering of the partons does not correspond to the one required. We point out that some antennas are symmetric under exchanges of partons. For instance,  $G_3^0(g, q, \bar{q})$  is the same as  $G_3^0(g, \bar{q}, q)$ . This is typical of antennas which has only collinear limits.

The subtraction terms 3.2 have exactly the same limits as the real contributions 3.14, as can be checked by looking at the limits of the three-partons and four-partons antennas in [6], and recalling that the reduced matrix elements are integrated against the three-partons jet function  $J_3^3(\tilde{p}_1, p_2, \tilde{p}_3)$  which prevents the parton outside of the antenna and the redefined hard radiators to undergo infrared limits.

Just for the sake of completeness, we point out that the symmetry factors are necessarily the same as the ones for the real matrix elements 3.14, since we are just replacing their singular limits with their factorised forms.

The game is not over yet: our subtraction terms correctly resemble the infrared structure of the matrix elements of the real contributions, but we need to make sure the integrated antennas in the antenna phase space analytically cancel the poles of the virtual contributions. Performing the integral of the antennas in eq. 3.2 in the factorised antenna phase space, we obtain:

---

<sup>10</sup>Therefore the factors of  $\frac{1}{2}$ .

$$\begin{aligned}
d\sigma_{NLO}^S &= \frac{|\mathcal{M}_{NLO}^S|^2}{|\mathcal{M}_B|^2} d\Phi_3(p_1, p_2, p_3; q) J_3^{(3)}(p_1, p_2, p_3) = \\
&= g_s^4 \left\{ \frac{1}{12} N^2 \left[ 8 \frac{1}{3} \mathcal{F}_3^0(s_{23}) + 8 \frac{1}{3} \mathcal{F}_3^0(s_{13}) + 8 \frac{1}{3} \mathcal{F}_3^0(s_{12}) \right] + \right. \\
&\quad N_F \left[ N \left( \mathcal{D}_3^0(s_{13}) + \mathcal{D}_3^0(s_{12}) + \right. \right. \\
&\quad \left. \left. \mathcal{E}_3^0(s_{13}) + \mathcal{E}_3^0(s_{12}) \right) + \right. \\
&\quad \left. - \frac{1}{N} 2 \mathcal{A}_3^0(s_{23}) \right] + \\
&\quad \left. N_F^2 \left[ \mathcal{E}_3^0(s_{13}) + \mathcal{E}_3^0(s_{23}) \right] \right\} \\
&\times d\Phi_3(p_1, p_2, p_3; q) J_3^{(3)}(p_1, p_2, p_3)
\end{aligned}$$

Extracting the poles with the infrared singularity operators  $\mathbf{I}^{(1)}$ , again using the results<sup>11</sup> listed in [6], we can verify the analytic cancellation of the integrated subtraction terms with the unintegrated virtual cross section:

$$\mathcal{Poles}(d\sigma_{NLO}^S) + \mathcal{Poles}(d\sigma_{NLO}^V) = 0 \quad (3.28)$$

This further confirms the correctness of the proposed subtraction term in eq. 3.2.

We might specify some details in the analytic cancellation of the poles. The antenna phase space 2.20 is just, up to normalisation, the three-particles phase space in  $d$ -dimensions. In terms of the Mandelstam invariants  $s_{ij}$ , it is symmetric under exchanges of them [45]:

$$dPS_3 = (2\pi)^{3-2d} 2^{-1-d} (q^2)^{\frac{2-d}{2}} d\Omega_{d-1} d\Omega_{d-2}(s_{12}s_{13}s_{23})^{\frac{d-4}{2}} ds_{12} ds_{13} ds_{23} \delta(q^2 - s_{12} - s_{13} - s_{23}). \quad (3.29)$$

---

<sup>11</sup>The infrared structure of the antennas, as already mentioned, is reported in [45]. We inform the reader that there is a little typo in eq. 7.32 of [45]. It is to be replaced with:

$$\mathcal{Poles}(\hat{G}_3^1(1_g, 3_q, 4_{\bar{q}})) = 2(\mathbf{I}_{qg,F}^{(1)}(\epsilon, s_{13}) + \mathbf{I}_{qg,F}^{(1)}(\epsilon, s_{12}) - 2\mathbf{I}_{gg,F}^{(1)}(\epsilon, s_{134})) G_3^0(1_g, 3_q, 4_{\bar{q}})$$



When combined with the three-particles phase space, the infrared singularity operators  $\mathbf{I}^{(1)}$ , if they appear alone in a sum, do not care anymore about the invariant they act on; for instance:

$$dPS_3 \mathbf{I}^{(1)}(s_{12}) = dPS_3 \mathbf{I}^{(1)}(s_{13}) \quad (3.30)$$

Another relevant note is that, in the cancellation between the poles of  $F_3^1(g, g, g)$  and  $\mathcal{E}_3^0(q', q, \bar{q})$ , the infrared singularity operators might appear different at first sight. In fact, these two antennas has singular structures proportional to  $I_{gg,F}(s_{ij})$  and  $I_{qg,F}(s_{ij})$ , respectively. Nevertheless, the cancellation occurs as required, since, for the same invariants,  $I_{gg,F}(s_{ij}) = 2 I_{qg,F}(s_{ij})$ , as can be checked<sup>12</sup> with eq. 2.27.

### 3.3 Numerical implementation

Once we have understood the singular structure of the matrix elements and obtained the subtraction terms, we are ready to produce numerical results. We provide a precise analysis of the most common event shapes for the process under study. The numerical implementation has been carried out with the program **EERAD3** [11]. It serves as an efficient way to implement the antenna subtraction method as well as all of the most used jet variables. It is flexible, since it can be easily modified to include the analysis for the decays of a neutral color particle into hadrons, such as the Z boson or the Higgs boson.

We reproduce the LO and NLO perturbative coefficients to Higgs decays in the following form<sup>13</sup>:

**( $b\bar{b}$ ) final states:**

$$\text{Br}(b\bar{b}) \frac{1}{\sigma_0(b\bar{b})} \frac{d\sigma(b\bar{b})}{dy} = \text{Br}^{\text{LO}}(b\bar{b}) \left( \frac{\alpha_s(l)}{2\pi} \right) \frac{dA}{dy} + \mathcal{O}(\alpha_s^2). \quad (3.31)$$

**( $gg$ ) final states:**

$$\text{Br}(gg) \frac{1}{\sigma_0(gg)} \frac{d\sigma(gg)}{dy} = \text{Br}^{\text{LO}}(gg) \left( \frac{\alpha_s(l)}{2\pi} \right) \frac{dA}{dy} + \text{Br}^{\text{NLO}}(gg) \left( \frac{\alpha_s(l)}{2\pi} \right)^2 \frac{dB}{dy} + \mathcal{O}(\alpha_s^3). \quad (3.32)$$

---

<sup>12</sup>Had we used  $G_3^0(g, q, \bar{q})$  antennas instead, the cancellation would perhaps have been more apparent, being the fact that these antenna has a singular structure proportional to  $I_{gg,F}(s_{ij})$ . We recall, again, that using one or the other antenna yields exactly the same results.

<sup>13</sup>Since the beginning we would like to point out our notation, which might sound a bit imprecise: when we write cross sections we always mean decay rate. This is to keep with the same notation as for the Z boson decays, in which the cross section  $e + e^- \rightarrow Z \rightarrow \text{partons}$  factorizes explicitly into the Born process and the hadronic decays of the Z boson.

where  $l = \mu^2/s^2$ ,  $\mu$  is the energy scale at which we evaluate the process and  $s$  the renormalisation scale. Since our normalisation is given by the Born matrix element at leading order, all the energy dependence of the cross section lies in the strong coupling constant  $\alpha_s(l)$ . The dependence on the energy scale appears also in the branching functions, where it affects both the HEFT coupling  $\lambda$  and the Yukawa coupling  $y_b$ .

To numerically test the correctness of the subtraction terms presented, we change the lower cut  $y_0$  of the phase space integration. This parameter formally yields the sensitivity to the limiting regions of the phase space and the numerical cancellation of the singular behaviours should be insensitive to it. This behaviour was successfully checked, implying that the subtraction terms ensure that the contribution of potentially singular regions of the final state phase space does not contribute to the numerical integrals, but is accounted for analytically.

In order to implement our analysis, we wrote the code relative to the antennas needed as well as the file containing the matrix elements for the LO contribution, the NLO real matrix elements, the NLO virtual ones and the NLO subtraction term. We wrote it in such a way that it is straightforward to add the contribution for NNLO corrections. The program **EERAD3** is available at [11] and the code used to compute the NLO corrections to hadronic Higgs boson decays can be found at [https://github.com/GuglielmoColoretti/EventShapes\\_HiggsTOgg\\_QCD\\_NLO.git](https://github.com/GuglielmoColoretti/EventShapes_HiggsTOgg_QCD_NLO.git).

The structure of the program is such that it allows to compute each perturbative coefficient (A and B in eq. 3.32) independently, as well as all the colour contribution separately. One can further select the event shape and set the precision of the statistics, namely the number of points to be used in the numerical integration. This is achieved with a so called input card, namely a text file with the selected specifics (section 4.1 of [11]).

The main program is **eerad3.f** and the files passed to it are called in the **Makefile**. In our case, the **Makefile** contains all the matrix elements and the subtraction terms. All details can be found in [11] and the specific ones related to our analysis in the git repository above. In particular, the main difference between the folder in [11] and the one in the git repository is that our analysis extends only up to NLO, and **eerad3.f** is designed to compute also NNLO corrections. This means that some files present in the **Makefile** of [11] are to be omitted if one wish to reproduce our results. In fact, we suggest to download the program from the git repository, where we have already arranged everything in order to compute three-jets event shapes to hadronic Higgs decays. For the sake of clarity, we specify that the new files written for our analysis are the ones contained in the **src** folder of the git repository.

The usage of the program can be found in [33]. Nevertheless, for the sake of

completeness, we briefly outline it here too, underlining the updates and the NLO usage. The main program, as already mentioned, is `eerad3.f`. It outputs a series of histograms containing the information regarding the event shapes selected. The files called by the program are the following:

`ecuts.f` : jet algorithms and event shape definitions

`phaseee.f` : phase space routines

`eerad3lib.f` : library with special functions and auxiliary routines

`histo.f` : histogram handling routines

`aversub0H.f` : antennas and subroutines for subtraction terms at NLO

`sigHG.f` : matrix elements up to NLO and subtraction terms at NLO for three-jets events of Higgs decays to gluon-gluon

`sigHB.f` : matrix elements up to LO for three-jets events of Higgs decays to bottom-antibottom

The selection of the specifics of the output are controlled by a so called input card, which look like the following:

```

1d-6      ! y0
0          ! iaver
1d-5      ! cutvar
1          ! imom
1          ! iang
-1         ! nloop
0          ! icol
L          ! ichar
1 1        ! iwarm iprod
5 5        ! itmax1 itmax2
50000000 50000000 0 ! nshot3 nshot4 nshot5

```

Figure 3.6: Example of input card for `eerad3.f`.

where:

`y0` : technical cut-off for the phase space integration (dimensionless), should be between  $10^{-5}$  and  $10^{-8}$

`iaver` : selects the observables to be computed:

0: all event shapes distributions ( $B_W, C, M_H^2/s, (1 - T), B_T$ )

1: wide jet broadening  $B_W$

2:  $C$ -parameter  $C$   
 3: heavy jet mass  $M_H^2/s$   
 4: thrust  $(1 - T)$   
 5: total jet broadening:  $B_T$   
 6: jet rates and transition parameters in the Durham algorithm:  
 $R_3, R_4, R_5, y_{23}, y_{34}, y_{45}$   
 7: jet rates and transition parameters in the Jade algorithm:  $R_3, R_4, R_5, y_{23}, y_{34}, y_{45}$   
 8: all jet distributions in the Durham  $k_t$  algorithm and all logarithmic event shape distributions.

**cutvar** : lower cut-off on distributions, should be at least one order of magnitude larger than  $y_0$ .

**imom** : moment number applied as weight: if computing distributions, should be set to **imom**= 1

**iang** : angular optimisation of phase space: on (**iang** = 1) or off (**iang** = 2).

**nloop** : perturbative order: LO (**nloop**= 0), NLO (**nloop**= -1)

**icol** : colour factor
 

- 0: sum of all colour factors
- 1: LO  $N$
- 2: LO  $1/N$
- 3: LO  $N_F$
- 1: NLO  $N^2$
- 2: NLO  $N_F N$
- 3: NLO  $-N_F/N$
- 4: NLO  $N_F^2$

**ichar** : one character to identify output files

**iwarm** : produce a warm up integration grid (**iwarm**= 1) or read the grid from files (**iwarm**= 0)

**iprod** : produce histograms: yes (**iprod**= 1) or no (**iprod**= 0)

**itmax1,2** : number of iterations for warm up and production runs

`nshot3,4` : number of vegas points for three-partons, four-partons channels<sup>14</sup>

As for the output files, the naming of the histograms follows exactly [11]. Regarding the phase space integration with the vegas routine and the two additional programs `eerad3.dist.f` (to compute whole cross sections and distributions) and `eerad3.combine.f` (to obtain statistics with independent random seeds), they again do not differ from [11]. More details can be found in the git repository above.

### 3.4 Results

Following the definitions given in section 2.2.2, we here display the plots relative to the process considered. In each of the plots, the cross section is weighted by the corresponding Born cross section and branching function, as explained in section 3.1. For convenience, we weight the distributions by the observable.

Nowadays, experimental errors can be considered to be negligible. The sources of errors in theoretical results are two: the theoretical description of the transition from partons to hadrons (hadronisation process) and the uncertainty arising from the truncation of the perturbative series at a certain order, as resembled by scale variations. Albeit the uncertainty in the theoretical model accounting for hadronisation are still debated and perhaps underestimated, it is customary to address the scale uncertainty as the dominant source of theoretical errors.

For every event shape, we provide the ratio of the three-jets ( $gg$ ) contribution against the ( $b\bar{b}$ ) one at LO; for the corrections to the three-jets ( $gg$ ) final state, we also plot the  $A$  and  $B$  coefficients (eq. 3.32) as well as the full cross section at NLO. For the latter figure, we vary the energy scale by  $\pm 20$  GeV from the reference one of the Higgs mass. If varied more than this, we enter regimes in which our approximations (especially regarding the HEFT validity) are no more accurate. As discussed above, we also plot the event shapes for different lower cut-off  $y_0 = 10^{-8}, 10^{-7}, 10^{-6}$  as a numerical check on the subtraction terms. We see that the numerical stability improves for higher values of  $y_0$ . This is due to the fact that the cancellations among matrix elements and subtraction terms happen over larger order of magnitudes, hence enhancing numerical rounding errors. Therefore, while displaying the plots, we use a low cut-off ( $y_0 = 10^{-6}$ ) for the coefficients and the cross section. The number of points used in each run is  $10^7$ , which amounted to

---

<sup>14</sup>The last number `nshot5` is left for a foreseen extension of our analysis to NNLO, where also real matrix elements with five-partons final states are to be considered. For our purposes, namely NLO precision, this channel is not needed and thus the number of points used to integrate over it are set to zero.

around five days of computational runtime<sup>15</sup>.

The specific size and shape of the perturbative corrections depend on the observable considered. Nevertheless, they share some common behaviours.

All observables are dominated by the behaviour in the two-jet region where the observable usually tends to zero. Since hadronic events contain many hadrons, it is extremely unlikely that the value of any event shapes is precisely zero for all experimental events. We further point out that, as it is well known, the fixed order perturbation expansion is affected by logarithmic behaviours which might become large and therefore need to be resummed. In the infrared limit  $y \rightarrow 0$ , the perturbative coefficients have the form:

$$\begin{aligned} y \frac{dA}{dy} &\sim A_1 L + A_0 \\ y \frac{dB}{dy} &\sim B_3 L^3 + B_2 L^2 + B_1 L + B_0 \end{aligned} \quad (3.33)$$

where  $L = \ln(1/y)$ . Whenever  $L$  is sufficiently large, resummation effects become relevant, therefore we impose a cut on  $y$  to avoid such small values for which we do not trust the perturbative expansion. The cut for  $y$  is typically in the range  $0.001 - 0.01$ .

Everywhere, the shape of the observables are heavily influenced by cancellations between real and virtual contributions. The LO contribution  $A$  is very large and positive at small  $y$  values and decrease monotonically as  $y$  increases. The NLO, on the other hand, is negative at small  $y$  values and exhibits a turnover around  $y \sim 0.05$ .

We now discuss the results obtained for the event shapes considered.

---

<sup>15</sup>With  $10^8$  points, the program was halted on a cluster after 360 hours of run. The analysis with  $10^7$  is already quite satisfactory.

Thrust  $T$ :

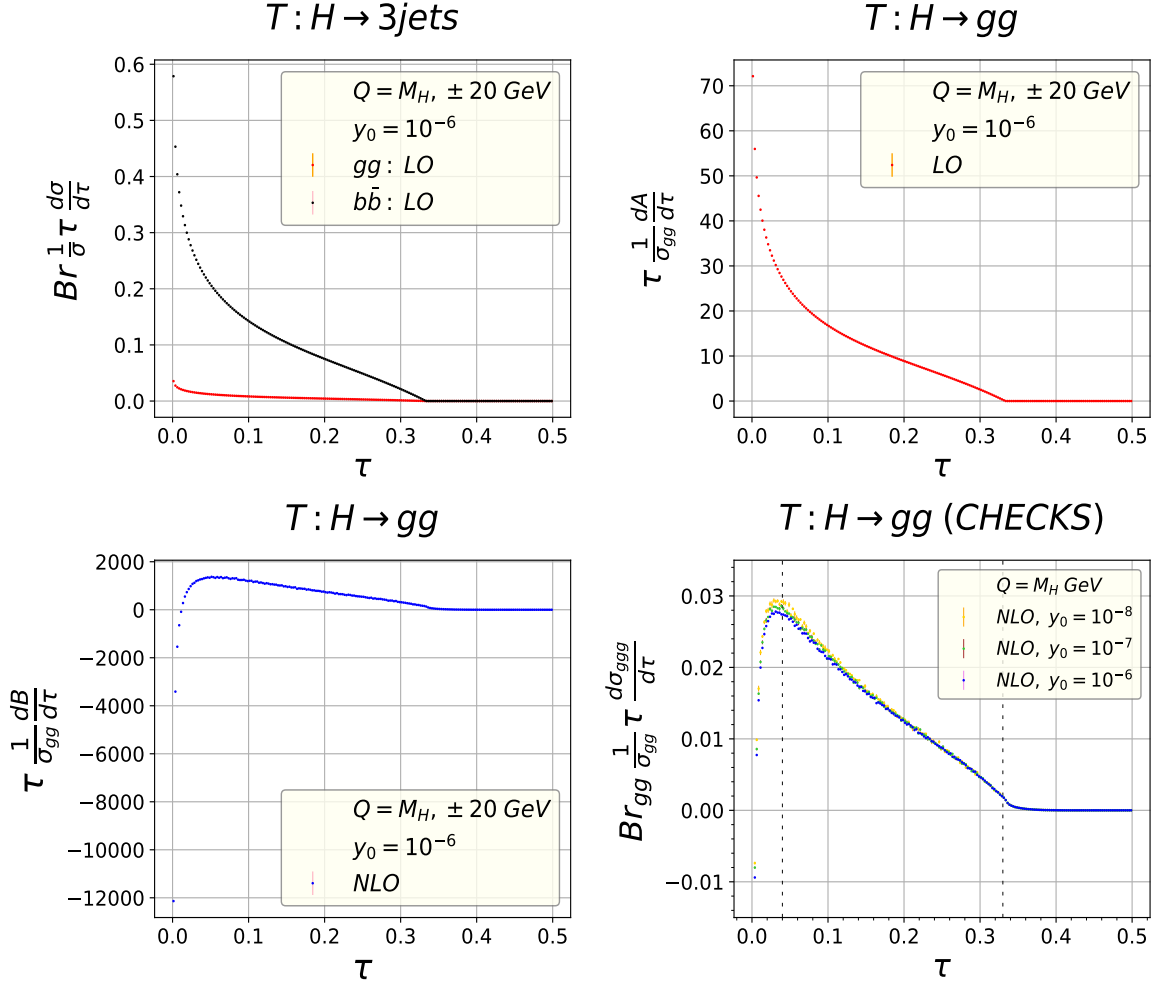


Figure 3.7: Thrust three-jets events analysis at Higgs mass energy  $M_H = 125.18$  GeV. From top-left to bottom-right: (i) LO comparison between gluon-gluon final states and bottom-antibottom final states; (ii) A coefficient; (iii) B coefficient; (iv) numerical check of subtraction terms at NLO.

Thrust is defined in 2.2.2. The LO hadronic Higgs decay is mainly dominated by the  $b\bar{b}$  contribution (Fig. 3.7). As for the  $gg$  final states, the LO contribution is very high and positive and grows monotonically for small  $\tau$ , whereas the NLO is negative and exhibits a turnover near moderate value of  $\tau$  (Fig. 3.7). The NLO corrections to this observable is dominant: in the regions in which the perturbation theory can be trusted, namely  $0.04 < (1 - T) < 0.33$ , it amounts to almost 65% of the event shape.

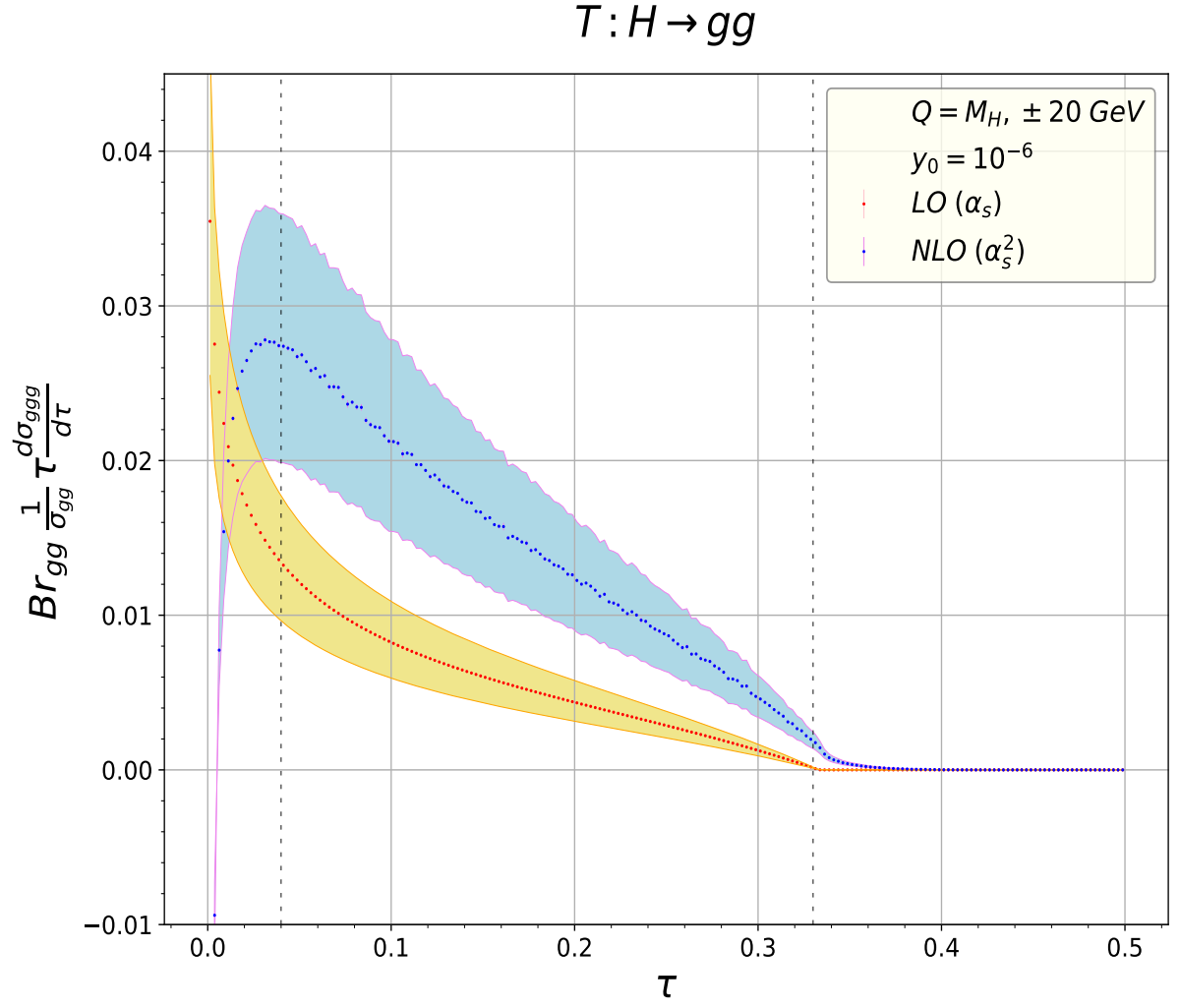


Figure 3.8: Thrust distribution: LO and NLO cross section of three-jets events. The shaded regions are bounded by energy scales  $Q = (125.18 \pm 20)$  GeV.



Heavy jet mass  $\rho$ :

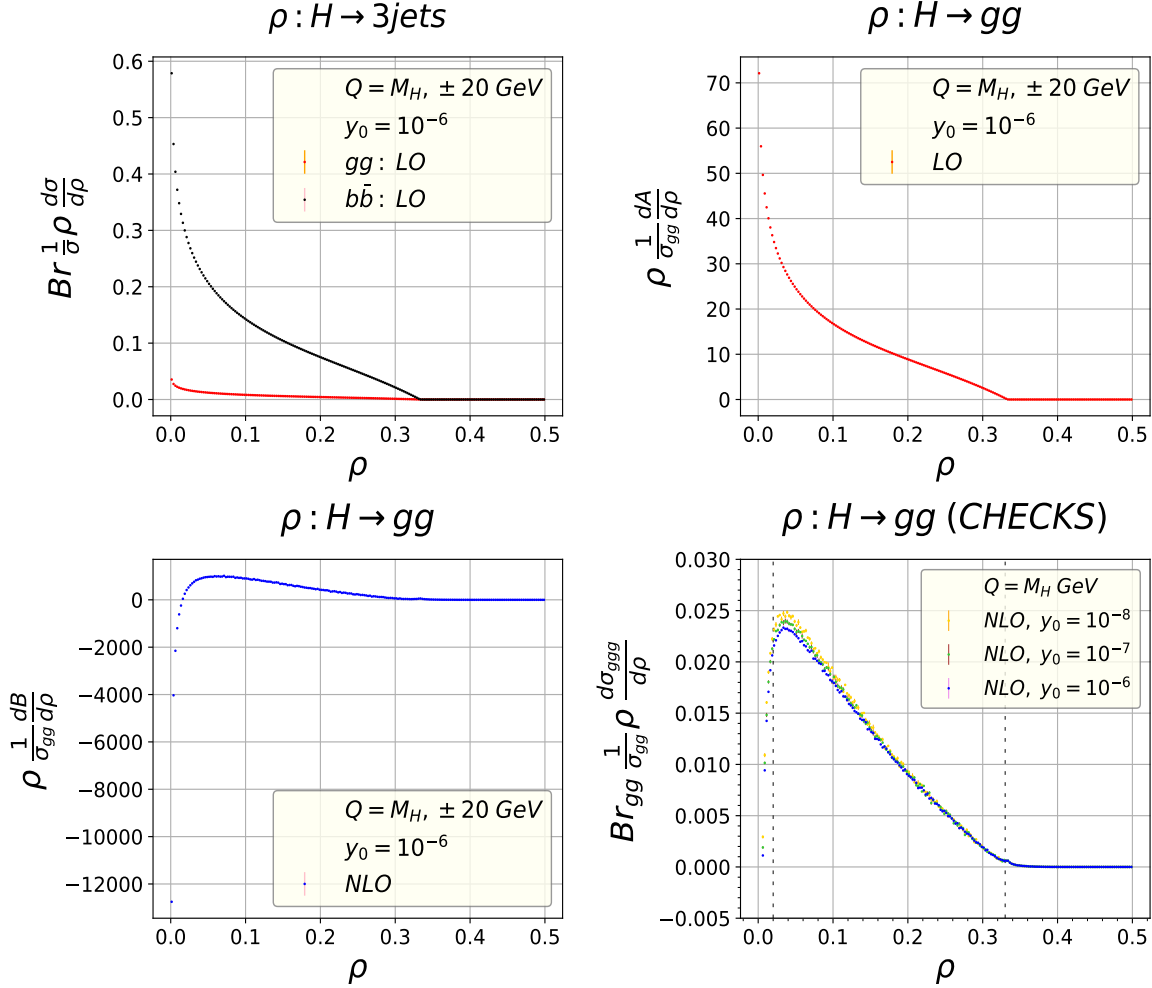


Figure 3.9: Heavy jet mass three-jets events analysis at Higgs mass energy  $M_H = 125.18$  GeV. From top-left to bottom-right: (i) LO comparison between gluon-gluon final states and bottom-antibottom final states; (ii) A coefficient; (iii) B coefficient; (iv) numerical check of subtraction terms at NLO.

The definition of the heavy jet mass given in section 2.2.2 is the larger invariant mass of the two hemispheres formed by separating the event by a plane normal to the thrust axis. The LO hadronic Higgs decay is mainly dominated by the  $b\bar{b}$  contribution (Fig. 3.9). As for the  $gg$  final states, at LO this event shape is the same as the thrust. Instead, at NLO, the heavy jet mass amounts to smaller corrections with respect to the thrust (Fig. 3.10). In the regions in which perturbation theory yields reliable results, i.e.  $0.02 < \rho < 0.33$ , the NLO correction is 57% of the event shape.

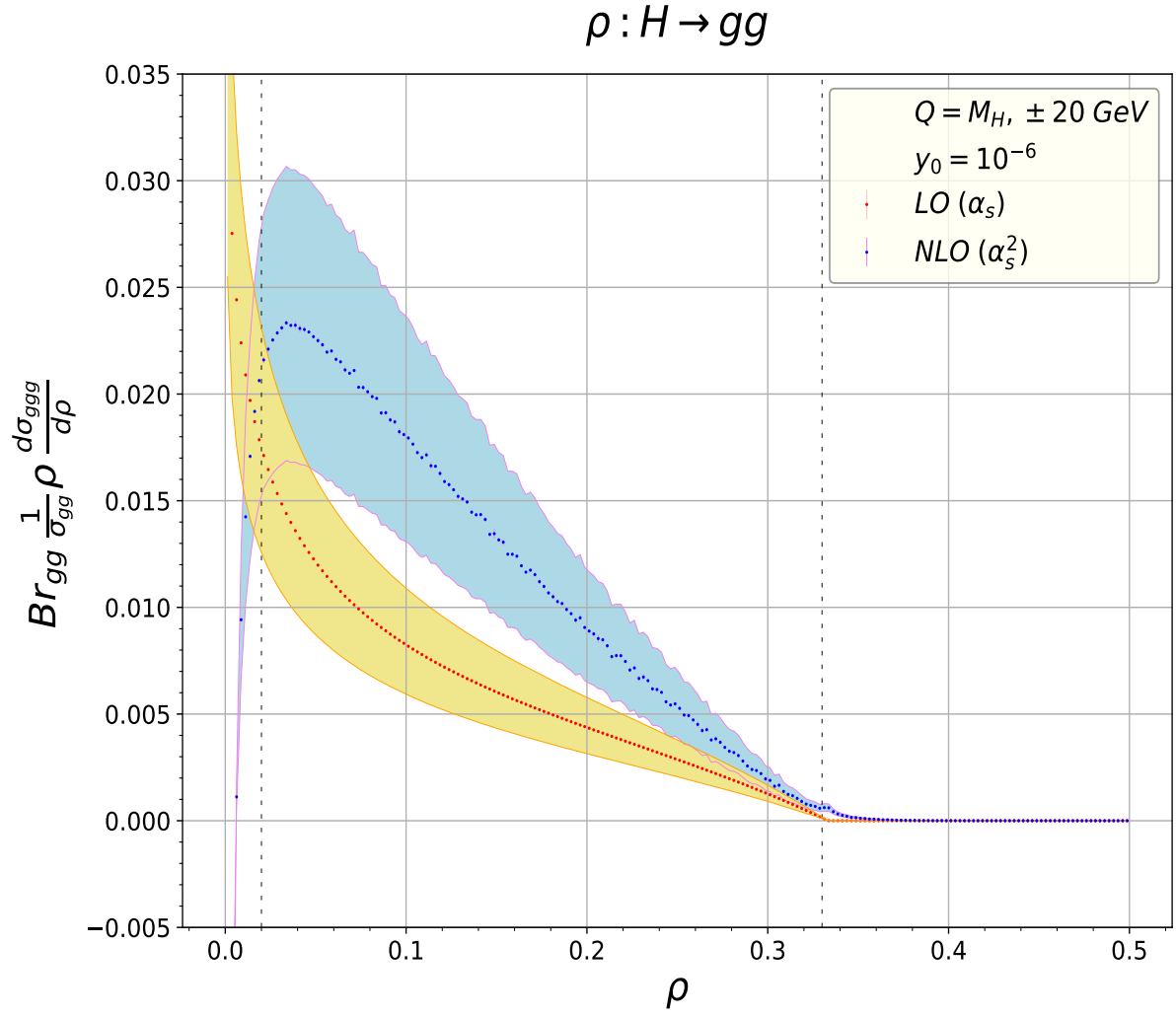


Figure 3.10: Heavy jet mass distribution: LO and NLO cross section of three-jets events. The shaded regions are bounded by energy scales  $Q = (125.18 \pm 20) \text{ GeV}$ .

$Y_3$ :

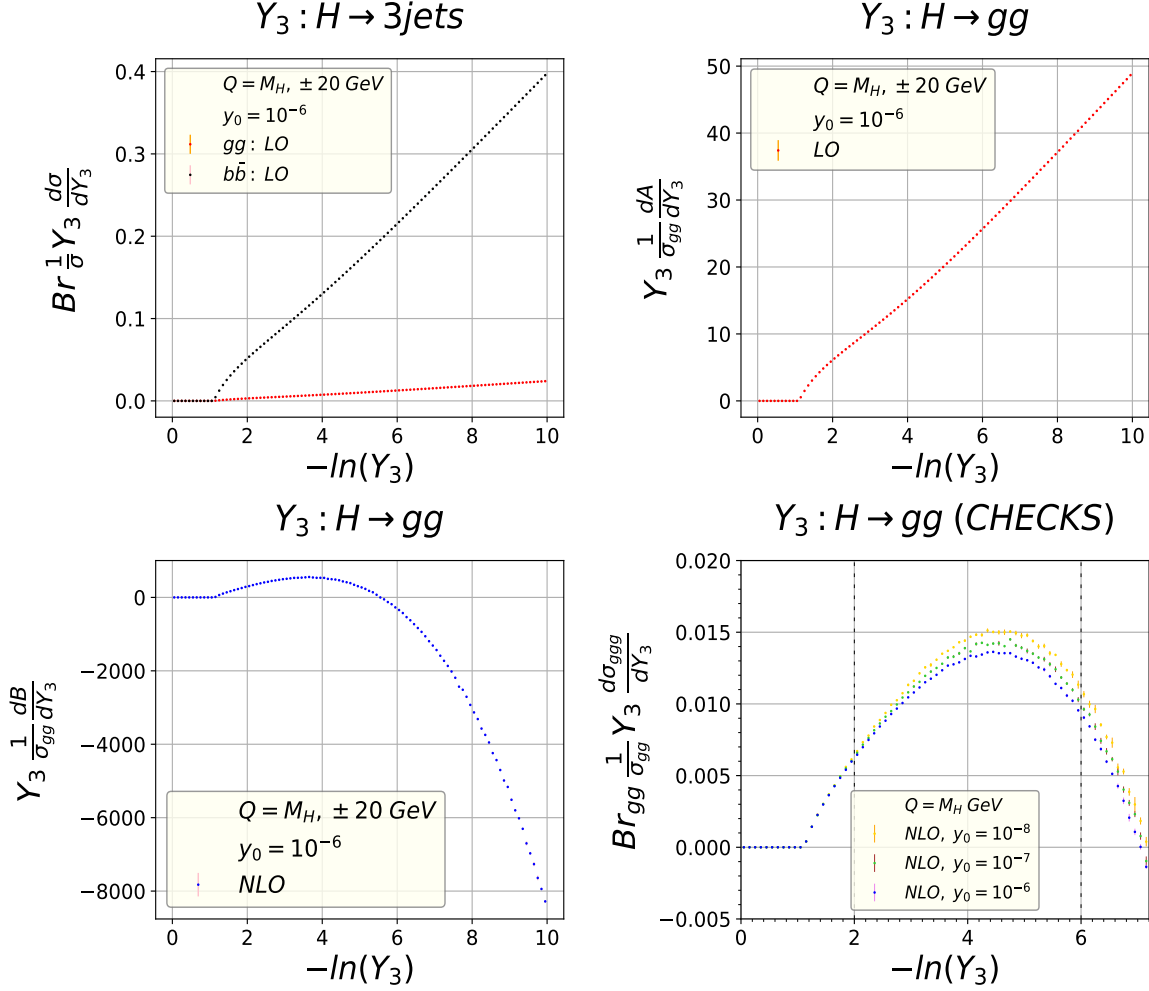


Figure 3.11:  $Y_3$  three-jets events analysis at Higgs mass energy  $M_H = 125.18 \text{ GeV}$  in the Durham algorithm. From top-left to bottom-right: (i) LO comparison between gluon-gluon final states and bottom-antibottom final states; (ii) A coefficient; (iii) B coefficient; (iv) numerical check of subtraction terms at NLO.

$Y_3$  is defined in 2.2.2. This variable gives information on the transition from a two-jets event to a three-jets event. The LO hadronic Higgs decay is mainly dominated by the  $b\bar{b}$  contribution for this observable, too (Fig. 3.11). As for the  $gg$  final states, the LO contribution is very high and positive and grows monotonically for small values of  $Y_3$ , whereas the NLO is negative and exhibits a turnover near moderate value of  $Y_3$  (Fig. 3.12). Outside the range  $2 < Y_3 < 6$ , perturbative expansion is not enough and resummation effects (as well as hadronisation) need

to be considered. The NLO corrections to this observable is not as rough as for the thrust: it amounts to almost 31% of the event shape.

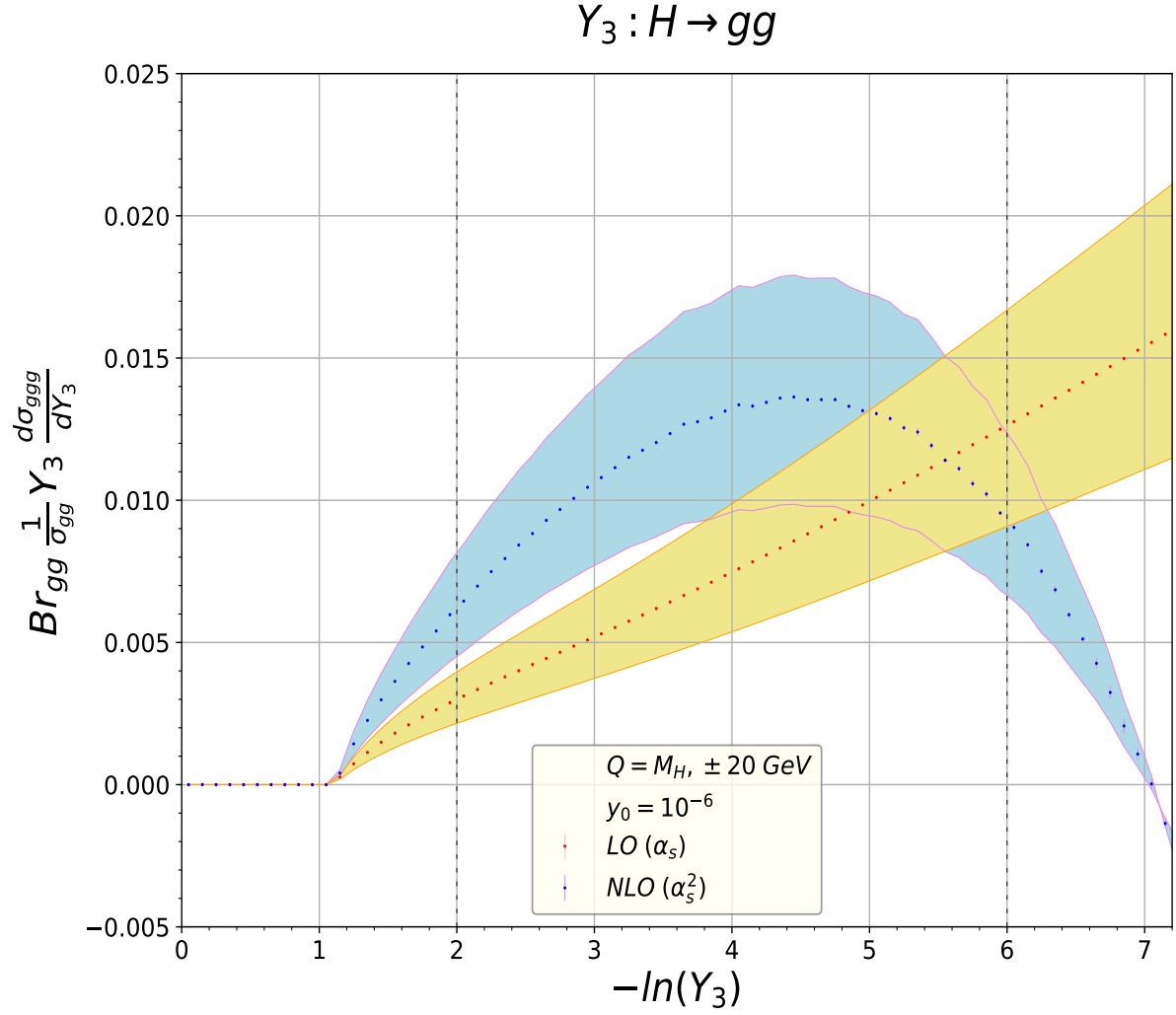


Figure 3.12:  $Y_3$  distribution: LO and NLO cross section to three-jets events in the Durham algorithm. The shaded regions are bounded by energy scales  $Q = (125.18 \pm 20) \text{ GeV}$ .

Jet broadenings  $B_T$ ,  $B_W$ :

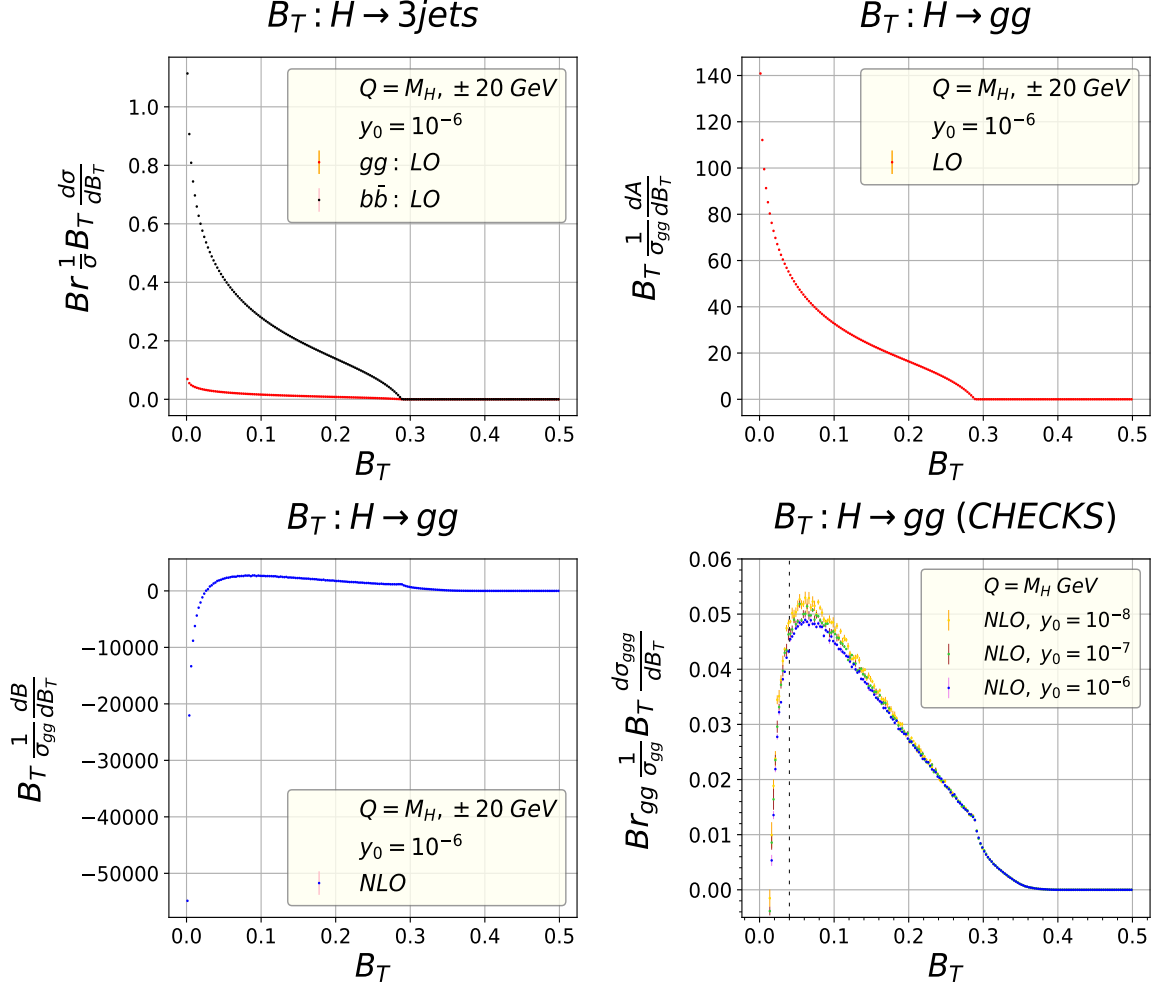


Figure 3.13:  $B_T$  three-jets events analysis at Higgs mass energy  $M_H = 125.18 \text{ GeV}$ . From top-left to bottom-right: (i) LO comparison between gluon-gluon final states and bottom-antibottom final states; (ii) A coefficient; (iii) B coefficient; (iv) numerical check of subtraction terms at NLO.

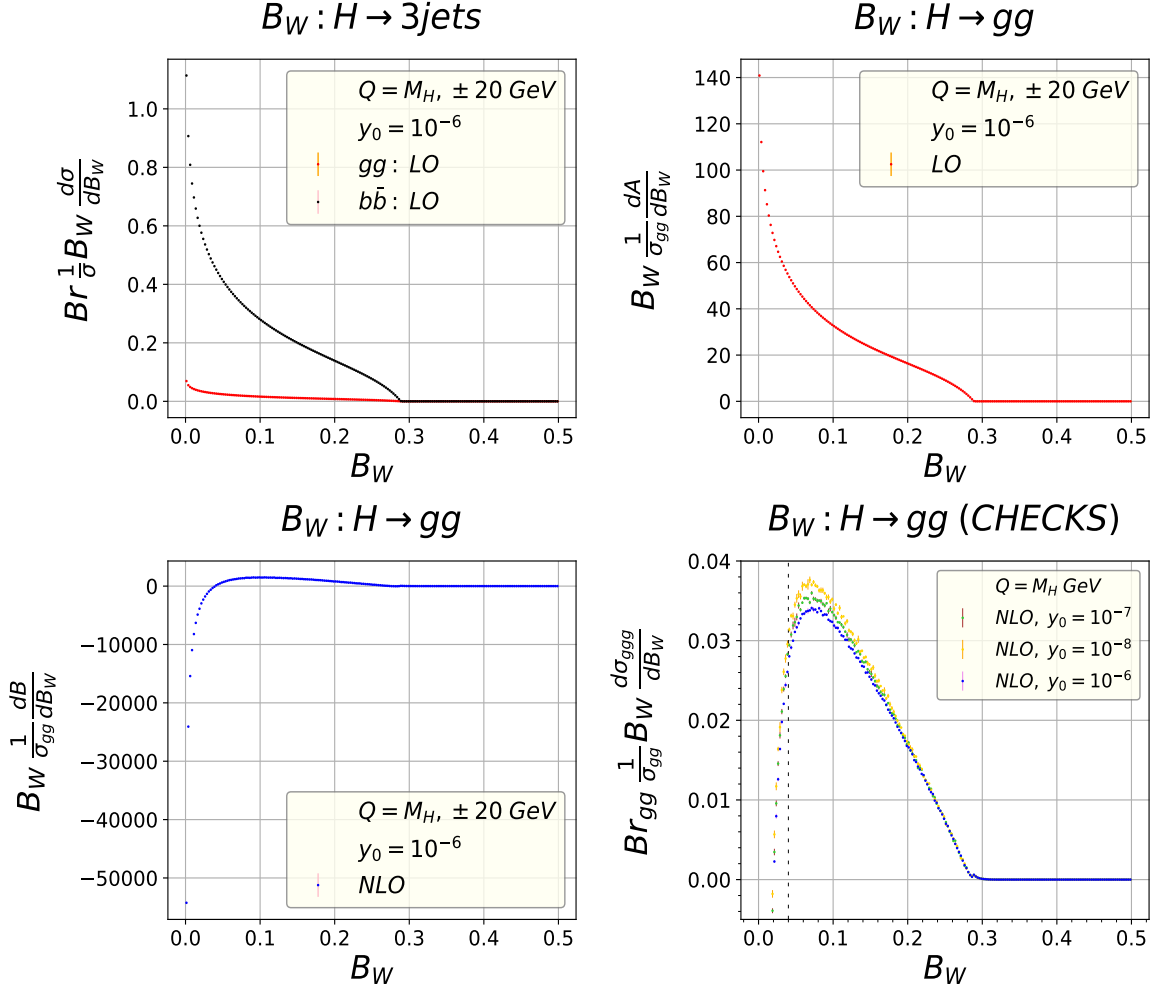


Figure 3.14:  $B_W$  three-jets events analysis at Higgs mass energy  $M_H = 125.18$  GeV. From top-left to bottom-right: (i) LO comparison between gluon-gluon final states and bottom-antibottom final states; (ii) A coefficient; (iii) B coefficient; (iv) numerical check of subtraction terms at NLO.

Jet broadening functions  $B_T$  and  $B_W$  are defined in 2.2.2. The LO hadronic Higgs decay is mainly dominated by the  $b\bar{b}$  contribution (Fig. 3.15, 3.16). As for the  $gg$  final states, the LO contribution is very high and positive and grows monotonically for small values of the variables, whereas the NLO is negative and exhibits a turnover near moderate value of the variables. The NLO corrections is larger for  $B_T$  than for  $B_W$ . For values of  $B_T$  and  $B_W$  smaller than 0.04, resummation must be considered. In the region in which the perturbative series can be trusted, the NLO contribution is 79% for  $B_T$  and 50% for  $B_W$ .

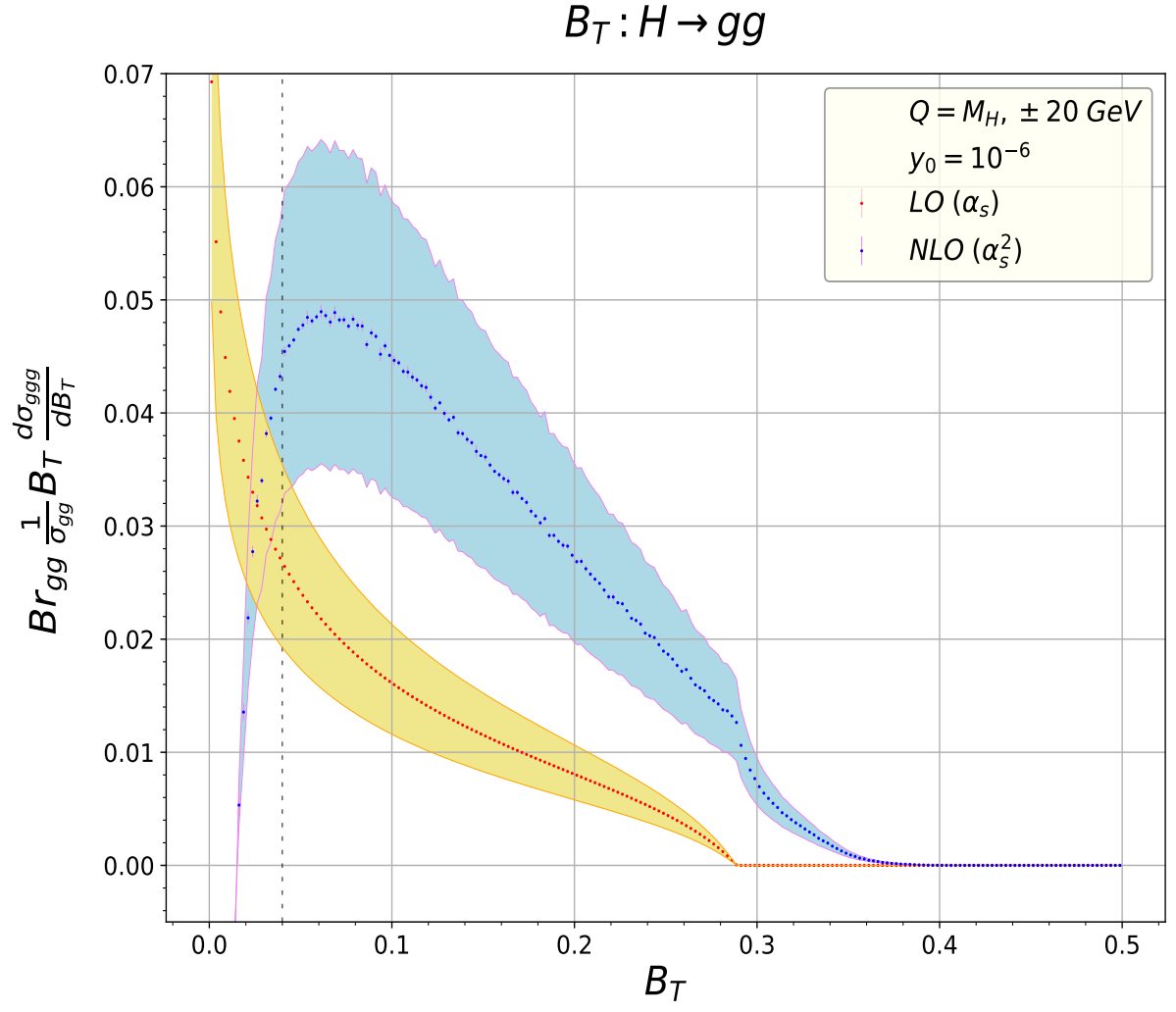


Figure 3.15:  $B_T$  distribution: LO and NLO cross section of three-jets events. The shaded regions are bounded by energy scales  $Q = (125.18 \pm 20) \text{ GeV}$ .

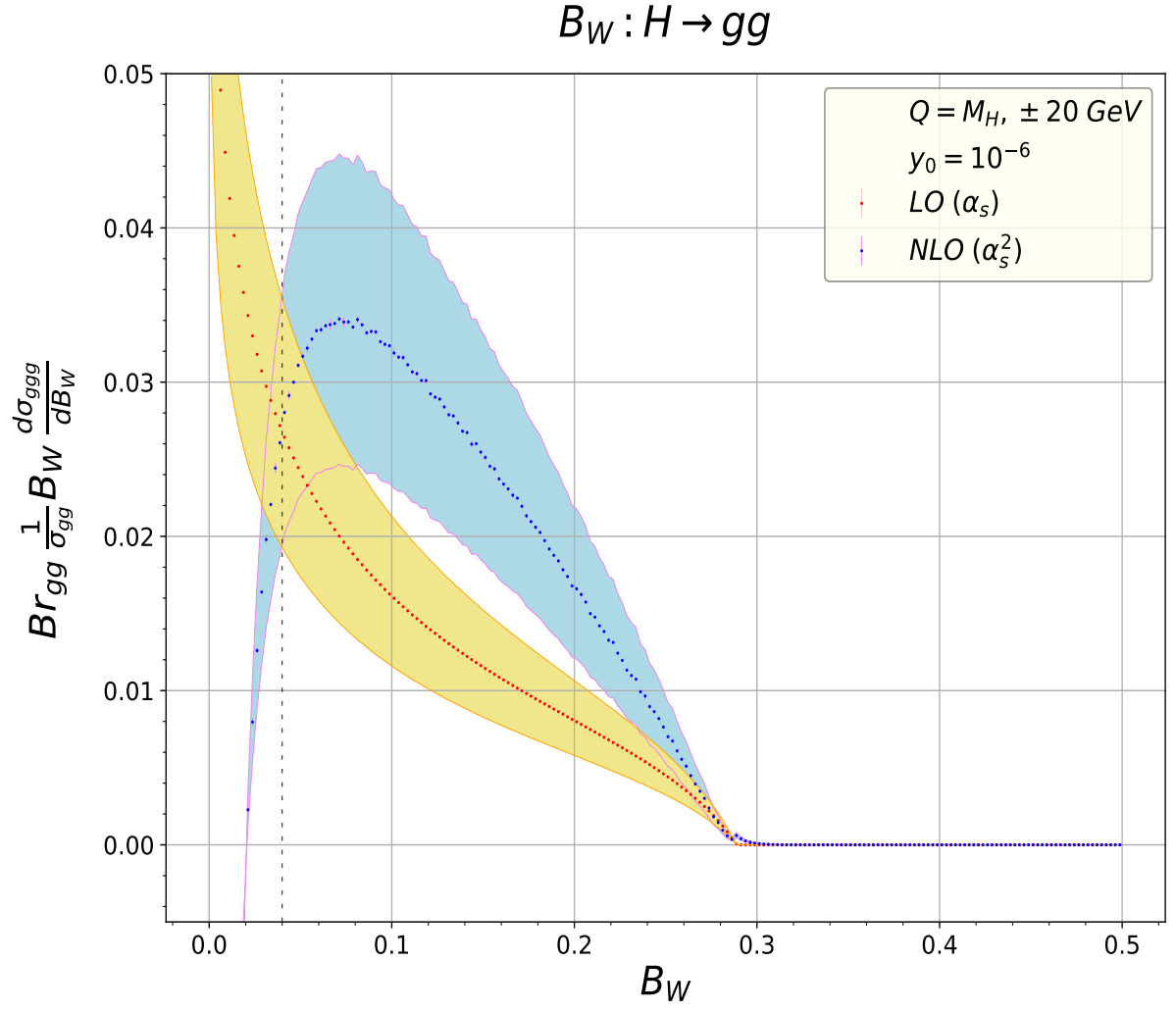


Figure 3.16:  $B_W$  distribution: LO and NLO cross section of three-jets events. The shaded regions are bounded by energy scales  $Q = (125.18 \pm 20) \text{ GeV}$ .



C parameter  $C$ :

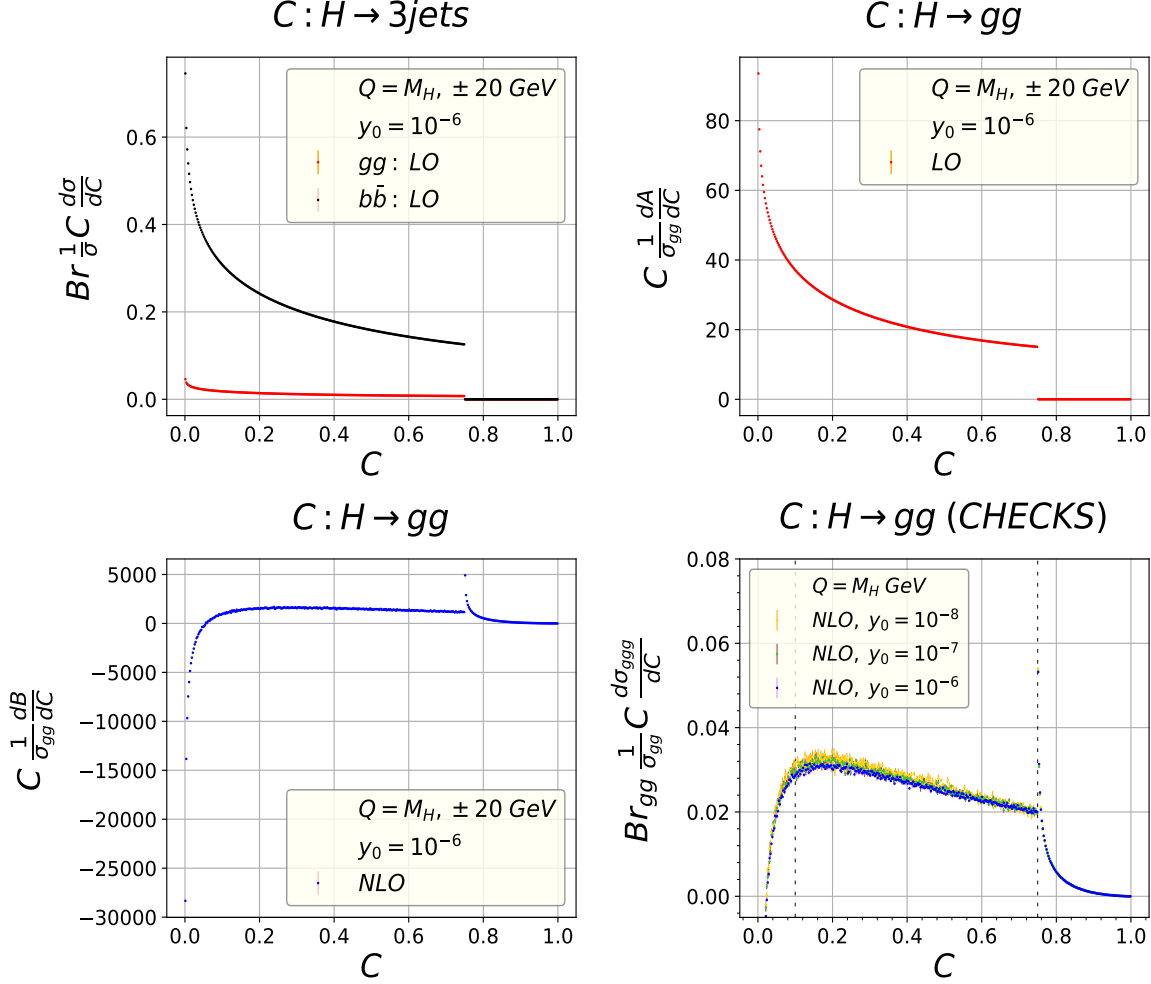


Figure 3.17: C parameter three-jets events analysis at Higgs mass energy  $M_H = 125.18$  GeV. From top-left to bottom-right: (i) LO comparison between gluon-gluon final states and bottom-antibottom final states; (ii) A coefficient; (iii) B coefficient; (iv) numerical check of subtraction terms at NLO.

C parameter is defined in 2.2.2 and it is a function obtained from a tensor in momentum space. The LO hadronic Higgs decay is mainly dominated by the  $b\bar{b}$  contribution (Fig. 3.17). The C parameter presents large logarithmic contributions below 0.01 which must be resummed (Fig. 3.18). There are also large logarithms around  $C \sim 1.75$  which spoils perturbation theory computations; these are due to soft gluon divergences in the physical region (displayed as the so called Sudakov shoulder in the plots). The NLO corrections to this observable is dominant: in

the regions in which the perturbation theory can be trusted it amounts to almost 59% of the event shape.

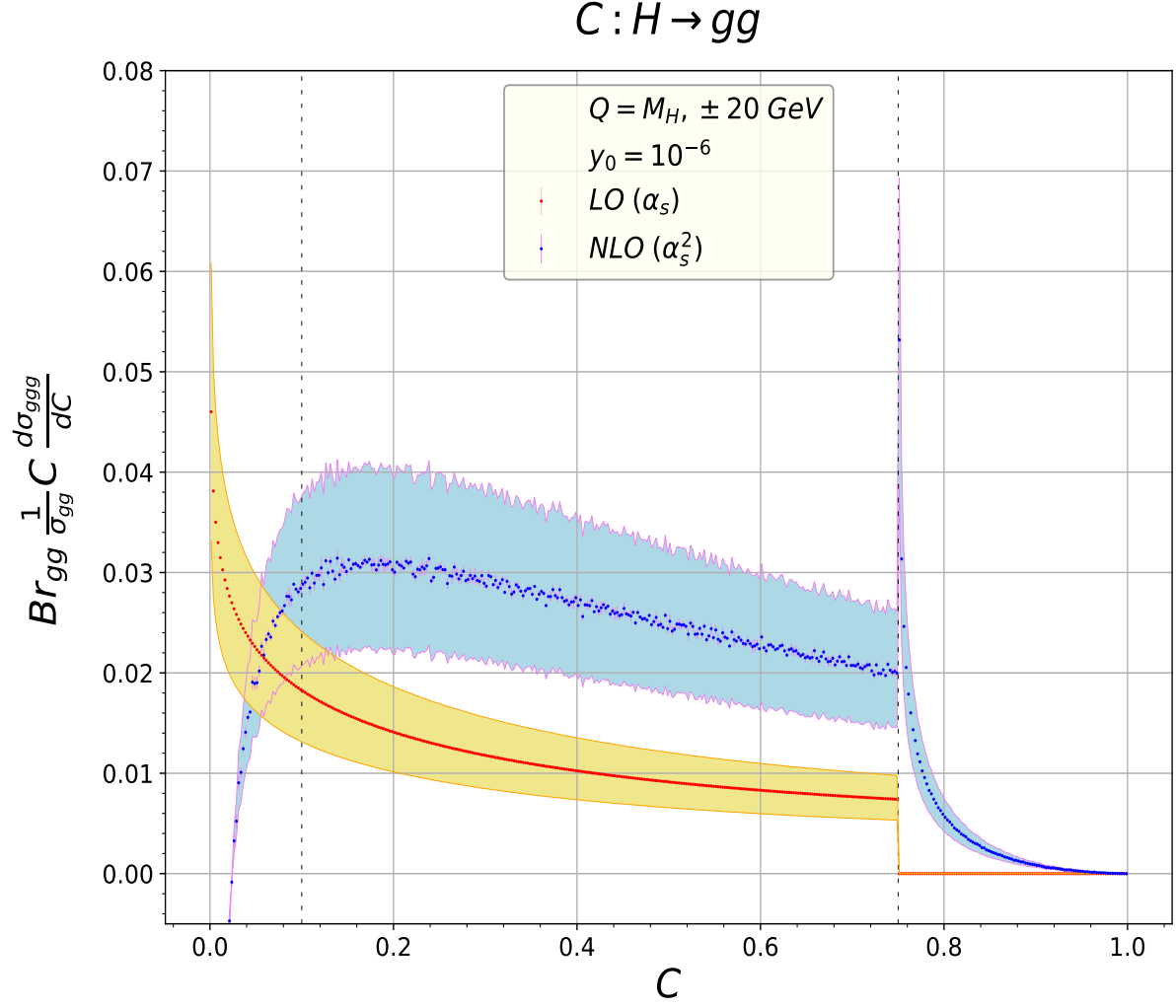


Figure 3.18:  $C$  parameter distribution: LO and NLO cross section of three-jets events. The shaded regions are bounded by energy scales  $Q = (125.18 \pm 20) \text{ GeV}$ .

# Conclusions and outlook

The goal of this thesis is to provide a precise study of QCD corrections to the most common event shapes variables for hadronic Higgs decays to three-jets events. The results are obtained up to next-to-leading order (NLO) accuracy for the gluon-gluon final state and up to leading-order (LO) accuracy for the bottom-antibottom pair final state. To produce our results, we employ the antenna subtraction method, presenting the first subtraction term for the process under study which correctly resembles all the (single-parton) infrared limits of the real four-partons matrix elements.

The numerical results are produced using the program **EERAD3**, which uses (for the gluon-gluon final state) the subtraction term as well as the three-partons tree-level and three-partons one-loop matrix elements  $H \rightarrow$  (three-partons) and the four-partons tree-level matrix elements  $H \rightarrow$  (four-partons). The numerical program yields the full kinematical information on the partonic final state and can be applied to generic infrared safe three-jet observables. We provide the (**FORT**RAN) code used to obtain our results. Computations and checks on the matrix elements have been conducted with **FORM** and MadGraph5.

The study of the most common six event shapes variables are collected in histograms and displayed in figures. We obtained NLO corrections between 30% – 80% of the full contributions. Importantly, the size of the corrections differs among different observables.

Our results serve as a theoretical prediction for future experiments at a foreseen  $e + e -$  collider able to reach Higgs mass energies of 125.18 GeV.

# Appendix A: angular terms

Angular terms manifest themselves in collinear limits of matrix elements when a final state gluon splits into a pair of quark-antiquark or into two gluons. This is due to the spin (helicity) dependence of the splitting function appearing in collinear limits. In turns, the squared matrix elements (hence the antennas, too) factorizes in the usual way up to some leftover terms, namely angular terms. The important point to make here is that angular terms integrate to zero in the respective phase space, thus not affecting the analytical cancellations of infrared poles. In principle, we can then neglect them. Nevertheless, we are aiming to subtraction terms which are local, meaning that they resemble the infrared singularities before any integration is carried out, and thus allowing a point-by-point check of the correct numerical behaviour of the subtraction terms, guaranteeing considerable improvements of the numerical stability.

To inspect the angular terms in the proper way, one has to keep track of the transverse components of the momenta of the collinear partons. Denoting the collinear direction with  $P^\mu$  ( $P^2 = 0$ ), with  $n^\mu$  an auxiliary light-like vector needed to specify the transverse component  $k_\perp$  ( $k_\perp \cdot P = k_\perp \cdot n = 0$ ), the collinear limit of partons  $p_1$  and  $p_2$  is defined in [41] as the limit  $k_\perp \rightarrow 0$  and reads:

$$\begin{aligned} p_1^\mu &= zP^\mu + k_\perp^\mu - \frac{k_\perp^2}{z} \frac{n^\mu}{2P \cdot n}, \\ p_2^\mu &= (1-z)P^\mu - k_\perp^\mu - \frac{k_\perp^2}{(1-z)} \frac{n^\mu}{2P \cdot n} \end{aligned} \tag{3.34}$$

with

$$s_{12} \equiv 2p_1 \cdot p_2 = -\frac{k_\perp^2}{z(1-z)}$$

In the small  $k_\perp$  limit (i.e. neglecting terms more singular than  $\frac{1}{k_\perp^2}$ ) we recover all the angular dependence in the four-partons antenna functions. For instance:

$$F_4^0(1, 2, 3, 4) \xrightarrow{i_g || j_g} \frac{1}{s_{ij}} P_{gg \rightarrow G}^{\mu\nu}(z) (F_3^0)_{\mu\nu}((ij), k, l)$$

A similar behaviour appears in every antenna function which has an infrared limit addressing a gluon splitting into quark-antiquark or into two gluons (e.g.  $G_0^4$ ,  $H_0^4$  and so on).

The spin-dependent splitting functions  $P_{\mu\nu}$  appearing in these equations were given in [43]. The tensorial three-partons antenna functions  $(X_0^3)_{\mu\nu}$  can be derived in the same way as with the scalar three-partons antenna functions from physical squared matrix elements. Their tensorial structure is obtained by leaving the polarisation index of the gluon associated with the momentum  $P_\mu$  uncontracted. On contraction of the tensorial three-partons antenna functions with a physical gluon polarisation average, we recover their scalar counterparts. In general, it seems we need to use spin-dependent antenna functions to account for the leftover angular terms. This problem can be circumvented as follows.

For each four-parton antenna function  $X_4^0$  yielding angular terms in a given simple collinear limit, we consider an angular function denoted with  $\Theta_{X_3^0}$ . This function needs to meet two fundamental requirements: (1) cancelling all angular dependence of the respective antenna function in the collinear limit considered, namely cancelling all the leftovers angular terms; (2) integrating to zero over the corresponding unresolved phase space. The last requirement is particularly strict, since it ensures that the analytical cancellation of the infrared poles is not affected by this procedure.

The local counterterms free of angular functions are obtained through the replacement:

$$X_4^0(1, i, j, 2) \rightarrow X_4^0(1, i, j, 2) - \Theta_{X_3^0}(i, j, z, k_\perp) \quad (3.35)$$

with

$$\Theta_{X_3^0}(i, j, z, k_\perp) = \left[ \frac{1}{s_{ij}} P_{ij \rightarrow (ij)}^{\mu\nu}(z, k_\perp) (X_3^0)_{\mu\nu}(1, (ij), 2) - \frac{1}{s_{ij}} P_{ij \rightarrow (ij)}(z) X_3^0(1, (ij), 2) \right] \quad (3.36)$$

where  $X_3^0$  is the appropriate antenna function obtained considering the limits of  $X_4^0$  when partons  $i$  and  $j$  build the parent parton  $(ij)$ ,  $P_{ij \rightarrow (ij)}^{\mu\nu}$  is the spin-dependent splitting function and  $P_{ij \rightarrow (ij)}$  the appropriate spin-averaged one and  $z$  is the collinear momentum fraction expressed in terms of invariants formed by the momenta of the four-partons antenna function.

Importantly,  $\Theta_{X_3^0}(i, j, z, k_\perp)$  integrates to zero over the unresolved antenna phase space since:

$$\int d\phi \, k_{\perp}^{\mu} k_{\perp}^{\nu} f(k_{\perp}^2) = -\frac{d^{\mu\nu}}{d-2} k_{\perp}^2 f(k_{\perp}^2) \quad (3.37)$$

and

$$d^{\mu\nu} = g^{\mu\nu} - \frac{P^{\nu} n^{\mu} + P^{\mu} n^{\nu}}{n \cdot P}$$

being the gluon polarisation sum in the axial gauge. Applied to the spin-dependent splitting function  $P_{ij \rightarrow (ij)}^{\mu\nu}$ , the above relation yields the spin-averaged splitting function  $d^{\mu\nu} P_{ij \rightarrow (ij)}$ . If further contracted with the tensorial antenna function  $(X_3^0)_{\mu\nu}$ , we obtain the product of the spin-averaged splitting function with the scalar antenna function  $P_{ij \rightarrow (ij)}(X_3^0)$ . Then, by construction,  $\Theta_{X_3^0}(i, j, z, k_{\perp})$  integrated in the unresolved antenna phase space vanishes.

# References

- [1] Ian J. R. Aitchison. “Supersymmetry and the MSSM: An Elementary introduction”. In: (May 2005). arXiv: [hep-ph/0505105](https://arxiv.org/abs/hep-ph/0505105).
- [2] Richard Keith Ellis, William James Stirling, and Bryan R. Webber. *QCD and collider physics*. Cambridge University Press, 2003.
- [3] Toichiro Kinoshita. “Mass Singularities of Feynman Amplitudes”. In: *Journal of Mathematical Physics* 3.4 (July 1962), pp. 650–677. DOI: [10.1063/1.1724268](https://doi.org/10.1063/1.1724268).
- [4] A. Gehrmann-De Ridder and E.W.N. Glover. “A complete (s)calculation of the photon + 1 jet rate in e+ e annihilation”. In: *Nuclear Physics B* 517.1-3 (1998), 269–323. ISSN: 0550-3213. DOI: [10.1016/S0550-3213\(97\)00818-3](https://doi.org/10.1016/S0550-3213(97)00818-3). URL: [http://dx.doi.org/10.1016/S0550-3213\(97\)00818-3](http://dx.doi.org/10.1016/S0550-3213(97)00818-3).
- [5] Charalampos Anastasiou, Kirill Melnikov, and Frank Petriello. “A new method for real radiation at next-to-next-to-leading order”. In: *Physical Review D* 69.7 (2004). ISSN: 1550-2368. DOI: [10.1103/PhysRevD.69.076010](https://doi.org/10.1103/PhysRevD.69.076010). URL: <http://dx.doi.org/10.1103/PhysRevD.69.076010>.
- [6] Aude Gehrmann-De Ridder, Thomas Gehrmann, and E.W. Nigel Glover. “Antenna subtraction at NNLO”. In: *Journal of High Energy Physics* 2005.09 (2005), 056–056. ISSN: 1029-8479. DOI: [10.1088/1126-6708/2005/09/056](https://doi.org/10.1088/1126-6708/2005/09/056). URL: <http://dx.doi.org/10.1088/1126-6708/2005/09/056>.
- [7] Takeo Inami, Takahiro Kubota, and Yasuhiro Okada. “Effective gauge theory and the effect of heavy quarks in Higgs boson decays”. In: *Zeitschrift für Physik C Particles and Fields* 18.1 (1983), 69–80. ISSN: 1431-5858. DOI: [10.1007/BF01571710](https://doi.org/10.1007/BF01571710).
- [8] Frank Wilczek. “Decays of Heavy Vector Mesons into Higgs Particles”. In: *Phys. Rev. Lett.* 39 (21 1977), pp. 1304–1306. DOI: [10.1103/PhysRevLett.39.1304](https://doi.org/10.1103/PhysRevLett.39.1304). URL: <https://link.aps.org/doi/10.1103/PhysRevLett.39.1304>.
- [9] URL: <https://www.nikhef.nl/~form/>.

- [10] R. Frederix et al. “The automation of next-to-leading order electroweak calculations”. In: *Journal of High Energy Physics* 2018.7 (2018). ISSN: 1029-8479. DOI: 10.1007/jhep07(2018)185. URL: [http://dx.doi.org/10.1007/JHEP07\(2018\)185](http://dx.doi.org/10.1007/JHEP07(2018)185).
- [11] A. Gehrmann-De Ridder et al. “EERAD3: Event shapes and jet rates in electron–positron annihilation at order  $\alpha^3$ ”. In: *Computer Physics Communications* 185.12 (2014), 3331–3340. ISSN: 0010-4655. DOI: 10.1016/j.cpc.2014.07.024. URL: <http://dx.doi.org/10.1016/j.cpc.2014.07.024>.
- [12] A. Gehrmann-De Ridder et al. “Infrared structure of  $e^+ e^- \rightarrow 3$  jets at NNLO”. In: *JHEP* 11 (2007), p. 058. DOI: 10.1088/1126-6708/2007/11/058. arXiv: 0710.0346 [hep-ph].
- [13] Johannes M Henn and Jan C. Plefka. *Scattering amplitudes in gauge theories*. Springer-Verlag Berlin Heidelberg, 2014.
- [14] Vittorio Del Duca, Lance Dixon, and Fabio Maltoni. “New color decompositions for gauge amplitudes at tree and loop level”. In: *Nuclear Physics B* 571.1-2 (2000), 51–70. ISSN: 0550-3213. DOI: 10.1016/S0550-3213(99)00809-3. URL: [http://dx.doi.org/10.1016/S0550-3213\(99\)00809-3](http://dx.doi.org/10.1016/S0550-3213(99)00809-3).
- [15] Malin Sjödal and Stefan Keppeler. “Tools for calculations in color space”. In: *PoS DIS2013* (2013). Ed. by E. Kajfasz, p. 166. DOI: 10.22323/1.191.0166. arXiv: 1307.1319 [hep-ph].
- [16] John Cornwell. *Group Theory in Physics: an introduction*. Academic Press, 1997.
- [17] Lance J. Dixon. “A brief introduction to modern amplitude methods”. In: *Theoretical Advanced Study Institute in Elementary Particle Physics: Particle Physics: The Higgs Boson and Beyond*. Oct. 2013. DOI: 10.5170/CERN-2014-008.31. arXiv: 1310.5353 [hep-ph].
- [18] Henriette Elvang and Yu-tin Huang. “Scattering Amplitudes”. In: (Aug. 2013). arXiv: 1308.1697 [hep-th].
- [19] Stephen J. Parke and T. R. Taylor. “Amplitude for  $n$ -Gluon Scattering”. In: *Phys. Rev. Lett.* 56 (23 1986), pp. 2459–2460. DOI: 10.1103/PhysRevLett.56.2459. URL: <https://link.aps.org/doi/10.1103/PhysRevLett.56.2459>.
- [20] John Collins C. *Renormalization. An introduction to renormalization, the renormalization group, and the operator-product expansion*. Cambridge University Press), 1984.



- [21] G. 't Hooft and M. Veltman. “Regularization and renormalization of gauge fields”. In: *Nuclear Physics B* 44.1 (1972), pp. 189–213. ISSN: 0550-3213. DOI: [https://doi.org/10.1016/0550-3213\(72\)90279-9](https://doi.org/10.1016/0550-3213(72)90279-9). URL: <https://www.sciencedirect.com/science/article/pii/0550321372902799>.
- [22] Charalampos Anastasiou et al. “D-dimensional unitarity cut method”. In: *Phys. Lett. B* 645 (2007), pp. 213–216. DOI: 10.1016/j.physletb.2006.12.022. arXiv: hep-ph/0609191.
- [23] Stefan Pokorski. *Gauge field theories, second edition*. Cambridge University Press, 2000.
- [24] A. Bassetto, Nardelli G., and R. Soldati. *Yang-Mills theories in algebraic non-covariant gauges*. World Scientific, 1991.
- [25] R. J. Crewther et al. “Chiral Estimate of the Electric Dipole Moment of the Neutron in Quantum Chromodynamics”. In: *Phys. Lett. B* 88 (1979). [Erratum: Phys.Lett.B 91, 487 (1980)], p. 123. DOI: 10.1016/0370-2693(79)90128-X.
- [26] G. 't Hooft. “Symmetry Breaking through Bell-Jackiw Anomalies”. In: *Phys. Rev. Lett.* 37 (1 1976), pp. 8–11. DOI: 10.1103/PhysRevLett.37.8. URL: <https://link.aps.org/doi/10.1103/PhysRevLett.37.8>.
- [27] R. D. Peccei and Helen R. Quinn. “Constraints imposed by CP conservation in the presence of pseudoparticles”. In: *Phys. Rev. D* 16 (6 1977), pp. 1791–1797. DOI: 10.1103/PhysRevD.16.1791. URL: <https://link.aps.org/doi/10.1103/PhysRevD.16.1791>.
- [28] Steven Weinberg. “A New Light Boson?” In: *Phys. Rev. Lett.* 40 (4 1978), pp. 223–226. DOI: 10.1103/PhysRevLett.40.223. URL: <https://link.aps.org/doi/10.1103/PhysRevLett.40.223>.
- [29] F. Wilczek. “Problem of Strong  $P$  and  $T$  Invariance in the Presence of Instantons”. In: *Phys. Rev. Lett.* 40 (5 1978), pp. 279–282. DOI: 10.1103/PhysRevLett.40.279. URL: <https://link.aps.org/doi/10.1103/PhysRevLett.40.279>.
- [30] Kazuo Fujikawa. “Path Integral Measure for Gauge Invariant Fermion Theories”. In: *Phys. Rev. Lett.* 42 (1979), pp. 1195–1198. DOI: 10.1103/PhysRevLett.42.1195.
- [31] Charalampos Anastasiou and Kirill Melnikov. “Pseudoscalar Higgs boson production at hadron colliders in next-to-next-to-leading order QCD”. In: *Phys. Rev. D* 67 (3 2003), p. 037501. DOI: 10.1103/PhysRevD.67.037501. URL: <https://link.aps.org/doi/10.1103/PhysRevD.67.037501>.

- [32] I. Brivio et al. “The complete HEFT Lagrangian after the LHC Run I”. In: *The European Physical Journal C* 76.7 (2016). ISSN: 1434-6052. DOI: 10.1140/epjc/s10052-016-4211-9. URL: <http://dx.doi.org/10.1140/epjc/s10052-016-4211-9>.
- [33] Vittorio Del Duca et al. “Higgs boson decay into b-quarks at NNLO accuracy”. In: *Journal of High Energy Physics* 2015.4 (2015). ISSN: 1029-8479. DOI: 10.1007/jhep04(2015)036. URL: [http://dx.doi.org/10.1007/JHEP04\(2015\)036](http://dx.doi.org/10.1007/JHEP04(2015)036).
- [34] Charalampos Anastasiou, Franz Herzog, and Achilleas Lazopoulos. “The fully differential decay rate of a Higgs boson to bottom-quarks at NNLO in QCD”. In: *Journal of High Energy Physics* 2012.3 (2012). ISSN: 1029-8479. DOI: 10.1007/jhep03(2012)035. URL: [http://dx.doi.org/10.1007/JHEP03\(2012\)035](http://dx.doi.org/10.1007/JHEP03(2012)035).
- [35] Steven Weinberg. *The quantum theory of fields. Volume 1: foundations*. Cambridge University Press), 1995.
- [36] Ruth Britto, Freddy Cachazo, and Bo Feng. “New recursion relations for tree amplitudes of gluons”. In: *Nuclear Physics B* 715.1-2 (2005), 499–522. ISSN: 0550-3213. DOI: 10.1016/j.nuclphysb.2005.02.030. URL: <http://dx.doi.org/10.1016/j.nuclphysb.2005.02.030>.
- [37] Ruth Britto et al. “Direct Proof of the Tree-Level Scattering Amplitude Recursion Relation in Yang-Mills Theory”. In: *Physical Review Letters* 94.18 (2005). ISSN: 1079-7114. DOI: 10.1103/physrevlett.94.181602. URL: <http://dx.doi.org/10.1103/PhysRevLett.94.181602>.
- [38] Zvi Bern and Gordon Chalmers. “Factorization in one-loop gauge theory”. In: *Nuclear Physics B* 447.2-3 (1995), 465–518. ISSN: 0550-3213. DOI: 10.1016/0550-3213(95)00226-i. URL: [http://dx.doi.org/10.1016/0550-3213\(95\)00226-I](http://dx.doi.org/10.1016/0550-3213(95)00226-I).
- [39] S.D Badger and E.W.N Glover. “Two-loop splitting functions in QCD”. In: *Journal of High Energy Physics* 2004.07 (2004), 040–040. ISSN: 1029-8479. DOI: 10.1088/1126-6708/2004/07/040. URL: <http://dx.doi.org/10.1088/1126-6708/2004/07/040>.
- [40] Stefano Catani and Massimiliano Grazzini. “The soft-gluon current at one-loop order”. In: *Nuclear Physics B* 591.1-2 (2000), 435–454. ISSN: 0550-3213. DOI: 10.1016/S0550-3213(00)00572-1. URL: [http://dx.doi.org/10.1016/S0550-3213\(00\)00572-1](http://dx.doi.org/10.1016/S0550-3213(00)00572-1).

- [41] S. Catani and M.H. Seymour. “A general algorithm for calculating jet cross sections in NLO QCD”. In: *Nuclear Physics B* 485.1-2 (1997), 291–419. ISSN: 0550-3213. DOI: 10.1016/S0550-3213(96)00589-5. URL: [http://dx.doi.org/10.1016/S0550-3213\(96\)00589-5](http://dx.doi.org/10.1016/S0550-3213(96)00589-5).
- [42] A. Gehrmann-De Ridder, T. Gehrmann, and G. Heinrich. “Four particle phase space integrals in massless QCD”. In: *Nucl. Phys. B* 682 (2004), pp. 265–288. DOI: 10.1016/j.nuclphysb.2004.01.023. arXiv: [hep-ph/0311276](https://arxiv.org/abs/hep-ph/0311276).
- [43] Stefano Catani. “The singular behaviour of QCD amplitudes at two-loop order”. In: *Physics Letters B* 427.1-2 (1998), 161–171. ISSN: 0370-2693. DOI: 10.1016/S0370-2693(98)00332-3. URL: [http://dx.doi.org/10.1016/S0370-2693\(98\)00332-3](http://dx.doi.org/10.1016/S0370-2693(98)00332-3).
- [44] A. Gehrmann-De Ridder, T. Gehrmann, and E.W.N. Glover. “Gluon–gluon antenna functions from Higgs boson decay”. In: *Physics Letters B* 612.1-2 (2005), 49–60. ISSN: 0370-2693. DOI: 10.1016/j.physletb.2005.03.003. URL: <http://dx.doi.org/10.1016/j.physletb.2005.03.003>.
- [45] A. Gehrmann-De Ridder, T. Gehrmann, and G. Heinrich. “Four-particle phase space integrals in massless QCD”. In: *Nuclear Physics B* 682.1-2 (2004), 265–288. ISSN: 0550-3213. DOI: 10.1016/j.nuclphysb.2004.01.023. URL: <http://dx.doi.org/10.1016/j.nuclphysb.2004.01.023>.
- [46] David A. Kosower. “Antenna factorization of gauge-theory amplitudes”. In: *Physical Review D* 57.9 (1998), 5410–5416. ISSN: 1089-4918. DOI: 10.1103/PhysRevD.57.5410. URL: <http://dx.doi.org/10.1103/PhysRevD.57.5410>.
- [47] A. Gehrmann-De Ridder, T. Gehrmann, and E.W.N. Glover. “Quark–gluon antenna functions from neutralino decay”. In: *Physics Letters B* 612.1-2 (2005), 36–48. ISSN: 0370-2693. DOI: 10.1016/j.physletb.2005.02.039. URL: <http://dx.doi.org/10.1016/j.physletb.2005.02.039>.
- [48] Stefano Catani and Massimiliano Grazzini. “Infrared factorization of tree level QCD amplitudes at the next-to-next-to-leading order and beyond”. In: *Nucl. Phys. B* 570 (2000), pp. 287–325. DOI: 10.1016/S0550-3213(99)00778-6. arXiv: [hep-ph/9908523](https://arxiv.org/abs/hep-ph/9908523).